January 2009

Electrocorticographic Neural Correlates of Arm Movements and Associated Goal Orientation in Humans

Nicholas Anderson
Washington University in St. Louis

WASHINGTON UNIVERSITY IN ST. LOUIS

School of Engineering and Applied Science

Department of Biomedical Engineering

Dissertation Examination Committee:
Daniel Moran, Chair
Dennis Barbour
Eric Leuthardt
Steven Petersen
William Smart
Kurt Thoroughman

Electrocorticographic Neural Correlates of Arm Movements and Associated Goal Orientation in Humans

By

Nicholas Robert Anderson

A dissertation presented to the
Graduate School of Arts and Sciences
of Washington University in
partial fulfillment of the
requirements for the degree
of Doctor of Philosophy

December 2009
Saint Louis, Missouri

Electrocorticographic Neural Correlates of Arm Movements and Associated Goal Orientation in Humans

by

Nicholas R. Anderson

ADVISORS: Professor Daniel W. Moran and Professor Eric C. Leuthardt

December 2009

St. Louis, Missouri

This thesis analyzed the cortical representation of arm kinematics, target encoding, and goal encoding using subdural electrocorticographic (ECoG) recordings in humans. Using a joystick-based visuomotor task, subjects performed both a standard, delayed match-to-sample center-out task as well as a circular tracing task. Spectral analyses of the ECoG signals clearly showed significant cosine tuning for hand velocity, direction, position and speed throughout the cortex. In particular, velocity tuning was best represented spectrally in a high gamma band from around 90-150 Hz in the primary motor cortical regions. In dorsolateral prefrontal cortex (DLPFC), cortical activity in the 150-250 Hz band of the ECoG signal showed robust, non-directional encoding for the goal during both the delay period prior to moving as well as the final hold period. This study suggests that ECoG is an effectively modality for applications where both movement kinematics and goal selection need to be decoded. Given ECoG's higher spatial and spectral frequency content as well as its higher signal to noise ratio versus scalp-based electroencephalography (EEG), ECoG is an optimal signal choice in brain-computer interface (BCI) applications.

Acknowledgements

I would like to thank Professor Daniel Moran for his guidance and faith. I would like to thank Professor Eric Leuthardt for his encouragement and mentoring. Thanks also goes to Tim Blakely, Dustin Heldman, Kim Wisneski, Wei Wang, Sherwin Chan, Adam Rouse, Mohit Sharma, Jeff Rudy, Jonathan Breshears, Vinod Rao, Craig Markovitz, and Elise Devries for assisting in the experiments and analysis. Thanks to my thesis committee: Dennis Barbour, Eric Leuthardt, Daniel Moran, Steven Petersen, William Smart and Kurt Thoroughman.

Nicholas R. Anderson

Washington University in St. Louis
December 2009

Table of Contents

Table list

Figure list

Epigraph

"If knowledge can create problems, it is not through ignorance that we can solve them."

Isaac Asimov

1 Introduction

1.1 Motivation

Millions of people suffer from neurological injury as a result of stroke and other neurological disorders (e.g. ALS). Each of these diseases and injuries has a different mechanism but the resulting paralysis is universal (A.H.A. 2007; NSCIA 2007). Due to the nature of these different mechanisms, curing these conditions through biological mechanisms would require a myriad of different treatments. However, methods have been developed to help alleviate the symptoms of these diseases without curing the underlying cause. One common solution is a Brain Computer Interface or BCI. BCIs are systems that bypass the nervous system to allow control of external devices from signals generated by the brain, these interfaces have been in development for the past 45 years,(Licklider 1960). Extracting these signals directly from the motor cortex can bypass any physiological problems that would normally interrupt these signals, allowing the patient to communicate or interact with the outside world (Wolpaw, McFarland et al. 1991).

Historically, control signals have been extracted from the human cortex using Electroencephalography (EEG), which has been the basis for developing human BCI (Wolpaw and Birbaumer 2005). The state of the art of EEG systems have recently been moved from their laboratory roots into a clinical environment with resulting increased efficacy. Improved functionality from these clinically developed BCIs allow some of them to be administrated on a daily basis by the patient's nurse (Birbaumer 2006). This improved functionality bring us closer to the goal of BCI technology, that is to allow the paralyzed patient to interact as normally as possible with the outside world; however, normal function

is not possible with the low signal fidelity present in EEG. Higher signal fidelity, available using other recording modalities, should allow for more degrees of freedom and thus a more useful interface. Action potentials of single neurons or single units provide the highest signal fidelity, and theoretically the most useful control (Nunez and Srinivasan 2006).

Control using single units has primarily been performed in non-human primates and other animals. The development of single unit recordings for BCI control has been largely in parallel to the EEG interfaces (Fetz and Finocchio 1971; Schwartz, Kettner et al. 1988; Georgopoulos 1995; Nicolelis, Dimitrov et al. 2003). Single units have been shown to carry much more detailed information per unit volume than EEG because they can record many independent neurons rather than an average of these same neurons as a large group (Fetz and Finocchio 1975). Single units are limited in their human applications because they both damage the cortex upon insertion and have uncertain long-term stability. Due to the instability of single units (Kipke, Vetter et al. 2003; Vetter, Williams et al. 2004), interest has shifted to field potentials of small groups of neurons that may provide the signal fidelity present in single units, while also offering a level of safety and stability suitable for human use (Heldman, Wang et al. 2006; Hochberg, Serruya et al. 2006).

Field potentials currently show the most promise for long term encoding of brain activity for use in brain computer interfaces (Andersen, Burdick et al. 2004; Andersen, Musallam et al. 2004; Schwartz, Cui et al. 2006). These field potentials have been shown to carry information about both the synaptic and the action potentials (Heldman, Wang et al. 2006). In addition field potentials are more robust and less technically demanding than recording action potentials directly (Pesaran, Pezaris et al. 2002; Heldman, Wang et al. 2006). Field potentials have been recorded both by microelectrodes and electrocorticographic (ECoG) electrodes, and both methodologies have shown encouraging results. Field

potentials have been shown to correlate to a variety of motor and cognitive activities that show promise for BCIs (Crone, Hao et al. 2001; G Schalk 2007). In addition, the ECoG BCI has shown the ability to allow the user to learn to control a computer with just a few minutes of training. ECoG has proven to be more robust in clinical settings, however it has not yet shown to decode more degrees of freedom than its EEG counterpart (Leuthardt, Schalk et al. 2004; Schalk 2005).

The aims of this thesis are to further understand the underlying ECoG activity as it relates to arm/hand movements, thereby enabling the creation of BCIs with more degrees of freedom and more intuitive control. Specific Aim I seeks to relate ECoG activity with human arm movements. While this encoding has shown to be cosine tuned to hand velocity and position for non-human primates, no one has been able isolate the separate components of position and velocity in humans using ECoG. Specific Aim 2 looks at non-motor aspects of these signals and seeks to find a non-directional signal appropriate for closed loop target selection (e.g., mouse click) using goal information encoded in the prefrontal cortex.

1.2 Specific Aims

I. Determine the ECoG neural correlates of hand position and/or velocity coding during joystick-based visuomotor tasks.

Hypothesis: High frequency tuning for arm movements has been shown in both human ECoG and non-human primate Local Field Potentials (LFPs); therefore, we expect the cosine tuning to be evident in these higher frequencies (Heldman, Wang et al. 2006; Kai J.

Miller 2007). Recently, time domain signals have shown some correlation to arm movements in ECoG; these signals may show tuning outside of the expected cosine tuning (G Schalk 2007).

II. Record from the Dorsolateral Prefrontal Cortex (DLPFC) and assess the feasibility of target encoding signals for use in BCI

a. Determine if the neural correlates for target information can be recorded using ECoG.

Hypothesis: ECoG signals in non-human primates have shown correlation to both goal encoding and target direction (Niki and Watanabe 1976; di Pellegrino and Wise 1993; Tanji and Hoshi 2001; Iba and Sawaguchi 2003). Humans have shown activity in specific Brodmann areas when performing directional based target tasks; therefore, we expect some some goal encoding and possibly directionality of target information.

b. Explore the feasibility of using attention signals for discrete selection.

Hypothesis: Given the encoding of target information recorded with other modalities some encoding is likely to be seen using ECoG (McCarthy, Puce et al. 1996; D'Esposito, Ballard et al. 2000; Iba and Sawaguchi 2003; Ramsey, van de Heuvel et al. 2006). In addition this should be a useful non motor signal for use in a selection task, given appropriate exploration of the encoding to fully understand it.

1.3 Significance

This thesis is most directly applicable to furthering BCI technology, which is still in its infancy. In order for BCI technology to reach the potential of restoring function to paralyzed and impaired individuals, advances need to be made in the associated neuroscience and engineering. This work is a small step in both of these areas. We do not understand how the cortex encodes information well enough to then decode the information completely. We currently believe that both the information encoded in action potentials as well as in synaptic potentials are useful for closed loop control of a BCI, and thus both will be important to use for successful restoration of a large percentage of limb function. Local field potentials and ECoG are uniquely suited for this endeavor as they monitor both of these signals.

Previous studies using ECoG has shown the ability to detect the encoding of arm movements; however, Aim I seeks to more precisely understand this encoding at a level where it could be used for real time control. This is the first study of human arm function to separate the position and velocity of the movements so that the related neural encoding can be viewed independently. Aim II seeks to show that ECoG can be used to view phenomena of target encoding previously seen mostly in non-human primate single units (Niki and Watanabe 1976; di Pellegrino and Wise 1993; D'Esposito, Ballard et al. 2000; Pochon, Levy et al. 2001). We use many non-motor areas in order to accomplish motor tasks, thus completely restoring function will likely require use of non-motor areas that have not been extensively studied for use in BCI.

1.4 Thesis organization

The experiments performed were based on a modification of the classic Center Out paradigm and Circle Tracing (Georgopoulos, Schwartz et al. 1986; Schwartz 1994). The Center Out task is a paradigm in which a subject moves a cursor from a center location to a radially placed goal target. The tracing task was is a task where two spheres move in a circular radius. One of these spheres is subject controlled and pushes the second computer controlled cursor. The data collected for Specific Aim 1 and Specific Aim 2a was based on joystick movement paradigms beginning with the center-out task. Aim 2b is based on the statistical analysis of the results acquired in 2a within the context of using this target encoding signal as a selection task (e.g. mouse click).

Chapter 2 outlines the previous research in the BCI community and how this thesis will further the body of knowledge necessary for this area of study to move forward. Chapter 3 outlines the methods for data acquisition, followed by Chapter 4 covering simulated data and analysis. Results for Specific Aim 1 and Specific Aim 2 are discussed in Chapters 5 and 6, respectively. Finally, Chapter 7 provides conclusions and future directions for this research.

2 Background and Significance

Assistive and prosthetic technologies for patients who have suffered neural injuries have been in development for over 100 years. A promising new technology for assisting these patients is Brain Computer Interfaces (BCI). The work to create a useful BCI as a human prosthetic began only 30 years ago using the modality of EEG (Vidal 1973). While it seemed that creating an EEG based BCI would be a relatively simple endeavor, many practical and engineering problems were encountered (e.g., noise and user training times) (Wolpaw, McFarland et al. 2003; Schalk 2005). These issues have belabored the development of a pragmatic BCI for those with immediate need. While progress has been made on some of these issues in the original modality of EEG, moving to a recording modality with higher signal fidelity such as Electrocorticography (ECoG) may provide a simpler and easier solution.

In first creating a closed loop ECoG BCI engineers used gross motor movements given their previous success in EEG BCI (Leuthardt, Schalk et al. 2004). Due to the chosen experiments and the immaturity of ECoG as a recording paradigm, the state of the art ECoG BCI has shown about the same level of control as the state of the art EEG BCI using the same type of motor signals (McFarland, Sarnacki et al. 2005; Schalk, Miller et al. 2008). However, this level of control in ECoG has been achieved with relatively little training compared to EEG due to the increased fidelity of the ECoG signals. In the future, the signal strength and detail of the ECoG BCI may allow the use of different features than the EEG BCI (Leuthardt 2006).

Investigations into the use of motor features similar to those used in other recording modalities began by looking at joystick movements while recording ECoG (G Schalk 2007). In addition, investigations of non-motor signals for control of ECoG BCI shows significant promise (Wilson, Felton et al. 2006). Isolating more complex signals using ECoG would be a significant advancement for neuroscience as it has the potential to fill gaps in our understanding left by other available modalities. Application of these signals to BCI could add additional degrees of freedom, and potentially lead to the development of better prosthetic devices for patients who suffer from neurological injuries.

2.1 Recording Cortical Activations

Human cortical activations were first measured using Electroencephalography (EEG) by Hans Berger in 1929 (Berger 1929). Prior to Berger's creation of this new technology, stimulation mapping had been used to chart the brain (Brodmann 1905). EEG was the first cortical recording technology, and a big advance in neuroscience because it is passive instead of active, thus it can provide temporal and frequency information about cortical signals whereas stimulation can only suggest location (Berger 1929). This electrophysiological information is important when trying to elucidate the neurophysiology of the human cortex. However, while EEG can provide much information about physiology it lacks the resolution, and detail, of other modalities (e.g. single units or local field potentials)(Nunez and Srinivasan 2006). With the use of single units or local field potentials, we can begin to understand the function of individual cortical areas and apply this understanding to create reasonably useful BCIs.

Since its inception in the 1970s, BCI has progressed seemingly independently in non-humans and humans because of the vast difference in recording paradigms. Human mapping and BCI has been done primarily with EEG, while single unit microelectrode recordings have been used in non-human primates (Fetz, Finoccio et al. 1971; Vidal 1973; Schmidt 1980; Georgopoulos, Schwartz et al. 1986; Schwartz, Kettner et al. 1988; Wolpaw, McFarland et al. 1991; Donoghue, Sanes et al. 1998; Nicolelis, Dimitrov et al. 2003). These two technologies have recently been tenuously bridged by the use of local field potentials (LFP) and Electrocorticography (ECoG) (Leuthardt, Schalk et al. 2004; Heldman, Wang et al. 2006). There is still some debate as to how these signals fit in to the existing landscape of recording methodologies. However, these technologies have provided for increased signal fidelity over EEG while avoiding many of the problems associated with single units (Leuthardt 2006).

2.1.1 Single Units

Single units are recorded by microelectrodes –(high-impedance devices that record the electrical activity (action potentials) of individual cells (Bremer 1958)). Single units are individual neurons, providing high spatial resolution, and are a proven recording paradigm for neurophysiology and BCI (Fetz and Finocchio 1971; Niki and Watanabe 1976; Georgopoulos, Kalaska et al. 1982; Schwartz, Kettner et al. 1988). The high resolution but invasive nature of these electrodes makes them well-suited for many studies in non-human primates. These studies have been conducted over a large spectrum of cortical and subcortical areas, with the thrust areas for neurophysiologists interested in BCI focused on motor and motor attention regions. Motor regions include primary motor (M1), pre-motor,

supplementary motor, and the motor attention regions including prefrontal cortex, dorsolateral prefrontal cortex (DLPFC), MT, LIP and others.

Microelectrodes have yielded many significant results in the study of motor regions, beginning with the demonstration that a monkey's arm movements are correlated with action potentials (Polit and Bizzi 1979). Building upon this result, it was shown that hand direction is represented in motor cortex (Georgopoulos, Schwartz et al. 1986). Also, arm position was shown to encoded by a sub population of motor cortical neurons (Evarts, Fromm et al. 1983). Further experiments indicated that velocity, rather than position was preferentially represented in motor cortex neurons (Fu, Suarez et al. 1993; Georgopoulos 1995). Furthermore, it was shown that in motor cortex, while the arm is being held still arm position is preferentially represented; however, during movement, velocities are dominantly represented (Moran and Schwartz 1999a; Moran and Schwartz 1999b; Wang, Chan et al. 2007). Finally, it was found that during movements velocity can be separated into speed and direction (Schwartz and Moran 1999c; Moran and Schwartz 2000). The encoding of cortical activity can be decoded using all three of these components if they are separated in the experimental design.

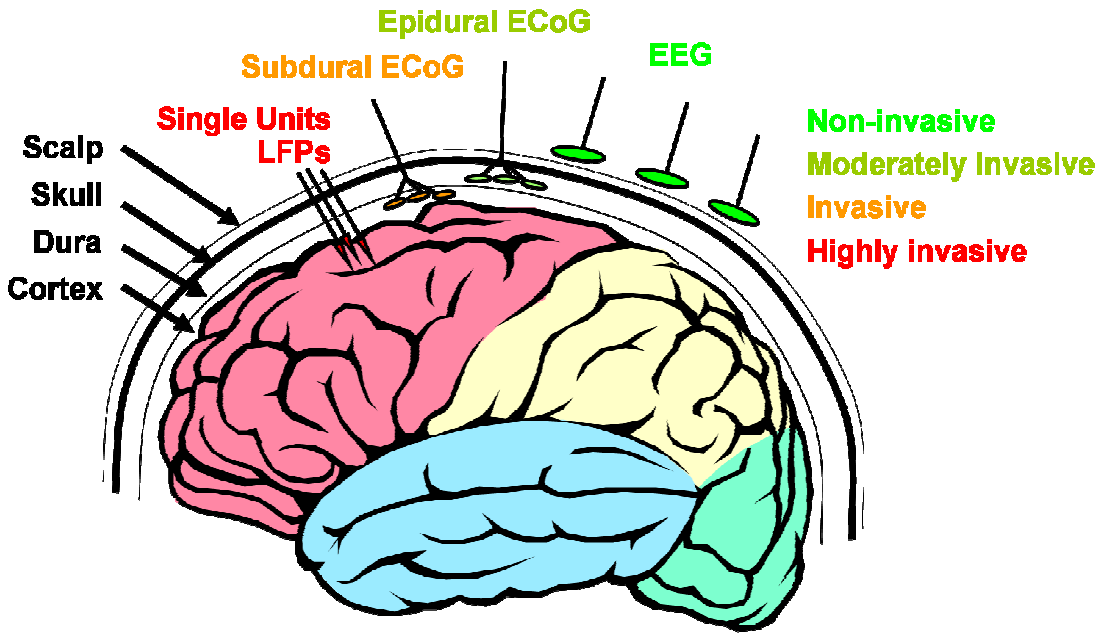

Figure 2.1.1: Methodologies for detection.
There are number of methods for recording cortical signals, they have different levels of invasiveness and signal detection ability. (Heldman 2007)

Kinematic encoding similar to that found in motor cortex has been found to correlate to activity in the dorsolateral prefrontal cortex (DLPFC) of non-human primates (Pochon, Levy et al. 2001). These studies have focused on how the information is encoded and have shown significant correlation to different attentional activities in the task. The correlations were found beginning with individual neurons showing increased firing rates during presentation and delay for a match to target task in primates prefrontal cortex (Fuster and Alexander 1971; Kubota and Niki 1971). Although these original studies were not delayed matching tasks, they pointed out an important cortical area involved in target matching tasks. Further investigations of this area have concentrated on the spatial nature of these signals (Niki 1974; Kubota and Funahashi 1982; Funahashi, Bruce et al. 1990).

The neurophysiology of many of these studies show tuning in the prefrontal cortex area to direction of response, but did not try to decorrelate cue direction from response direction. These responses, when decorrelated, appear to correspond more to cue direction than response direction in primates (Niki and Watanabe 1976; Funahashi, Bruce et al. 1993) . This cue directional encoding seems to be independent of stimulus modality as it has been shown to be present in prefrontal cortex areas in primates for both visual and auditory stimuli (Vaadia, Benson et al. 1986). While these neurophysiological studies correlated the response in DLPFC primarily to cue direction, questions remained if this activity was seen as independent of response and response modality.

These response modality questions have begun to be answered using implantable eye coils, which allowed controlled eye movements and showed there were spatial fields for these neurons. From these studies individual neurons in primate prefrontal cortex appeared to encode for cues in a specific contra-lateral area. Some of these contra-laterally encoded neurons showed directional target encoding and others showed non-directional target encoding (Funahashi, Bruce et al. 1989). These results were confirmed in work which saw encoding of cue direction in both prefrontal and premotor areas (di Pellegrino and Wise 1993). Using eye coil information, it has been shown that the cue direction is encoded in primate dorsolateral prefrontal cortex even when the response does not have a directional component (Sawaguchi and Yamane 1999). In addition to the encoding of current cue direction other signals have been identified (Takeda and Funahashi 2002; Tsujimoto, Genovesio et al. 2008), including non directional signals where neurons recorded showed an increase in activity post saccade as a "termination of target encoding signal" (Takeda and Funahashi 2002) All of this work in single units provides an indication of how individual cells behave but not of the population which is recorded by other modalities.

The tuning of components in motor cortex obtained through single units have yielded impressive results when used in BCIs (Schwartz, Taylor et al. 2001; Donoghue 2002; Velliste, Ferel et al. 2008). Monkeys have shown the ability to control cursors in multi-dimensional space based on components detected with microelectrodes during arm movements (Fetz and Finocchio 1971; Schwartz, Taylor et al. 2001; Velliste, Ferel et al. 2008). The level of control has been more robust as the encoding of the neural activity in different areas has become better understood, and the associated decoding algorithms become more sophisticated (Donoghue 2002). Due to this increased understanding and enhanced decoding techniques, single units have recently been used to control robotic arm devices (Fetz 1999; Taylor, Tillery et al. 2002; Carmena, Lebedev et al. 2005).

2.1.2 Electroencephalography (EEG)

While EEG lacks the signal fidelity of single units, much research has been done using EEG on motor and cognitive systems. EEG has very good temporal resolution compared to other non invasive techniques (e.g. fMRI, PET), making it useful for a variety of studies as well as BCI (Pfurtscheller and Aranibar 1977; Vidal 1977; Wolpaw and McFarland 1994). In addition, it has proven useful in studying lower frequency encoding in the cortex, particularly from the cortical gyruses (Pfurtscheller and Cooper 1975; Nunez and Srinivasan 2006). EEG recordings have been used to record from motor cortex and many other cortical areas (Bertrand ; Vidal 1977; Pfurtscheller, Neuper et al. 1997).

Gross motor movements were the first and simplest experiments performed using EEG (Penfield and Boldrey 1937) . EEG was then shown to correlate beyond different muscle groups to different movements of the same muscle group (Zetterberg. 1969; Roland, Skinhoj et al. 1980). Arm movements are of particular interest to those performing studies

with EEG because they have cross-modality support (i.e. they are also recorded by microelectrodes), and these recordings of cortical potentials do show correlation to arm movements (Touge, Werhahn et al. 1995). While EEG cannot provide the tuning results of other recording modalities, it continues to be important in providing an overall picture of cortical activity and important comprehensive timing information (Foxe and Simpson 2002).

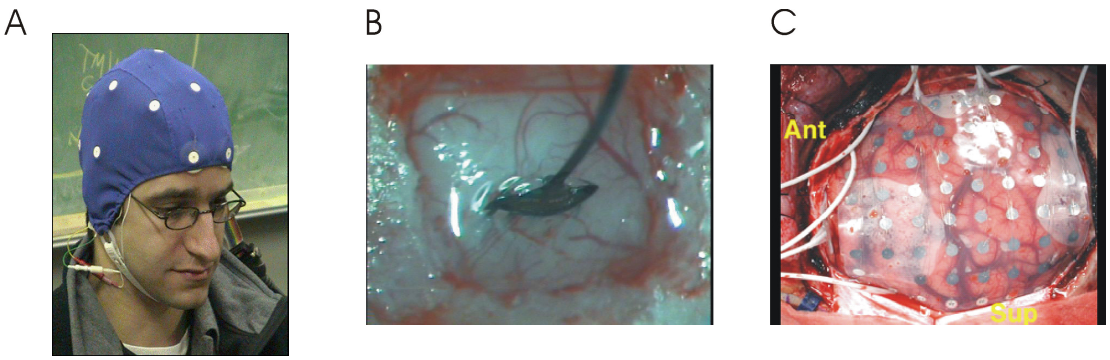

Figure 2.1.2: Recording modalities.
EEG (A), single units (B), and ECoG (C) are the primary means of acquiring neural signals for BCI applications. (Heldman 2007)

EEG has been the focus of human BCI research because it is very safe and inexpensive, resulting in a large number of labs running this paradigm.(Wolpaw, McFarland et al. 1991; Wolpaw and McFarland 1994; McFarland, Lefkowicz et al. 1997). A substantial amount of information can be recorded from EEG that is useful for BCIs. Currently available clinical BCI are based on EEG and allow a patient to control a computer in multiple ways for communication. The many years of signal process work and computer programming that have been invested in EEG have made it the most successful modality for BCIs at the present time. (Wolpaw, McFarland et al. 1991; Wolpaw and McFarland 2004; McFarland, Sarnacki et al. 2005; Birbaumer 2006). Despite EEG's success as a paradigm for BCI, it has some limitations that keep it from realizing the level of success initially hoped for.

There are many limitations that have slowed the progress of clinically available BCIs for patient use. Many of the issues that have slowed development of a BCI in EEG would have been encountered using any recording methodology. Some of these issues have been resolved by advances in technology. Other issues are engineering issues such as; human factors that go into creating a new interface to a machine, or developing algorithms that decode neural signals in a way that makes sense for a BCI. Currently, the major issues impeding the development of EEG BCI are those related to the physics restraining the methodology and no longer signal processing or hardware (Nunez and Srinivasan 2006). First, EEG has poor spatial resolution. Six square centimeters of cortex are needed to create a signal detectable with EEG, which means that at most people could have approximately four control signals from the motor cortex (two on each hemisphere) (Birbaumer 2006; Nunez and Srinivasan 2006). Second, EEG has a low signal to noise ratio, which comes in part from the heterogeneous impedance of the tissue between the cortical sources and the EEG electrodes (Kostov and Polak 2000; Guger, Edlinger et al. 2003; Nunez and Srinivasan 2006). These problems are compounded by the fact that the interfaces require months of training before meaningfully accurate control can be realized (Wolpaw 2004). Patients who need BCIs for daily living can not afford to train for months while their condition degrades, merely to gain a small degree of non-restorative control.

2.1.3 Magnetoencephalography (MEG)

Magnetoencephalography is closely related to EEG, in that it detects the magnetic component (rather than the electrical component) of the signal on the surface of the skull. It is different from EEG in that EEG records signals primarily from the gyri of the cortex whereas MEG records primarily from the sulci (Cohen 1968; Zimmerman 1970). The MEG

technique has much better source localization than EEG because it does not depend on head geometry and signals are not randomly scattered. EEG signals are randomly scattered by the differential permittivity of the tissue between the electrodes. The permeability that would affect the magnetic signals recorded by MEG is relatively uniform, resulting in better source localization (Martin, Houck et al. 2006).

MEG was plagued by noise for decades because the magnetic signals it records are incredibly small in magnitude (Huk and Vieth 1993). Recently, advances in computers and the associated algorithms have allowed compensation for the noise, resulting in a host of new research using MEG (Merlet 2001; Stam 2005). This research has included both studies on basic neuroscience as well as application to BCI technology (Stippich, Freitag et al. 1998; Mellinger, Schalk et al. 2007).

MEG has the ability to provide more specific results about underlying neural activity (Martin, Houck et al. 2006). Individual finger activity has been detected with the use of MEG because of its superior localization of individual sources (Nakamura, Yamada et al. 1998; Jarvelainen and Schurmann 2002). One study in MEG was able to predict movement position based on MEG data without dissociation of position and velocity (Georgopoulos, Langheim et al. 2005) Hand speed and coordination from prefrontal cortex to posterior regions has been correlated to MEG (Jerbi, Lachaux et al. 2007). These results have not shown correlation to hand movement direction or position. This could be because MEG does not perform well at higher frequencies, or simply because the data was low pass filtered at 100 Hz (Jerbi, Lachaux et al. 2007).

Prefrontal cortex has been the focus of many different studies in MEG, including for motor related tasks (Sasaki, Nambu et al. 1996; Kawaguchi, Ukai et al. 2005; Nakata, Inui et al. 2005). These studies have focused on the go/no-go related signals and not on possible

directional tuning or target encoding. Go/no-go signals give a cue to a subject and then instruct the subject whether to perform the action associated with that cue. The go/no-go signal is closely related to target signals and is encouraging for the prospect of target signals located in the dorsolateral prefrontal cortex.

From the available studies, it is apparent that the work utilizing MEG has focused more on clinical and epilepsy related research than on motor control or BCIs (Barkley 2004; Castillo, Simos et al. 2004). One of the reasons for the lack of BCI application is that the MEG system is as expensive as a fMRI system. This makes MEG much more difficult to afford and apply to BCIs then EEG (Mellinger, Schalk et al. 2005). Thus, for MEG to reach its potential as a BCI, it would need to be scaled down and reduced in cost (Birbaumer, Kubler et al. 2000; Wolpaw, Birbaumer et al. 2002) . In addition, MEG BCIs currently show improvement to EEG BCIs only in reduced training times and not in the other metrics that are used to gauge BCI performance (e.g. dimensions of control, accuracy) (Mellinger, Schalk et al. 2007). MEG as a BCI modality has the advantage of better signal to noise ratio and better source localization than EEG, but it is less widely used than cheaper but invasive methods (Leuthardt, Schalk et al. 2004).

2.1.4 Functional Magnetic Resonance Imaging (fMRI)

Functional Magnetic Resonance Imaging (fMRI) is the most common recording methodology for cortical activation studies in humans. It yields better spatial resolution than any other non-invasive modality, and can also simultaneously record activity from the whole brain, which is not available with any other modality (Rao, Binder et al. 1993; Cohen and Bookheimer 1994). Experiments on both motor systems and intentional systems are performed using fMRI. These experiments performed on humans tend to show less specific

results than the related non-human primate literature but give a better picture of the overall brain activity (Matelli, Rizzolatti et al. 1993; Moran and Schwartz 1999a).

fMRI studies have not been widely used in decoding the activations in motor cortex because of the difficulty in recording movements in fMRI machine space (Gassert, Dovat et al. 2005). In the studies that have been done, fMRI has shown that different areas are activated for different types of arm movements (Menon, Glover et al. 1998; Nirkko, Ozdoba et al. 2001). In addition, these studies have shown that fMRI is sensitive to fluctuations in signals that arise depending upon the direction of movement. (Lotze, Erb et al. 2000). fMRI can not be used to confirm the spectral and temporal information because the signal currently measures the hemodynamic response, not electrical activity. The hemodynamic response has been shown to correlate to electrical activity, but lacks the subtle changes in frequency response associated with electrical activity (Jueptner and Weiller 1995; Moseley, deCrespigny et al. 1996). In addition the hemodynamic response is slower than the electrical response associated with neuronal activity (Turner, Howseman et al. 1998). The extent and complexity of directional encoding is likely missed in fMRI because of the aforementioned limitations. The decoding of direction has proven to be a highly successful signal for control of BCI and the diminished capacity to detect this signal in fMRI puts it at a disadvantage for BCI applications (Schwartz 2004). While fMRI is not the best paradigm for motor studies or BCI applications, it has been yielded more complete data for other areas of interest.

fMRI has been used in humans to identify the dorsolateral prefrontal cortex (DLPFC) as an area of interest for coding target information, which supports the single unit work conducted in primates (D'Esposito, Ballard et al. 2000; Levy, Nichols et al. 2001; Pochon, Levy et al. 2001; Tanji and Hoshi 2001; Corbetta and Shulman 2002). Similar to the

single unit studies, fMRI studies demonstrated significant activation in the human analog area of cortex for the encoding of target information and motor initiation; however, they differed in that they did not show any positional information encoded in these areas (D'Esposito, Ballard et al. 2000; Pochon, Levy et al. 2001). This may be because of the low temporal resolution of fMRI or the fact that the fMRI signal is actually the hemodynamic response in the brain and is not a neural signal. Although unlikely, it is possible that humans or at least untrained humans simply do not encode for direction or position in this area of cortex and instead have adopted a new strategy for completing this type of task.

The high spatial resolution and non-invasive nature of fMRI have led some scientists to pursue it as a possible methodology for a BCI (Weiskopf, Veit et al. 2003). Through this work they have shown that it is possible for a person to control the signals that can be detected with fMRI (Weiskopf, Mathiak et al. 2004). In addition to the traditional motor tasks, dorsolateral prefrontal cortical areas have been explored using cognitive tasks (Ramsey, van de Heuvel et al. 2006). These data indicate that a variety of fMRI detectable signals can be controlled by the user and also, more importantly, that signals in the dorsolateral prefrontal cortex can be controlled by humans for the purposes of BCI. Despite this success, the expense of the equipment and the relatively low temporal resolution make fMRI an unlikely candidate for practical applications of BCI, compared to less expensive alternatives that can provide comparatively good results (Wolpaw, Birbaumer et al. 2002).

2.1.5 Intracortical Local Field Potentials

Local field potentials recorded with microelectrodes have recently yielded very encouraging results (Heldman, Wang et al. 2006). In addition, LFPs have better spatial, frequency, and temporal resolution than fMRI and EEG. Neuro-anatomy studies have shown that populations of neurons collectively carry larger amounts of information than single neurons alone and since high frequency LFP represent a population response from a group of single units. For example, multiple researchers have found that different neurons in M1 encode for both position and velocity (Georgopoulos, Schwartz et al. 1986; Moran and Schwartz 1999a; Wang, Chan et al. 2007). Thus by recording LFPs one can find encoding for both position and velocity, where as recording from one neuron would likely only show encoding of one component.

LFPs have recently been shown to record activity related to action potentials, which is particularly important because action potentials encode much of the information in the cortex. EEG records from large populations of neurons, but it does not record information directly related to action potentials. It is believed the low frequency activations recorded by EEG represent synaptic activity (Nunez and Srinivasan 2006). LFPs can record both the synaptic potentials and the action potentials of cells that are close to the recording area (Heldman, Wang et al. 2006). The action potentials appear to be largely encoded in the frequency range from 75 Hz and above this frequency range is not widely recorded using EEG (Heldman 2007). Because LFPs have the ability to record the most available information, they show promise for cognitive control of a BCI.

For the past decade several groups have looked at local field potentials with varying results. Until recently LFPs were investigated only in frequency regions lower than 50 Hz and showed results similar to EEG (Sanes and Donoghue 1993; Donoghue, Sanes et al. 1998). More complex results have been found by investigating the frequencies above 75 Hz. This higher frequency band has yielded better results from LFPs compared to previous studies using, other modalities, which is logical, given the LPF's correlation to action potentials in this band (Scherberger, Jarvis et al. 2005; Heldman, Wang et al. 2006). The sensitivity of high frequency LFPs can be seen in Figure 2.3, which shows that the preferred direction of a cosine tuned cell correlates to the preferred direction of the LFP taken from an electrode near that area (Heldman, Wang et al. 2006).

The correlation between high frequency LFP and action potentials gives a good indication that a high degree of kinematic encoding should be seen in LFPs. Heldman et al demonstrated speed tuning in M1 of non-human primates using two related target based tasks(Heldman 2007). Despite the correlation to speed tuning, the same study found that direction, velocity, and position tuning did not yield statistically significant results. This is believed to be the result of field cancellation due to overlapping receptive fields of the cells (Heldman 2007). First, it is of note that although the direction and position results did not show statistically significant results they did show tuning in many individual cases. It is believed that tuning for direction and position was not seen by Heldman et al because of the overlap of receptive fields. These LFPs were recorded from small groups of adjacent neurons that had different receptive fields thus canceling out any directional tuning that would be seen. In addition, it is of note that these LFP recordings were done with micro electrodes that were designed for single unit recording and studies of the appropriate size and geometry have not been performed for electrodes to record LFPs at this level.

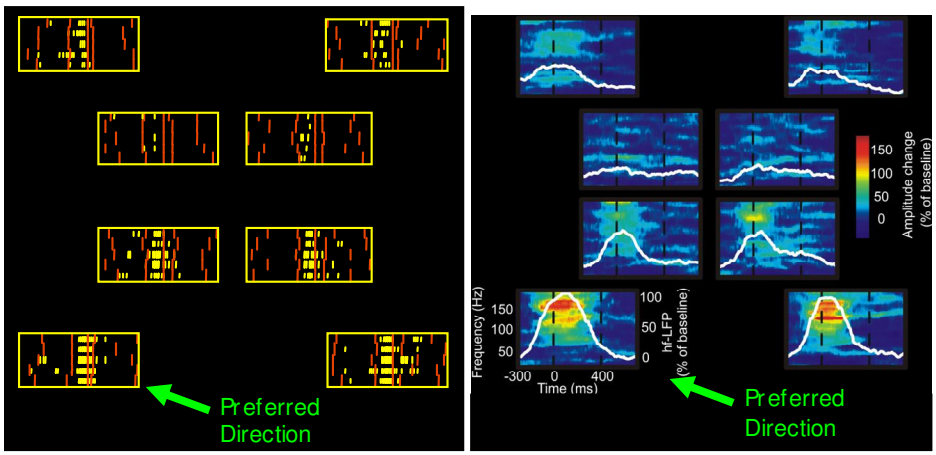

Figure 2.1.3: Single units and LFPs
Comparison of single units action potentials with local field potentials (Heldman 2007)

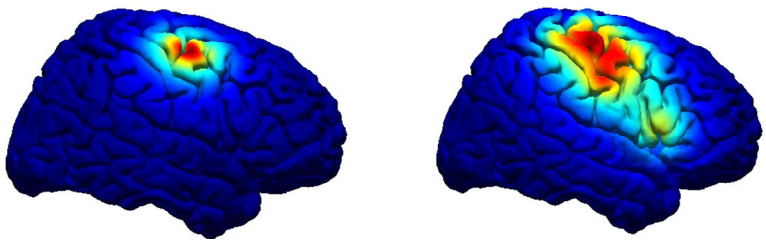

Screened for feature **Feature used for control**

Figure 2.1.4: Screening compared to control
Screened for feature vs feature used by patient for control (Leuthardt 2006)

2.1.6 Electrocorticography (ECoG)

Electrocorticography (ECoG) has been in use as a clinical paradigm for several decades and has been of interest to neuroscience researchers for about a decade (Toro, Cox et al. 1994). ECoG is an intermediate modality between EEG and LFPs. ECoG is recorded on the surface of the brain, whereas EEG is recorded on the surface of the skull, allowing ECoG to have better spatial selectivity and signal fidelity. Clinicians use ECoG because it offers better spatial localization then EEG (Toro, Deuschl et al. 1994). In addition, there is another very important advantage that ECoG offers over EEG; ECoG has a much better signal to noise ratio at higher frequencies (Leuthardt, Schalk et al. 2004). As seen in studies with LFPs, this higher frequency range is where additional relevant information can be found. The advantages of ECoG, when compared to EEG, should allow for better mapping of the encoded information and underlying anatomy involved with motor as well as non-motor areas.

ECoG offers advantages similar to LFPs; however, there are key differences between LFPs and ECoG. First, LFPs are recorded with much smaller electrodes (tens of microns) whereas ECoG is recorded with millimeter sized electrodes. Secondly, LFPs are recorded inside the cortical layers, while ECoG is recorded from the cortical surface.

It is also important to note that ECoG is dissimilar from single unit microelectrode recordings in that both ECoG and LFPs record high frequency information that is correlated with action potentials rather than the action potentials themselves (Heldman, Wang et al. 2006). As discussed earlier, action potentials have been shown to be highly correlated to movement kinematics and LFPs have shown some correlation to movement kinematics (Heldman, Wang et al. 2006). Recent studies have demonstrated ECoG's ability in detecting these movement signals as well (Miller, Leuthardt et al. 2007).

ECoG has been shown to be a good method for mapping spatial and frequency information correlated to movements. Gross motor movements have been extensively mapped out using ECoG (Kai J. Miller 2007). Recent results have shown joystick movement to be correlated to cortical potentials recorded with ECoG. In these experiments, movements could be predicted based on the amplitude of the ECoG signal recorded (G Schalk 2007). However, the joystick movements used did not differentiate position from velocity so the cortical signals could not be decomposed into kinematic components. The next step toward characterizing ECoG signals correlated to joystick movements is to decompose these signals into various kinematic components. Properly designed joystick experiments can help dissociate the different components of movements. The next logical step is to record cortical signals obtained during joystick movements that dissociate position from velocity. In addition, through careful experimental design, other ECoG responses can be explored at the same time. Since ECoG arrays typically cover a broad cortical surface, it would be advantageous to design experiments that simultaneously examine motor and non motor areas.

Motor cortex represents a small area compared to the total area of cortex, and other areas of cortex could potentially prove useful for BCIs given appropriate quantification of the available signals. One non-motor area that is important in daily functioning is associated with goal acquisition. Much of what humans do on a day to day basis is goal-oriented, and decoding this information could be useful for a BCI. The most likely non-motor location to be useful in goal selection is the prefrontal cortex. The prefrontal cortex has been extensively mapped in non-human primates using the delay-match-to-target task and using fMRI in humans (D'Esposito, Ballard et al. 2000; Tanji and Hoshi 2001). In addition, the DLPFC appears to encode for motor initiation and target position which are closely related

to target encoding (Jahanshahi, Dirnberger et al. 2001). Recent studies are encouraging for ECoG because they have found target encoding results in fMRI (Ramsey, van de Heuvel et al. 2006). Recently, recordings of ECoG have shown statistical significance in target based tasks; however, the studies only looked at frequencies generally associated with EEG (Rektor, Sochurkova et al. 2006). Thus, this area should be one of the first evaluated to determine whether ECoG signals are present and can be utilized for closed loop control. ECoG can currently be used to control two dimensional interfaces with accuracy that is similar to that using EEG interfaces. The advantage ECoG has shown is shorter training time. ECoG control only requires a few minutes to learn (Schalk, Miller et al. 2008) as opposed to EEG that requires months of training. ECoG has a higher signal fidelity than EEG and should now be explored to create more robust and intuitive BCI. This higher signal fidelity is of particular importance because the spatial extent of the signals from gross movements, shown in Figure 2.4, has become a hindrance to achieving higher dimensions of control. Just one signal for a gross movement used in this fashion takes up several square centimeters of cortical area, limiting the degrees of freedom possible with that cortical area. ECoG has shown an ability to decode signals that are of much smaller spatial extent than gross motor signals, including more specific motor signals (e.g. decoding directional movements) and also signals that are a combination of attention, sensory, and motor (Schwartz, Moran et al. 2004; Rektor, Sochurkova et al. 2006; G Schalk 2007). By better understanding how these signals are encoded at the level of ECoG, they can be applied to BCIs and provide more degrees of freedom.

2.2 Neural Decoding

The human brain converts sensory input and electrical impulses into motor outputs. These electrical impulses encode information in a variety of anatomical and spectral codes which are represented as a epiphenomena in ECoG (Brodmann 1905; Norton 1928; Berger 1929). The information exists across different Brodmann areas in the brain and at many different frequencies that can be sorted into features using spectral transformations (Krusienski, Schalk et al. 2006). Once the information is broken down into features, it can be further correlated to the experimental paradigm (Dalton 1969; Evarts and Tanji 1976; Georgopoulos, Kettner et al. 1988).

2.2.1 Techniques for computing spectral power

Auto regressive (AR) spectral estimation is one of the techniques most commonly used in biosignal applications because it solves difficulties associated with other techniques. The two major problems solved by the AR estimation technique are those of phase reversal and windowing effects. The problems that still remain include choosing the correct model order for this technique and determining whether the estimation created by the AR filter is better than the transformation provided by the fast fourier transform (FFT).

The AR filter is modeled using only poles making it very good at dealing with very sharp changes in the spectra (Marple 1987). Conversely, the FFT is an all zeros method, both equations are shown in Equation 2.2.1 and Equation 2.2.2. Poles (in the denominator) lead to fast changes in the power estimation as they cause the denominator to approach 0. Conversely in Equation 2.2.2 one can see that the FFT has all the variables for power

estimation in the numerator. This makes it much harder to fit to sharp spectral features due to the large changes required in the variables to make medium changes to the estimate.

$$P(f) = \frac{a_o}{\left|1 + \sum_{k=1}^{M} a_k z^k\right|^2} \quad \textbf{(2.2.1)}$$

$$X_k = \sum_{n=0}^{N-1} x_n e^{-\frac{2\pi i}{N} nk} \quad \textbf{(2.2.2)}$$

The FFT works very well on long time periods of stationary data. However the major problems the FFT causes for analyzing EEG data, is due to the windowing of the small samples. This effect may not be present for the relatively large samples obtained from ECoG. The windows used for EEG generally are of dozens of samples while those for ECoG are for hundreds of samples (Wolpaw, McFarland et al. 2003; Leuthardt, Schalk et al. 2004). To get around this problem all together, the AR filter does not have to be windowed because it can deal with very small windows of time and sharp spectral changes.

The AR filter has been used appropriately for EEG but has not been evaluated extensively for use with ECoG (Krusienski, Schalk et al. 2006). It has thus far been assumed that the AR filter is the appropriate choice for ECoG motor experiments while there has been no documented quantification as to how to choose the model order (G Schalk 2007; Kai J. Miller 2007). Outside of biosignals, a computational method would be used to determine the model order of the AR filter. These computational methods, such as the Akaike Information Criterion, can provide a model order for the filter; however, the results have shown to not be optimal for biosignals. In the EEG domain, new methods have been developed to choose an optimal filter order based on certain metrics(Dean J. Krusienski 2006). Similarly these methods have been used for ECoG but not systematically

quantified. These methods should be quantified for use, specifically for motor screening tasks, before this filtering method is continued

2.2.2 Mathematical encoding of movement information

Finding position and velocity encoding in humans brain activity would be significant because it would demonstrate that humans encode information in the same way as non-human primates. While this separable activity has been shown in single units, and somewhat in micro-local field potentials, it has never been dissociated in ECoG. This dissociation would allow for BCI with more degrees of freedom. Currently, two degrees of control are possible, but it takes seven to control a human arm, which is the eventual goal. If it does not provide significantly better control than what is offered by EEG, the invasive nature of ECoG will reduce its strength as an option for practical application (Leuthardt, Schalk et al. 2006).

Single unit decoding has a long history of mathematical rigor, including cosine tuning in the motor cortex (Georgopoulos, Kalaska et al. 1982). Georgopolous introduced the idea of cosine tuning for neurons controlling arm movements (Georgopoulos, Schwartz et al. 1986). These neurons would fire maximally in the preferred direction (defined by the direction of movement that caused maximal firing). The preferred direction was found by using linear regression (Equation 2.2.1). In Equation 2.2.3 $d(\mathbf{M})$ is the firing rate for a given neuron during a movement with a given direction defined by the x,y, and z components (m_x, m_y, m_z) and then determining b, b_x, b_y, and b_z which are coefficients from linear regression. Converting Equation 2.2.3 into polar coordinates yields Equation 2.2.4 illustrating the "cosine tuning" of the regression.

$$d(M) = b + b_x m_x + b_y m_y + b_z m_z \quad \textbf{(2.2.3)}$$

$$d(M) = b + k\cos(\theta - \theta_{pd}) \quad \textbf{(2.2.4)}$$

The activity of the cortical areas is denoted by d(M) and the baseline firing rate is b (sp/sec). The portion of the activity that is correlated to arm movement corresponds to $k\cos(\theta - \theta_{pd})$. In addition to these physical encoding factors there is a temporal encoding delay between the neural activity and the corresponding movements.

These equations have been converted into a form that is useful for different movement parameters by Moran et al. as well as others (Moran and Schwartz 1999a; Moran and Schwartz 1999b; Wang, Chan et al. 2007). These equation were used on LFPs data by Heldman et al. to find the preferred directions of features rather than firing rates (Heldman 2007). Equations 2.2.5-6 are taken from Heldman et al. and show how position and velocity can be fitted to the features in question. By fitting individual features to these equations, one can determine the percentage of activity correlated to position and velocity. Equation 2.2.5 utilizes the mean positions (*x,y,* and *z)* and finds the tuning (*B* values) for them. Similarly equation 2.2.6 finds the tuning criteria for the mean velocities in the *x,y,* and *z* directions.

$$\overline{P} = B_0 + B_{p,x}\overline{x} + B_{p,y}\overline{y} + B_{p,z}\overline{z} \quad \textbf{(2.2.5)}$$

$$\overline{P} = B_0 + B_{v,x}\overline{\dot{x}} + B_{v,y}\overline{\dot{y}} + B_{v,z}\overline{\dot{z}} \quad \textbf{(2.2.6)}$$

2.3 Novel directions explored in this thesis

This thesis explorers two new areas of BCI on neuroscience research. Chapter 5 addresses encoding of arm kinematics in ECoG data, Specific Aim 1. The second is covered in Chapter 6 addresses the unique encoding of DLPFC, Specific Aim 2. ECoG offers a unique perspective over previous techniques because it has electrodes specifically designed for large scale, close proximity, LFP recordings and also records wide areas of cortex (Heldman, Wang et al. 2004; Heldman 2007). These electrodes have started to be a successful paradigm with some early successes in motor decoding and BCI control (Leuthardt, Schalk et al. 2004; Schalk, Kubanek et al. 2007; Schalk, Miller et al. 2008; Wisneski, Anderson et al. 2008).

Showing the neural correlates of arm movements is an important step in creating a useful BCI using ECoG. ECoG is a very stable invasive system for recording neural activity; and as such it provides a possible medium for creating a useful BCI. However, thus far ECoG has been limited to using gross motor movement paradigms for creation of BCI which limit its functionality (Leuthardt, Schalk et al. 2004; Schalk, Miller et al. 2008). By mapping arm movements in a more specific manner ECoG can potentially be used to create a more useful multidimensional BCI.

Specific Aim 2 is the first time a delay match to sample task is used to explore the non-directional ECoG correlates of target based tasks. The end vision is to use the non directional ECoG correlates as a selection signal in a BCI. Other groups have shown that the DLPFC is an area that can be controlled for use on a BCI (Andersen, Burdick et al. 2004; Ramsey, van de Heuvel et al. 2006). At the same time the use of selection tasks have

been shown to increase the accuracy of BCI (McFarland, Sarnacki et al. 2005). Meanwhile , information in the DLPFC encodes directional and non directional information that may be useful for a selection task (Niki and Watanabe 1976; Funahashi, Bruce et al. 1990; Sawaguchi and Yamane 1999). Evaluating which ECoG signals would be useful for a selection task is an important step in developing a reliable selection paradigm for BCI.

3 General Experimental Methods

The Human Studies Committee at Washington University in Saint Louis approved the research protocols used herein. These protocols were approved at Barnes Jewish Hospital and Saint Louis Children's Hospital, for human epilepsy subjects. All approved guidelines set forth were followed when conducting these experiments.

3.1 Data Collection

Data were collected from epilepsy patients during invasive electrcorticography (ECoG) monitoring. All patients who underwent the placement of ECoG grids were asked to participate, less than five percent did not consent. The age and clinical diagnoses of the patients varied. Each patient performed a battery of experiments designed to test the cortical responses in a variety of ways.

3.1.1 Subject Pool and Electrode Placement

Epilepsy patients who consented and assented to involvement in this study were the subjects in these experiments. Clinicians placed electrodes on the surface of the cortex for the purpose of seizure localization prior to resection; Figure 3.1.1 shows the placement of such a grid. The location and quantity of these electrodes were determined clinically. The experiments contained herein accounted for variance in electrode placement based on several previous studies at Washington University that have used these subject groups

(Leuthardt, Schalk et al. 2004; Miller, Leuthardt et al. 2007; Schalk, Kubanek et al. 2007; Schalk, Miller et al. 2008).

These data were recorded concurrently to a clinical system that monitored continuously for epileptic events (e.g. seizures). A large improvement in temporal and amplitude sensitivity has been made in this experimental setup from the previous studies. Previously, these data were retrieved from the clinical network. However, in this study, data were collected by splitting off the clinical signal recorded from these subjects for purposes of seizure localization. The new and superior setup is shown in Figure 3.1.2 and allowed for the experiments contained herein.

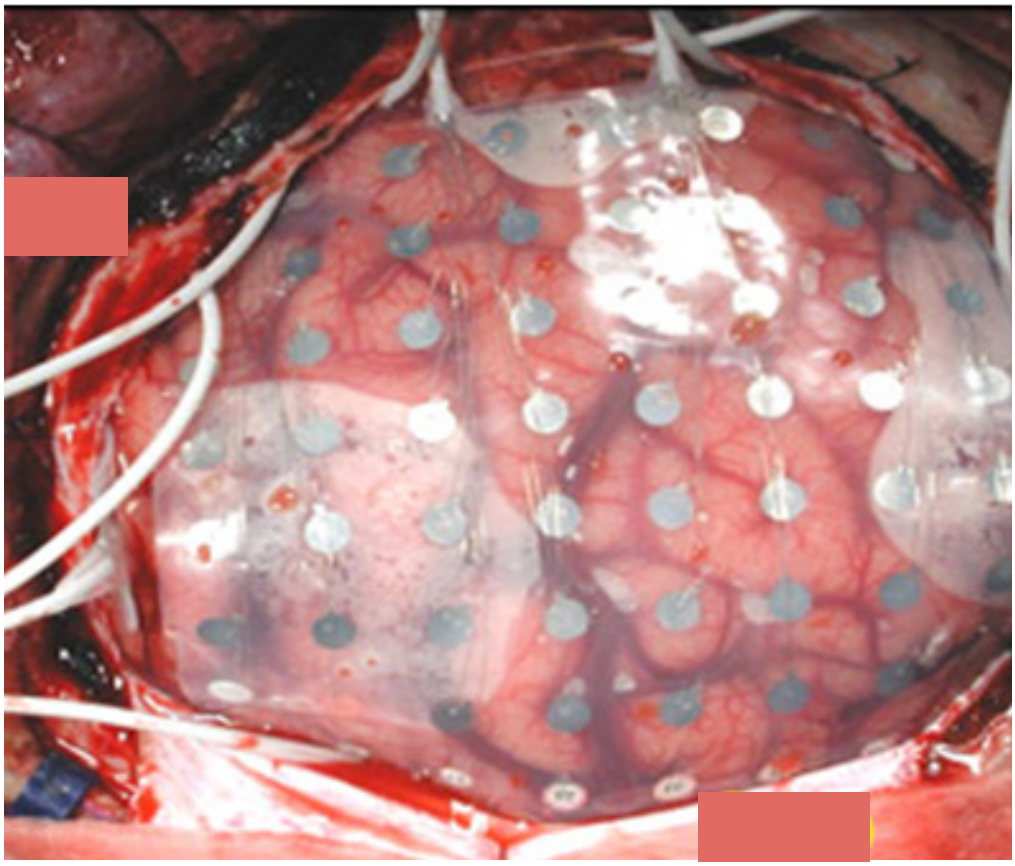

Figure 3.1.1: Electrocorticography
Electrodes placed on the surface of the cortex for the purpose of seizure localization.

The split signal was routed to four G.USB amplifiers connected to a computer running BCI2000. Each G.Usb amplifier can record 16 channels (for a total of 64 channels) and were purchased from Guger Technologies , Graz, Austria. The signals from these amplifiers were then routed to a computer containing BCI2000, a software designed to coordinate experiments with EEG or ECoG recordings (Schalk, McFarland et al. 2004). All experimental paradigms for this study used BCI 2000 to coordinate psychometric and kinematic stimulus with the cortical recordings.

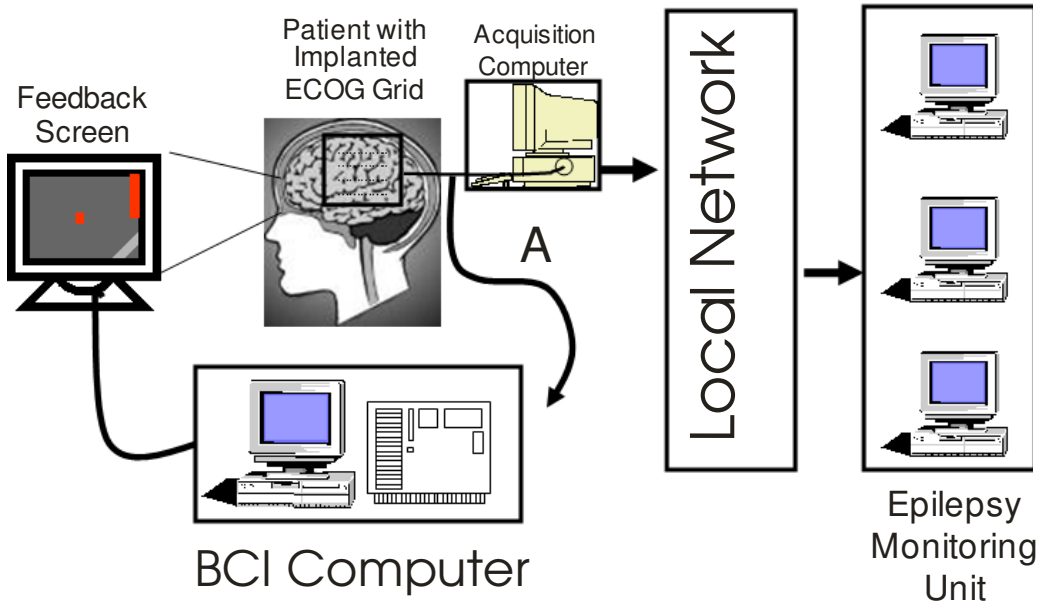

Figure 3.1.2: Splitting of the signal.
While previous studies had downloaded the ECoG signal off of the clinical network this study split the signal before it was recorded by the clinical system. This connection provided better temporal and amplitude sensitivity than the previous setup.

3.1.2 Systematic Localization of Electrodes

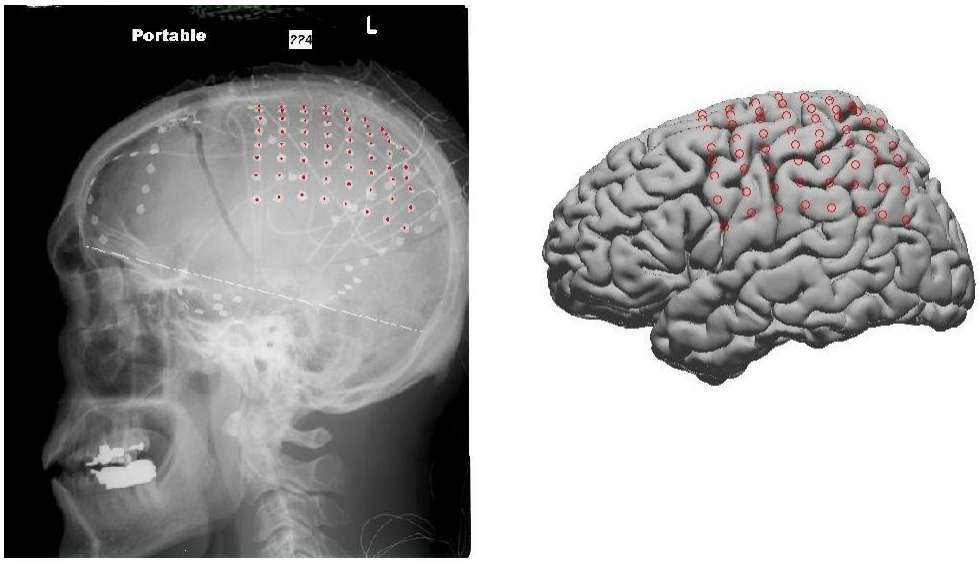

Figure 3.1.3: Example of electrode localization
Electrode locations on an x-ray using the LOC package developed by Kai Miller (Miller, Rao et al. 2007)

Care was taken to ensure precise electrode localization for these experiments. This could not be done directly as the electrodes were covered with the subject's dura mater and other tissue during the recordings. Between the time of electrode placement and recording these electrodes are imaged by a lateral x-ray of the subject's skull. These images were then used to localize electrode locations using the Talairach Coordinate system (Talairach and P. Tournoux PU - Thieme Medical Publishers 1988).

The calculation of Talairach coordinates of ECoG electrodes has been well documented and automated (Miller, Rao et al. 2007). This automated system was used to find the Talairach coordinates for each electrode, with 1 cm of variance to their actual location. The corresponding Brodmann areas were then found using the Talairach Daemon (Daemon). The Brodmann areas given by the Daemon were adjusted when they disagreed with what had been established clinically through stimulation and visual localization.

3.1.3 Subjects

Patient	Number	Sex	Handed	Age	Cognition
ZNZS	47	Male	Left	14	Normal
ZOZN	49	Male	Right	11	Normal
TOFS	51	Female	Right	27	Normal
TTES	54	Female	Right	46	Normal
ETOS	59	Female	Right	9	Normal
NTES	60	Male	Right	43	Normal
ZOOS	50	Male	Right	23	Normal
TOTS	52	Female	Right	11	Normal
EOES	58	Female	Right	11	Normal
FOTE	55	Female	Right	16	Normal
FZFE	67	Female	Right	48	Normal

Table 3.1.1: Subjects
Consenting subjects who participated in these experiments. Subject ZOOS was eliminated because the data collected was incomplete. Subjects EOES and ZOZN were eliminated due to non-compliance (refusing to follow instructions). Subject TOTS was eliminated due to noise issues caused by the clinical system yielding a total of seven subjects.

Data were collected from 11 subjects (listed in Table 3.1) for these experiments. Partial data was collected from three subjects because of non-compliance, or epileptic events. One subject had to be eliminated because change to the clinical system caused noise for both the experimental and clinical recordings . The remaining seven subjects performed the same three experiments using the same experimental conditions.

Experimental Environment

Experiments were performed by the subjects, in their hospital room, when they were feeling well enough to participate. The patients performed the experiments with a Microsoft Sidewinder II force feedback joystick which was placed at a comfortable distance to move with whole arm movements. These experiments or tasks were displayed on a computer monitor that was placed approximately 18 inches from the subject based on both best

viewing and comfort for the subject. The joystick was placed near the subject's contra lateral arm (contra lateral to electrode placement), this joystick was used to control the open loop task that was presented. This joystick provided forces to the center of the joystick and also resisted whichever direction the subject moved in. At maximum displacement from center the joystick provided x grams of force toward the center. When moving in a circle at maximum displacement there are x grams of force toward the center and y grams of force which resisted the circular movement of the subject. These forces provided increased effort from the subjects and thus increased activation on the cortex.

3.1.4 Controlling for Eye Position and Movements

The original experiments (i.e. Center Out and Tracing) have been performed in non-human primates and were then modified, in part to control for eye movements (Georgopoulos, Schwartz et al. 1986; Moran and Schwartz 1999a; Moran and Schwartz 1999b). It is of note that these tasks are generally performed without controlling or recording eye movement in non-human primates when recording from motor areas (Nicolelis, Dimitrov et al. 2003; Heldman 2007; Wang, Chan et al. 2007). However, for the purposes of these experiments we are also recording from areas associated with eye movements, particularly Brodmann Area 8 (Frontal Eye Fields).

The eye position of the subject was important because they correlate heavily with arm movements, and the primary interest is arm movements. A variety of measures were attempted to control eye movements including instruction, monitoring eye movements, and experimental design. Significant effort was placed into controlling for this possible confounding variable, and experimental design was eventually deemed the most successful approach.

When recording from visual areas it is common place to control eye position, in part because of the study of receptive fields (di Pellegrino and Wise 1993; Iba and Sawaguchi 2003). A receptive field is a region in the field of vision where a neuron responds to stimulus. The purposes of these tasks is not to ascertain receptive fields at the level ECoG records, nor would it be likely to see receptive fields at this level. However, due to this additional coverage attempts were made to account for the eye movements.

The first method attempted to control eye movements was to have the subject's foveate at the center of the task while also recording Electrooculogram (EOG). It was deemed that this could eliminate eye movements entirely, however subjects found the task too difficult with out being able to move their eyes. In addition, it became apparent that, EOG electrodes often would have to be placed close to areas that caused the subjects discomfort or pain. For these reasons the tasks were designed to minimize eye movements.

The Center Out task had delay periods added to analyze specific attentional components and they also eliminated potential eye movements from many of the periods of interest. The target was displayed during a period (Target Encoding) that was not analyzed (Figure 3.2.2); during this Target Encoding period there is an expectation of eye movements as the subject saccades to the target. Following this there was a delay where in the subject waited for a signal to move (go signal). This signal was an elimination of a center target and ring which kept the subjects attention and eyes focused on the center of the task, reducing eye movements during this important period. The last section wherein eye movements would be expected is following the go signal, wherein the subject would be expected to saccade to the goal target. This saccade would last only a short time (20-200 ms) for the entire movement period (1-2 s) and thus be largely averaged out.

The hold period of Center Out (Figure 3.2.2) was used to find position tuning. During this period it would be expected that the subject be foveated on the goal target and be holding the cursor on the goal target. During this section eye position and hand position would be highly correlated, however a way to eliminate this was not added to the task. It is now recommended that the reward or error signal be put in the center of the task to force the subject to look in that location during this hold period.

The Tracing task was programmed in two versions, with one designed to minimize eye movements. The traditional version uses a cursor radius that encompasses the whole size of the screen. To reduce this radius, a version was created that used arrows (Figure 3.2.1) that had a 54% reduction in radius, while still using the same arm movements (Table 3.2.2). This was the smallest radius of arrow that could be used while still having a distinction between the smaller and larger radii. We still expect smooth pursuit eye movements to be present during this task, but this was deemed an appropriate reduction of eye movements.

3.1.5 Manipulandum

The manipulandum used to perform the tasks outlined in Figure 3.2.1 was a Microsoft Sidewinder force feedback joystick. The forces applied from this joystick are outlined in Figure 3.1.4. The patient was resisted in movement of the joystick in every direction except when moving toward the center. The joystick provided continual force toward the center and as such would apply force to the subjects arm back to the center during any movement. This would provide perpendicular force (compared to movement direction) during Tracing and assistive force when returning the joystick to its center. Subjects were instructed to move the manipulandum using their whole arm and not just wrist movements. In addition, the tasks lent themselves to using the whole arm both given the arm movements required and the resistive force of the joystick. This will allow decoding of the neural correlates of arm movements rather than simply wrist or shoulder movements.

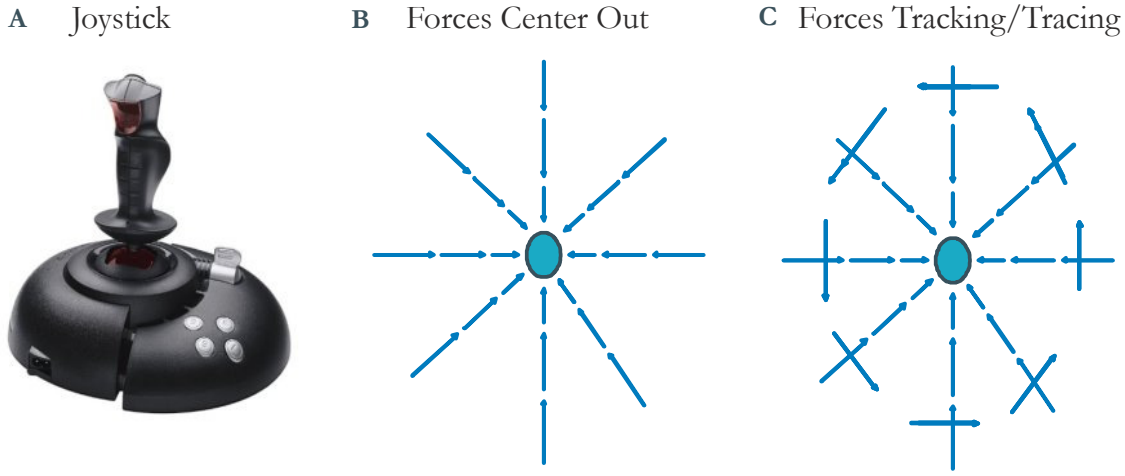

Figure 3.1.4: Manipulandum
A. The manipulandum (joystick) used in the experiments as shown from the front, it had force feedback as outlined above. Resistive and pushing towards the center of the joystick similar to an aircrafts yoke.. B. For Center Out the subjects experienced forces resisting their movement to the targets. C. For Tracing the subjects experienced forces resisting their movements as well as continual force towards the center.

3.2 Tasks

The following four experiments were performed by each subject: a center out task (Center Out), arrow tracing task (Tracing), a sphere tracing task, and a Speller task; all tasks are shown in Figure 3.2.1. Each task was designed to test for a different neural correlate. Center Out and the tracing tasks were meant to test for the neural correlates of directional movement. Center Out was also designed to work in combination with the Speller task to test for target encoding.

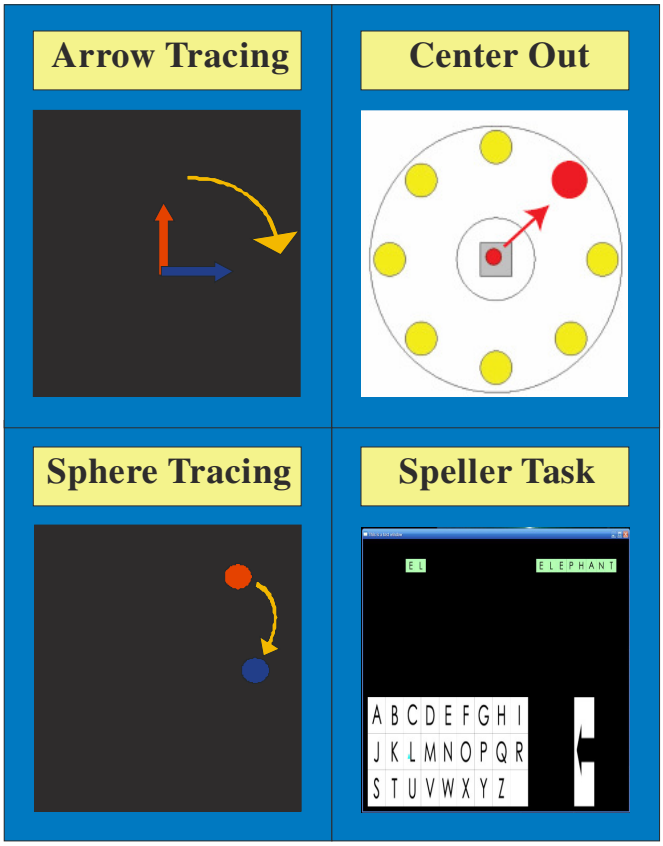

Figure 3.2.1: Task Diagram
The above tasks were performed by the subjects in these experiments. Each task was created for a specific cortical response, in order to establish whether that response was present and viewable at the level of ECoG.

3.2.1 Center Out

Center Out was derived from the classic center out task run by many earlier studies (Georgopoulos, Kalaska et al. 1982; Moran and Schwartz 1999a; Georgopoulos, Langheim et al. 2005; Heldman 2007). The Center Out task had 8 targets spaced 45 degrees away from each other (Figure 3.2.1). The subject was instructed to move the cursor to the target that shifts colors during a target acquisition period. Table 3.2.1 displays the subjects tested on this task. Center Out was divided into five different periods and included delay periods allowing attention and intentional components to be analyzed separate from motor components. The delay periods were of differing and variable lengths and are displayed in Figure 3.2.2.

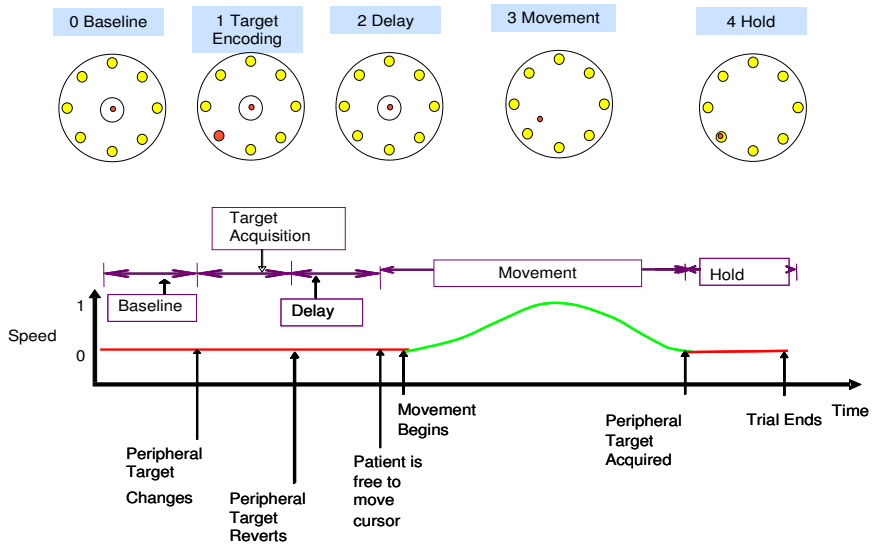

Figure 3.2.2: Temporal details of Center Out.
Each delay period was set up in order to view encoding of target information, attention, or intention without the motor responses related to movement. The red line and green line are a sample velocity curve of the subject's movements. During red periods the subject is not moving, and during green periods the subject is moving.

The first period is a delay (Baseline Period; 300 ms), used as a baseline in the analysis, is before the subject can encode the target. The goal target then briefly changes color (Target Encoding Period; 300-500 ms) to indicate that it is the goal target, which the subject is to attain for this trial. Another delay (Delay Period; 300 ms) follows the target-encoding period, allowing analysis of the intentional encoding of the target without the motor response. Subjects then move (Movement Period; variable ms) the cursor to the appropriate target. Upon reaching the target the subject has to hold for a length of time (Hold Period; 300-500 ms); allowing for analysis of goal accomplishment. A reward period follows wherein the original goal target changes to green if the trial was completed correctly or red if the trial was completed incorrectly. To complete the cycle of the task the cursor is re-centered by the subject so that each trial begins in the same location.

Center Out			
Patient	**Number**	**Hold**	**Click**
ZNZS	**47**	**x**	**x**
TTES	**54**	**x**	**x**
TOFS	**51**	**x**	**x**
ETOS	**59**	**x**	**x**
FOTE	**55**	**x**	
NTES	**60**	**x**	
FZFE	**67**	**x**	**x**
Total		**7**	**5**

Table 3.2.1: Center Out Subjects
The center out hold task was run on seven patients and the center out click task was run on 5 patients. The hold task was prioritized first, and was run on on more patients than the click task.

3.2.2 Tracing

The tracing tasks were originally programmed in several varieties, all of which were designed to decorrelate position and velocity kinematics. A circle would be traced by the subject so that the position and velocity components of the movement kinematics would be

orthogonal to each other (Figure 3.2.3). In Center Out these components are correlated so that it cannot be determined which component is being encoded. By making these components orthogonal and running the task in both directions (clockwise and counter-clockwise) it can be shown that either position or velocity is being encoded for preferentially.

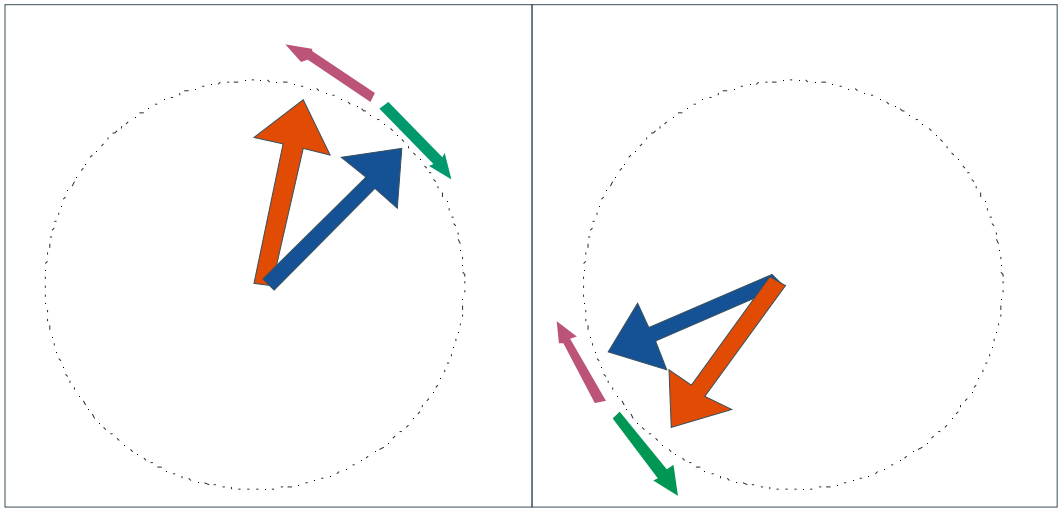

Figure 3.2.3: Tracing task with arrows
Demonstrates the dissociation of position from velocity for this task. For each position there are two anti-parallel directions and for each direction there are two positions. The green and purple direction arrows point in the same direction, despite being in opposite positions around the circumference. Similarly the position of the arrows on the left at one point on the circle has two opposite directions applied to it.

A prototypical tracing task done by monkeys uses two spheres where one sphere is controlled by the monkey to push the other sphere in a specified direction (Schwartz 1993; Moran and Schwartz 1999b). The direction changes from between trials, so that the velocity encoding can be compared to the position encoding. This was modified into a task for humans where one sphere pushed another in two dimensions around a circle (radius) encompassing the entire screen height. The goal of the task was to match the radius of the target sphere so that it could be pushed around the circle. In addition a task was devised where in one sphere would follow another traveling at a constant computer paced speed ("Tracking" task) in two dimensions. These tasks were run in a clockwise and

counterclockwise direction and in two radii (Table 3.2.2). An issue that arose when using a circle with a radius of the monitor width was that the eye movements were very large and correlated heavily with the arm movements.

	Large radius (cm)	Small radius (cm)
Center Out	12.7	
Sphere Tracing	8.25	4.125
Arrow Tracing	3.81	1.905
Joystick (Displacement)	5.334	2.667

Table 3.2.2: Tracing Radii
The Tracing tasks were run at two radii, and the Center only had the maximum radius. Joystick displacement is the distant from center the top of the joystick moves; it was the same for all the tasks. That is, the hand position to reach the large radius in all three tasks was the same.

Arrows of much shorter length (Table 3.2.2) than the height of the monitor were placed in the center of the screen. These arrows were used both in the tracing and tracking version , in both directions, and at both radii, the only difference being that they allowed a minimization of eye movements in this task. While the arm movements were the same as the previous task, the arrow diameters were smaller so the eye movements were smaller. The arrow Tracing task was prioritized to be run on subjects first as it had the best subject compliance and kinematics that were most interesting. Due to the prioritization of this task enough data was generated for analysis, 6 subjects were deemed to be a high enough number for this analysis. While each Brodmann area had to have coverage from at least three subjects to be considered. As such the other Tracking/Tracing tasks were not run on enough subjects for analysis. The number of subjects that performed each task is shown in Table 3.2.2.

Tracing Task					
Patient	**Number**	**Arrow Tracing**	**Arrow Tracking**	**Circle Tracing**	**Circle Tracking**
ZNZS	**47**	**x**	**x**	**X**	**x**
TTES	**54**	**x**	**x**	**X**	**x**
TOFS	**51**	**x**		**X**	
ETOS	**59**	**x**		**X**	
FOTE	**55**	**x**			
FZFE	**67**	**x**			
Total		**6**	**2**	**4**	**2**

Table 3.2.3: Tracing Subjects
The arrow tracing task was performed by 6 subjects, the arrow tracking task was performed by 2, the circle tracing task was performed by 3, and the circle tracking task was performed by 2. The arrow tracing task was prioritized highest because of the higher subject compliance and reduced eye movements, causing it to be run on many more subjects.

3.2.3 Speller

The last experiment was referred to as the Speller task. The subject would spell out words using the joystick to control the cursor (Figure 3.2.4). The task was designed so that a subject hitting a goal target could be compared to a subject passing over a non-goal target. This was accomplished by putting all of the targets next to each other on a grid.

There were some unresolved issues with the design of the task. The hold period on the each target was not long enough in comparison to the movement periods to give very good results. In addition there was no delay period after each target was acquired. Lastly, the letters should be presented to the subject one at a time rather than as a string so that the delay periods can be added later.

The issues mentioned kept the analysis from teasing out the attention details that it was designed to capture. The results were overwhelmed by the motor responses involved in all sections of the task. With the addition of delay periods and more careful motor control a similar task will likely have better results.

This task was run on four patients and did not yield novel results based on the corresponding analysis. No interesting results were found that could not be attributed to the

motor components of the task; therefore, no further analysis will be presented on this task in this dissertation.

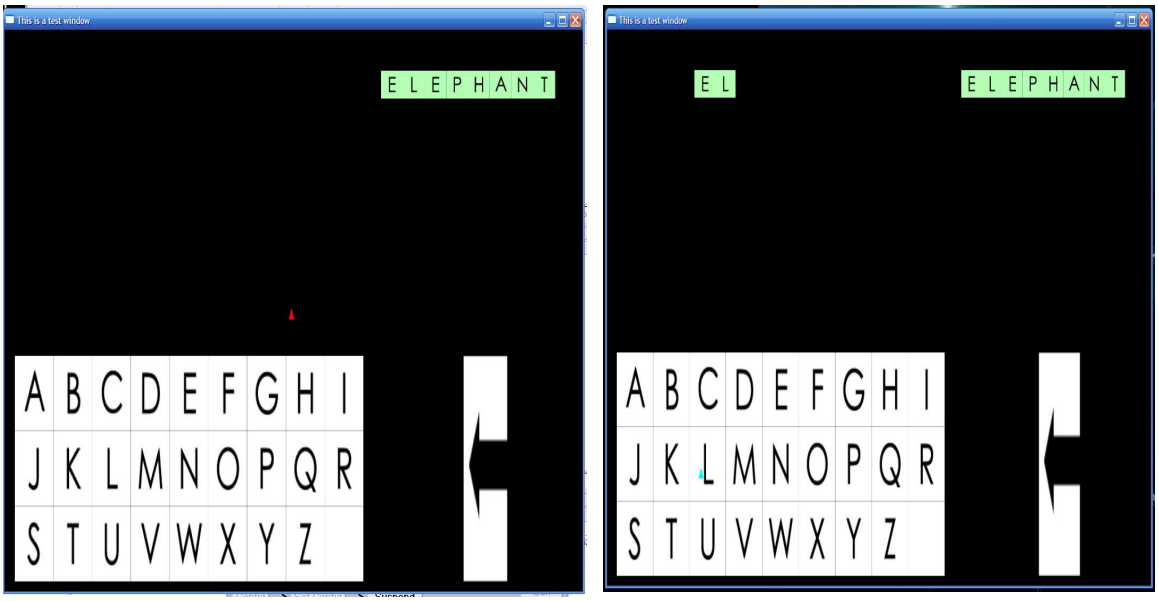

Figure 3.2.4: Speller task
The subject was instructed to spell out the word or pseudoword in the upper right hand corner using the cursor.

4 Analysis and Simulations

Simulated data was created based on expected performance of the models and analysis. Simulated data was created using cosine tuning models for kinematics (position,velocity, etc.). Data was also created that simulated non directional target encoding. Lastly, data was created that only contained noise to verify that encoding would not be seen on un-tuned data.

Spectral estimation and analysis was run for cosine tuning, goal tuning, and using a decision tree to test all of the applicable algorithms. The spectral estimation techniques accurately represented the encoded data. Each algorithm showed the expected result and also rejected the channels with incorrect or no tuning. The decision tree analysis was able to correctly identify when a target was encoded in the simulated data. The results were positive, confirming the validity of the analyses algorithms

4.1 Simulated Data

Simulated ECoG data was designed and created to encode for the expected results of both the Center Out and Tracing tasks. A simulated patient was created for both tasks with independent channels encoding position, velocity, amplitude, and noise. These channels were divided into different simulated Brodmann areas for the purposes of analysis.

The process of creating an encoded channel had three steps, creation of a kinematic signal, encoding of the signal in the spectra, and addition of noise. The creation of a kinematic (e.g. hand position) signals were all done manually. In Figure 4.1.1 a, position duing a center-out task was modeled as a straight line as a function of time. This signal was then used to amplitude modulate a carrier signal by multiplying its magnitude for each sample by a series of sinusoids across a frequency band. The sinusoids phases were then

randomized and combined into one modulated spectra. Lastly, 20% noise was added to these spectra by taking the existing modulated spectra and adding a random number (white noise).

4.1.1 Encoding of Center Out

Simulated Center Out ECoG data was encoded with position, velocity, amplitude tuning, and two types of noise. Position was a ramp function that increased as the simulated cursor position approached the preferred positions (Figure 4.1.1 a). Velocity encoding was represented as a Gaussian curve that increased when the simulations cursor was moving in the preferred direction (Figure 4.1.2 a). Amplitude encoding was represented by a ramp that increased as the simulated cursor approached any target (Figure 4.1.3 a).

Noise encoded channels were created in two ways. First, by taking purely random uniformly distributed encoding (white noise). The second by adding this white noise to a signal that had been put through the modulation process with no task related encoding. This noise was added to ensure that the modulation process was functioning exactly as expected, and not adding encoding.

The position tuned signals (Figure 4.1.1) show an increase when the simulation is positioned near 180 degrees and a decrease when the simulation is near 0 degrees. The preferred position in this case is 180 degrees and the anti-preferred position is 0 degrees. The intermediate directions are cosine tuned because the amplitude of the signal in a polar coordinate system mirrors that of a cosine tuned wave.

The position tuning used to encode Center Out simulated data can be seen in Figure 4.1.1 a. This position tuning was encoded into a simulated channel by amplitude modulating

a power signal centered at 90 Hz (Figure 4.1.1 b). The power of the spectra can be seen to mirror that of the encoding despite the randomization of the phases in the signal.

Noise was then added to this signal in addition to the noise inherent in the original signal due to the process of mixing the phases (Figure 4.1.1 c). This additional noise was designed to be 20 % of the maximum power present in the signal. Despite the addition of the noise, the original tuning can still be seen in the signal.

The power of this signal is centered at a frequency of 90 hz, which can only be viewed as a spectrogram, which converts the data into the time and frequency domain (Figure 4.1.1 d). This spectrogram shows the same tuning as the spectra in Figure 4.1.1 b, but also shows that the encoded frequency is centered around 90 Hz. Additionally, it shows that all of the power in the modulated signal is represented between 85 and 115, as was intended.

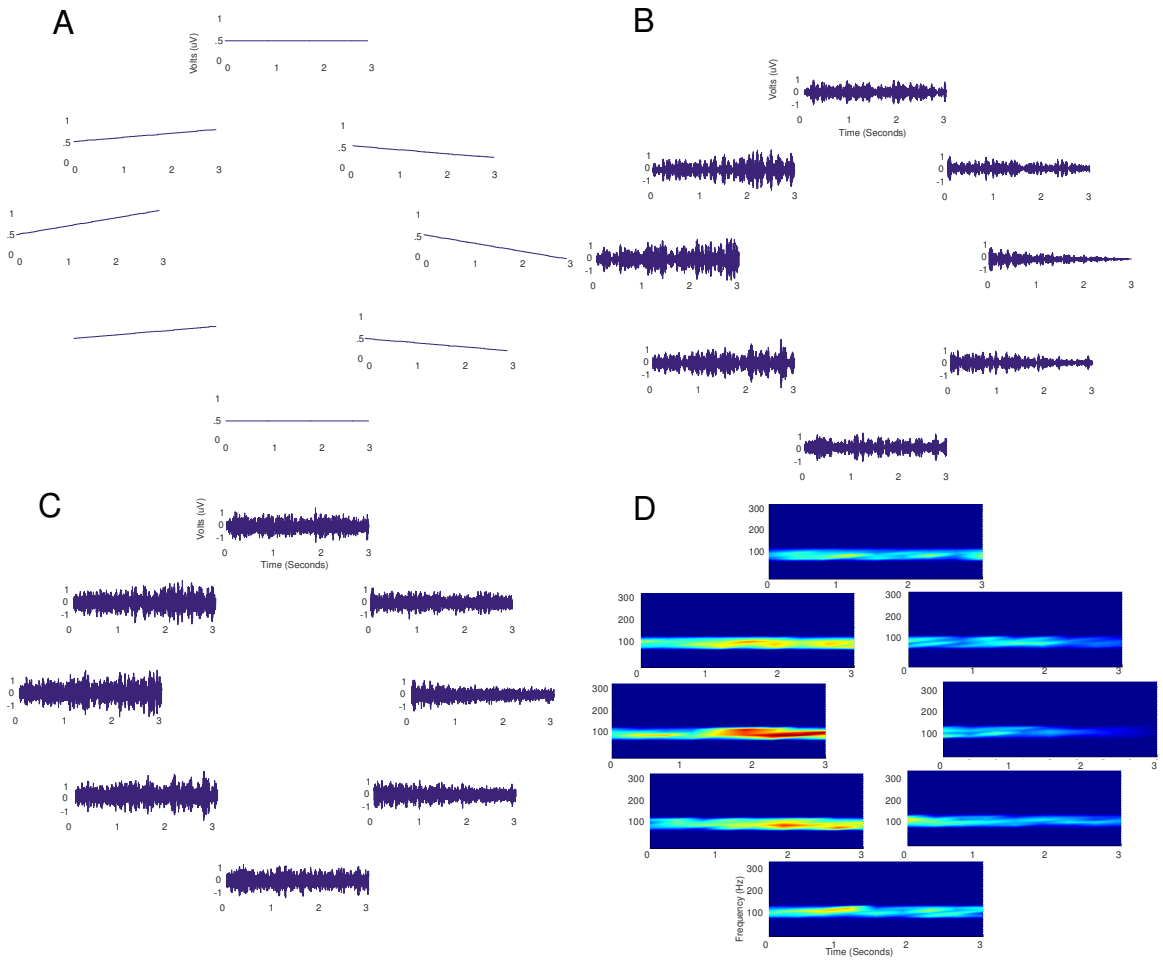

Figure 4.1.1: Position encoded sample data
Displaying different aspects to the process of encoding and eventual data. A. The position signal encoded into the simulated ECoG data. B. A sample of the traces created to form a position tuned signal, the tuning mirrors that of the encoding vectors. C. White noise is added to the traces from part B. White noise was added, in the form of a random number 20 % the magnitude of the tuning. D. Traces from part B viewed in the frequency domain, the color scale goes from 0 (blue) to 1 (red).

Velocity tuning was simulated for Center Out (Figure 4.1.2 a), as an increase during the simulated movement period for the preferred direction and a decrease for the anti-preferred direction. This cosine tuning is now related to direction and speed instead of just position. The basis for the velocity tuned signal was the expected velocity profile shown in

Figure 3.2.2. This standard velocity profile should correlate to the encoding of the actual data.

The velocity encoded spectra signal was created in the same way as the position tuned signal and is shown in Figure 4.1.2. b. The encoding of the spectra can be seen to match the tuning signal in Figure 4.1.1 a. The overall power is at its maximum when the simulated cursor is moving toward 180 degrees, indicating this is the preferred direction.

Noise was added to the velocity signal that represented 20 % of its maximum amplitude (Figure 4.1.2 c). With the addition of the noise, the tuning can still be seen in this signal and the preferred direction is still 180 degrees. The maximal and minimal power encoded in this signal and the other signals with added noise is higher than their no noise counterparts. By adding white noise to the signal, it raises the mean signal power by the mean of the noise.

A frequency domain version of the velocity encoded signal can be seen around the center tuned frequency in Figure 4.1.2 d. This figure is a spectrogram of the signal in Figure 4.1.2 b. Similar to the position encoding (Figure 4.1.1 d), this figure shows a center frequency of 90 Hz and is power encoded only in the appropriate frequency region.

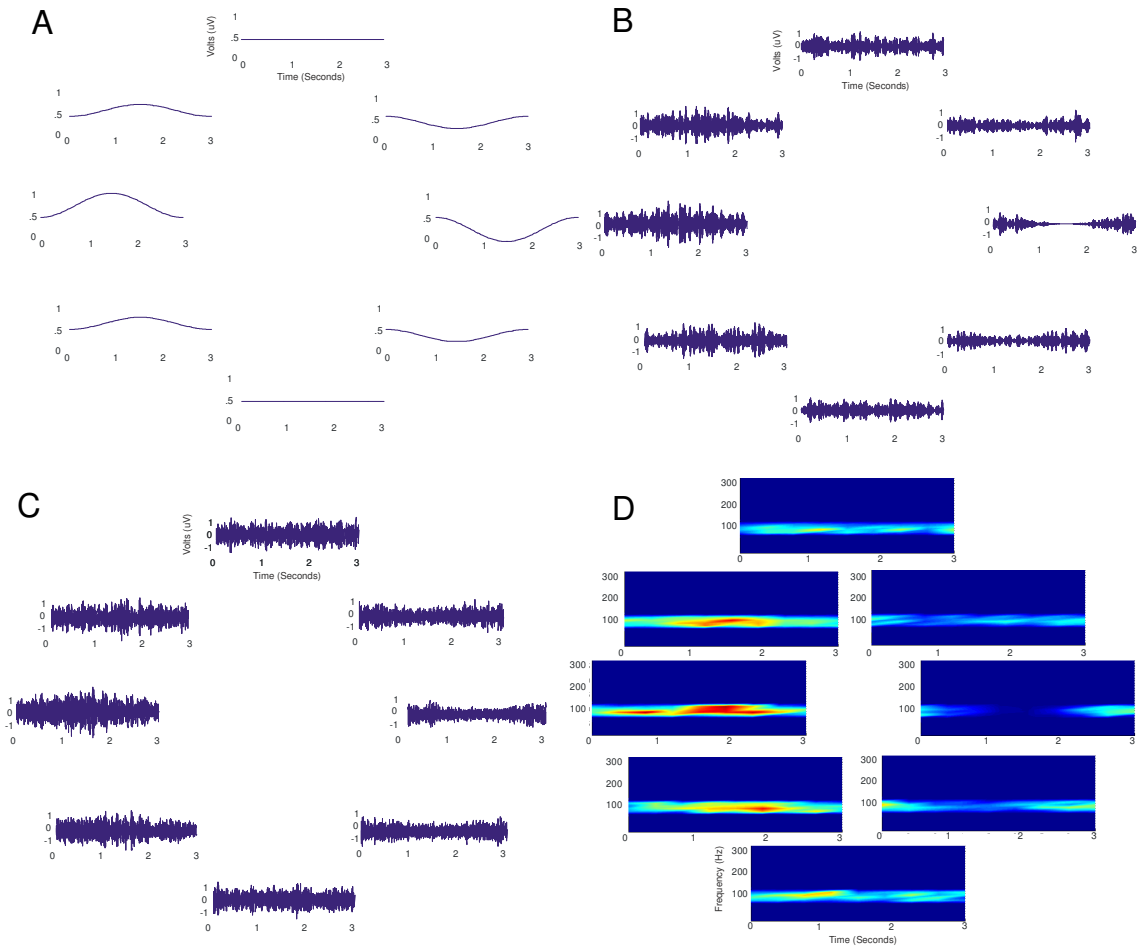

Figure 4.1.2: Velocity encoded sample data
Displaying different aspects to the process of encoding and eventual data. A. This is the amplitude that was placed into the amplitude modulation signal in order to create velocity tuned data. B. A sample of the traces created to form a velocity tuned signal, the tuning mirrors that of the encoding vectors. C. White noise is added to the traces from part B. D. Traces from part B viewed in the frequency domain, the color scale goes from 0 (blue) to 1 (red).

Amplitude or Target Encoding was only simulated for Center Out and is shown in Figure 4.1.3 a. The amplitude of the encoding increases as the simulation approaches the target regardless of the location. This encoding has no directionality, which is important

because the expected signal and corresponding analysis are decoding for a signal that has no directionality.

The amplitude encoding signal was used to modulate a spectrum as shown in Figure 4.1.3 b. This spectrum a simple ramp function is conceptually similar to the position tuning signal as it is a simple ramp function. However, there is no directionality to the tuning function or this associated spectrum. This non-directionality demonstrates the expected results when a subject has encoded for a goal.

When noise is added to these target encoded channels, the tuning is still evident (Figure 4.1.3 c). More and less noise was added to these channels in order to fine tune the analysis. A noise level of 60% of the maximum was eventually used in order to demonstrate the efficacy of the amplitude tuned signal.

This amplitude signal shows a corresponding increase only around the tuned frequency of 90 Hz, Figure 4.1.3 d. This corresponds to the tuning that was intended for this channel and shows that the spectrum is being encoded at the correct frequency.

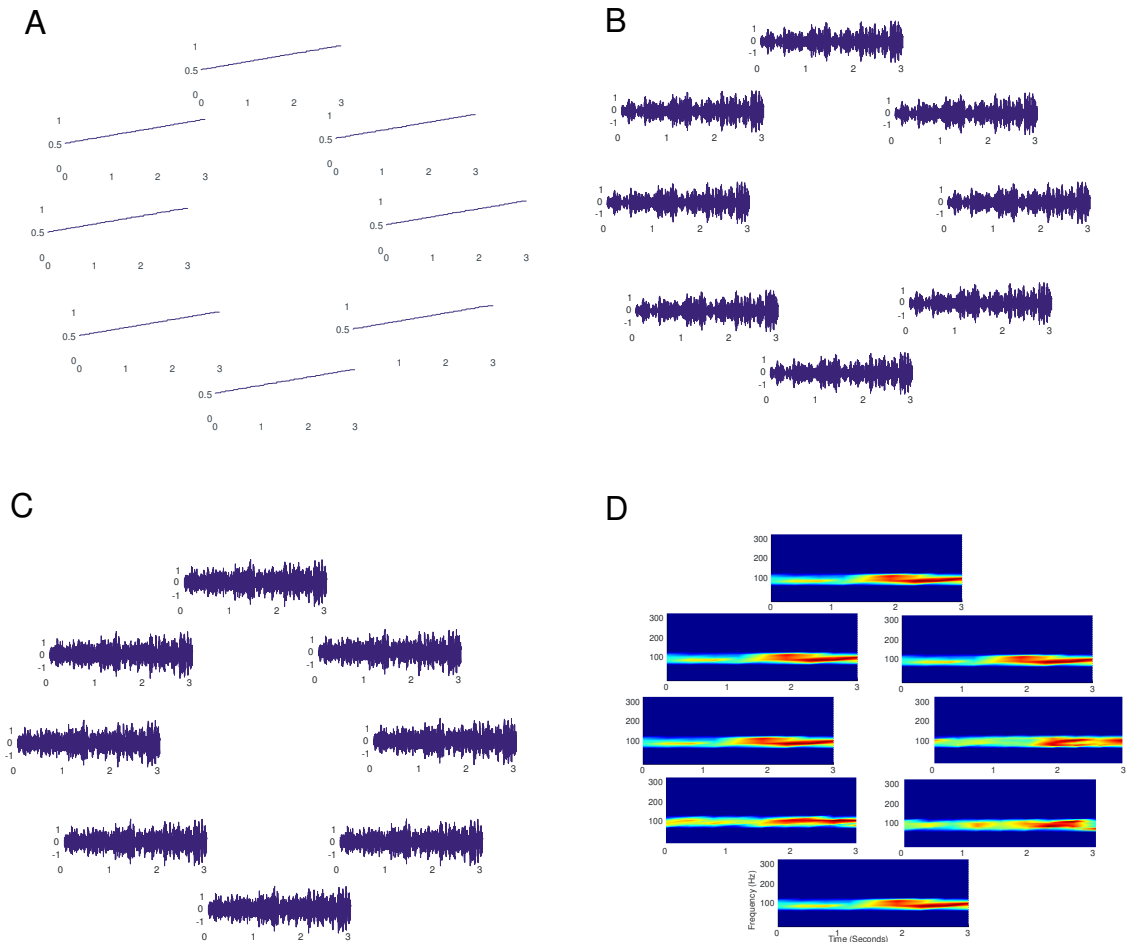

Figure 4.1.3: Amplitude encoded sample data
Displaying different aspects to the process of encoding and eventual data. A. This is the amplitude that was placed into the amplitude modulation signal in order to create amplitude tuned data. B. A sample of the traces created to form a amplitude tuned signal, the tuning mirrors that of the encoding vectors. C. White noise is added to the traces from part B. D. Traces from part B viewed in the frequency domain, the color scale goes from 0 (blue) to 1 (red).

4.1.2 Encoding of Tracing Kinematics in ECoG

A simulated Tracing ECoG signal was created for cosine tuning of position and velocity similar to the Center Out. Position and velocity time traces are 90 degrees out of phase in the simulations (Figure 4.1.5 a-b). This interplay between correlations of phase position encoding to velocity encoding was discussed earlier in Chapter three (see Figure 3.2.3).

The position and velocity kinematics of the tracing task were encoded in the same way as the center out task (Figure 4.1.4 c-d). These kinematic signals were multiplied by the modulation signal over time, then the phases were randomized, and all of the sinusoids were summed. The modulation of these signals is evident in the spectra as they mirror the tuning signal.

Noise was also added to these spectra (20% max power white noise). The corresponding noisy spectra are shown in Figure 4.1.4 e-f. They demonstrate both of the concepts discussed concerning the noisy spectra of Center Out. First, they show tuning despite the added noise. Second, they also have an increased mean due to the added white noise. The third important point these sub-figures represent is that the position and velocity remain 90 degrees out of phase.

Once the signal is moved back into the frequency domain, the 90 degree phase shift from position to velocity can be seen around the 90 Hz center (Figure 4.1.5 a-b). This figure is the spectrogram of the signals in Figures 4.14 c-d. It demonstrates the continued encoding in the expected band as well as the absence of power outside of this band.

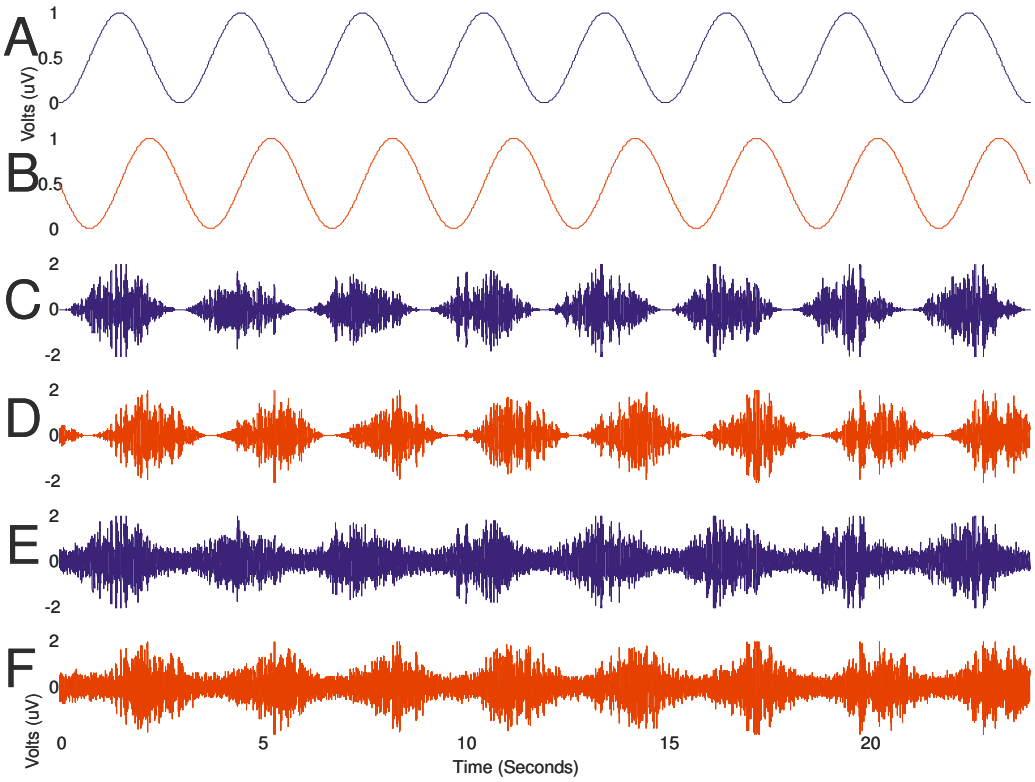

Figure 4.1.4: Position and Velocity encoded sample data
Displaying different aspects to the process of encoding and eventual data. A. This is the amplitude that was placed into the signal in order to create position tuned tracing data. B. Similarly, this is the amplitude for velocity tuned data. C-D sample of the traces created to form a position (C.) and velocity (D.) tuned signal, the tuning mirrors that of the respective encoding vectors. E-F. White noise is added to the traces from part C-D respectively.

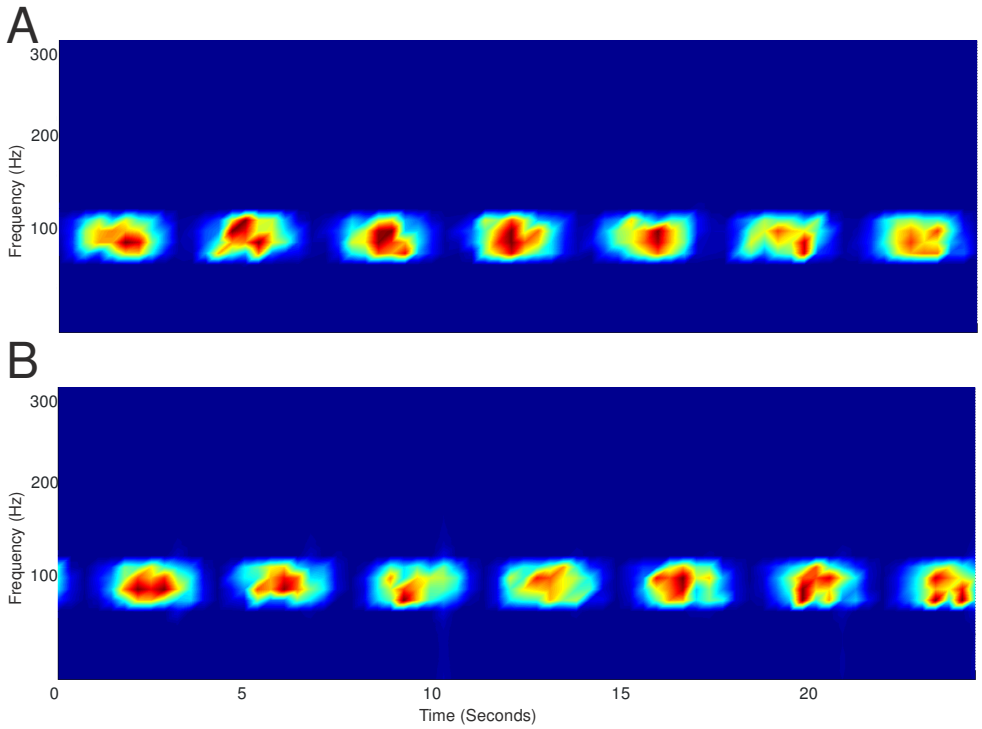

Figure 4.1.5: The spectra of position and velocity encoded sample data
A. The spectra of the position tuned signal, the amplitude changes as the sample data moves around the circumference of the circle. B. The spectra of the position tuned signal, the amplitude changes as the sample data moves around the circumference of the circle. Notice the velocity signal is 90 degrees out of phase with the position signal.

4.2 Spectral Estimation

Care in spectral estimation is important when analyzing ECoG data. Errors in the spectral estimation can be made if a technique that does not perfectly reconstruct the signal, such as the FFT, is used. In this case, the Maximum Entropy Method (MEM) was used, but it must be stressed that care was taken to ensure that the model order and windows were carefully considered and evaluated. A small change in either of these can vastly change the estimate MEM creates and alter any further analysis done using these estimated spectra.

The MEM, an autoregressive technique, was used because of its ability to fit sharp spectral periods and make estimation in short time windows (Press, Teukolsky et al. 1992). The MEM has been used for spectral estimation in both EEG and ECoG BCI (McFarland, Lefkowicz et al. 1997; Leuthardt, Schalk et al. 2004).

Two other methods were also evaluated to transform the data to the frequency domain, the Fast Fourier Transforms (FFT) and Gabor Filters. The FFT was rejected because the tasks time windows were too short to get accurate representations of the signal using the FFT, and it was necessary to use a spectral estimation technique. The Gabor filter is a spectral estimation technique that uses wavelets and varying temporal windows to create ,in general, a more accurate estimation of spectra than the MEM filter. Gabor filters were rejected based on their inability to provide a more accurate representation than the MEM filter for these experiments and analyses.

4.2.1 Bandwidth, Bandsize, and Window length

The MEM requires a bandwidth, bandsize, length of data, and a model order. Bandwidth is the overall frequency range used in analysis, the bandsize is the size of each individual feature, and each channel had a bandwidth of .5-280.5 Hz and a bandsize of 5 Hz.

These parameters are decided by the programmer and have to be determined prior to analysis either qualitatively or quantitatively. Quantitative methods were used herein wherever possible and qualitative methods were used when appropriate. Bandwidth was determined by experimental filter setting and amplifier performance, bandsize was chosen qualitatively, window length was quantitatively by experimental restrictions, and model order was chosen based on previous work (Anderson, Wisneski et al. 2009).

The estimation range was chosen to be between 0.5-280.5 Hz, due to a combination of factors. A lower range of 0.5 was chosen based on the filter settings during data collection; the original filter setting was chosen qualitatively, to facilitate fast and accurate measurements in the hospital room. The upper limit of 280.5 Hz was chosen based on the signal-to-noise ratio, at higher frequencies. The bandwidth also had to be an even multiple of the bandsize 5 Hz, 280.5 Hz allowed an even multiple. The amplifier performance above 290 Hz was poor, due to the lower powers that are expressed at these higher frequencies in the brain. As such it would not be possible to view a spectral change in the range above 290 Hz with any certainty.

Bandsizes from 1 Hz to 50 Hz were tested and 5 Hz was settled on qualitatively. It was originally expected that lower frequencies would perform better at lower bandsizes and higher frequencies would perform better at high bandsizes due to the nature of spectral estimation. However, upon further analysis and experience with the data it was found that 5 Hz did a good job and lower bandsizes did not increase accuracy.

A window length of 200 ms was chosen because it allowed for multiple samples to be taken for each trial even during the delay periods. The smallest delay periods were 300 ms and thus a window was needed that was shorter than this time period in order to create an accurate spectral estimate. 200 ms was chosen in combination with 20 ms stepping in a

sliding window technique because it allowed for the largest windows while still allowing for multiple samples per trial. The multiple samples created from this slidng window technique were averaged to help create a better estimation of the spectra present during that time period.

Averaging multiple samples is a common trade off used to reduce noise while preserving the desired signals. Multiple sample averaging may allow for a more accurate representation of the spectra by eliminating white noise, but it may also be reducing activations that are correlated to our stimulus. The activations at higher frequencies appear to exist for very short time windows on the order of tens of milliseconds. These short time period activations will be averaged out if long samples are taken or if windows are averaged together. The time periods in this analysis were long which was desired to show the robustness of these results, so this trade off was accepted, but should be noted.

4.2.2 MEM filter and model order

Autoregressive techniques and specifically the MEM have been analyzed for efficacy with use in EEG and ECoG (Anderson, Stolz et al. 1998; Anderson, Wisneski et al. 2009). Anderson et al found that a filter order of about 30 was ideal on data given a frequency band from 0-500 hz and no filtering. This was the filter order that we originally used to create an estimate of spectra for these experiments until a comb filter was applied to the data (Krusienski 2008; Anderson, Wisneski et al. 2009). A comb filter, is a series of notch filters that eliminate not only 60 Hz but also it's harmonics (120 Hz, 180 Hz, etc), or other narrow band noise.

Filtering data causes a large decrease in the number of weights the MEM filter needs to create an accurate representation of the spectra (Krusienski 2008). A band stop filter was applied to the recorded data at 60 Hz and it's harmonics that interfered with proper spectral estimation. In this case it was found that 20 weights worked to create an accurate representation of the spectra, once the comb filter was applied. This number of weights seemed to create an accurate representation when compared to previous work.

4.3 Analysis for Cosine tuning

4.3.1 Determination of Position, Direction, Velocity, and Speed

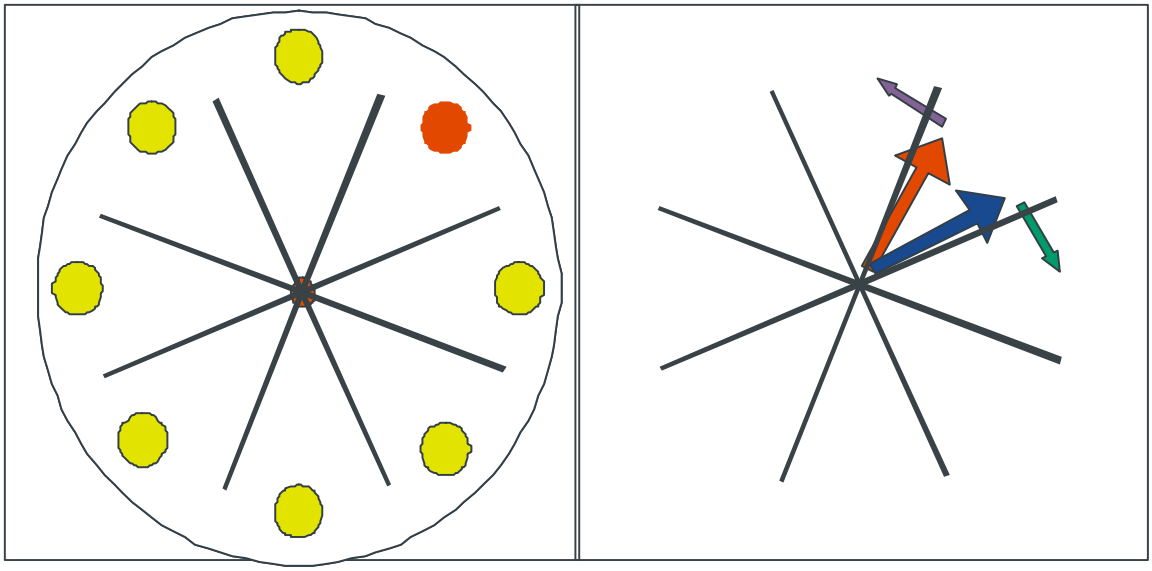

Figure 4.3.1: Dividing the tasks up into octants.
The center out task was broken up into octants by its 8 targets. There were only 8 targets so the maximum level of precision for tuning would be 1/8 of 360 degrees. Similarly the tracing task was broken down into octants so that the two tasks could be more properly compared. The data was first broken down based on rotations around the circle making each rotation on trial; each octant was then averaged for the tracing task so that one mean position and velocity were found within each octant. In this way there were than 8 samples for each rotation the subject accomplished.

In the Center Out task the position was taken as the mean position during the hold period for that trial, shown in Equation 4.3.1-2. There is minimal movement during the hold periods so these numbers should be consistent from trial to trial. Position for the

whole movement and mean paths can be seen for Center Out and Tracing in Figure 5.2.1. After a mean position was found for each trial, the positions were normalized by the maximum magnitude x and y position, respectively, (Equations 4.3.5-6). Normalization was used on all of the kinematics in order to normalize them to vary between -1 and 1. The normalization of ECoG data and kinematics is important, because when regressed (Equations 4.3.) normalized variables produce weights that can be directly compared across different encoding schemes.

The Tracing task analysis and samples were matched as closely as possible to Center Out task. The Tracing task was divided up into eight octants (Figure 4.3.1) in order to facilitate ease of analysis as well as cross task comparisons. Each time there was a change in direction the trial number was incremented. The mean of each octant in each trial was taken as one sample, Equations 4.3.1-2. This would give 8 samples for each trial, one for each octant. These samples were then normalized in the same fashion as Center Out, Equations 4.3.3-4.

$$\bar{x}_t = \frac{\sum_{n=1}^{N} x_n}{N} \quad \textbf{(4.3.1)}$$

$$\bar{y}_t = \frac{\sum_{n=1}^{N} y_n}{N} \quad \textbf{(4.3.2)}$$

$$\bar{x} = \frac{[\bar{x}_{t1}, \bar{x}_{t2} .... \bar{x}_{tN}]}{\max(|[\bar{x}_{t1}, \bar{x}_{t2} .... \bar{x}_{tN}]|)} \quad \textbf{(4.3.3)}$$

$$\bar{y} = \frac{[\bar{y}_{t1}, \bar{y}_{t2} .... \bar{y}_{tN}]}{\max(|[\bar{y}_{t1}, \bar{y}_{t2} .... \bar{y}_{tN}]|)} \quad \textbf{(4.3.4)}$$

In equations 4.3.1-4.3.4 x and y are the associated position of the cursor on the screen. x was the horizontal component of position and y was the vertical component of position.

Many of *x* and *y* measurements are taken over the period of one trial and are averaged into the variables $\bar{y}_t$ and $\bar{x}_t$ giving one measurement per trial. These measurements were then normalized by the maximum of all trials to create the normalized vectors of positions $\bar{x}$ and $\bar{y}$.

Velocity for Center Out task was taken from the average for a whole movement, and then transformed similar to position. The mean velocities and velocity at each position for actual data can be seen in Figure 5.2.2. Each trial had many velocities which were then averaged using Equations 4.3.5-6, this average would results in one sample per trial. This vector of average velocities was then normalized by the maximum velocity, shown in Equations 4.3.7-8. The un-normalized velocities were also used to find the speed component and direction using later transformations.

Velocity for the Tracing task was found in much the same was as position, for Tracing. To begin with the Tracing task was once again divided into octants. After dividing into octants a mean velocity was taken from each octant for each trial. Trials were defined by changes in direction, just as they were for defining position. Finally, the velocities were normalized by the maximum absolute velocity to give normalized samples of velocity. In addition to this measurement of velocity, the raw velocity values for Center Out and Tracing were used to calculate speed and direction.

$$\bar{\dot{x}}_t = \frac{\sum_{n=1}^{N} \dot{x}_n}{N} \qquad \textbf{(4.3.5)}$$

$$\bar{\dot{y}}_t = \frac{\sum_{n=1}^{N} \dot{y}_n}{N} \qquad \textbf{(4.3.6)}$$

$$\bar{\dot{x}} = \frac{\left[\bar{\dot{x}}_{t1}, \bar{\dot{x}}_{t2} .... \bar{\dot{x}}_{tN}\right]}{\max(\left|\left[\bar{\dot{x}}_{t1}, \bar{\dot{x}}_{t2} .... \bar{\dot{x}}_{tN}\right]\right|)} \quad \textbf{(4.3.7)}$$

$$\bar{\dot{y}} = \frac{\left[\bar{\dot{y}}_{t1}, \bar{\dot{y}}_{t2} .... \bar{\dot{y}}_{tN}\right]}{\max(\left|\left[\bar{\dot{y}}_{t1}, \bar{\dot{y}}_{t2} .... \bar{\dot{y}}_{tN}\right]\right|)} \quad \textbf{(4.3.8)}$$

Equations 4.3.5-4.3.8 are the velocity equivalent of the earlier equations for position; $\dot{x}$ and $\dot{y}$ are the associated velocity of the cursor on the screen. $\dot{x}$ was the horizontal component of velocity and $\dot{y}$ was the vertical component of velocity. Many of $\dot{x}$ and $\dot{y}$ velocity measurements are taken over the period of one trial and are averaged into the variables $\bar{\dot{y}}_t$ and $\bar{\dot{x}}_t$ giving one measurement per trial. These measurements were then normalized by the maximum of all trials to create the normalized vectors of velocity $\bar{\dot{x}}$ and $\bar{\dot{y}}$.

Speed was derived from the velocity components by taking their magnitudes. The raw velocities magnitudes were taken prior to normalization, Equation 4.3.9. The speeds were then normalized in the same fashion as position and velocity, Equation 4.3.10. The speed was found this way for both Center Out and Tracing tasks. The raw speeds were also used to find the direction kinematics.

$$\bar{s}_t = \sqrt{\bar{\dot{x}}_t^{\,2} + \bar{\dot{y}}_t^{\,2}} \quad \textbf{(4.3.9)}$$

$$\bar{s} = \frac{\left[\bar{s}_{t1}, \bar{s}_{t2} .... \bar{s}_{tN}\right]}{\max(\left|\left[\bar{s}_{t1}, \bar{s}_{t2} .... \bar{s}_{tN}\right]\right|)} \quad \textbf{(4.3.10)}$$

Speed was determined from the velocity components on a trial by trial basis. The speed, $\bar{s}_t$, of each trial was found by squaring each component from Equation 4.3.5-4.3.6 then summing them and taking the square root. From here the speed data across all trials is normalized into the vector $\bar{s}$ by dividing by the maximum speed.

Direction was also derived from velocity, by removing the speed. For each trial the x velocity and the y velocity were both divided by the speed giving a unit vector for direction, Equations 4.3.11-12. Transformation to a unit vector is an inherent normalization so no further normalization was needed. This was done both for Center Out and Tracing.

$$\bar{\dot{x}}_d = \frac{\left[\bar{\dot{x}}_{t1}, \bar{\dot{x}}_{t2} .... \bar{\dot{x}}_{tN}\right]}{\left[\bar{s}_{t1}, \bar{s}_{t2} .... \bar{s}_{tN}\right]} \quad \textbf{(4.3.11)}$$

$$\bar{\dot{y}}_d = \frac{\left[\bar{\dot{y}}_{t1}, \bar{\dot{y}}_{t2} .... \bar{\dot{y}}_{tN}\right]}{\left[\bar{s}_{t1}, \bar{s}_{t2} .... \bar{s}_{tN}\right]} \quad \textbf{(4.3.12)}$$

Direction is found by making each trial a unit vector. The un-normalized velocity of each trial is taken from Equations 4.3.5 and 4.3.6, listed as $\bar{\dot{x}}_{tN}$ and $\bar{\dot{y}}_{tN}$. The speed is taken from Equation 4.3.9 and is listed as $\bar{s}_{tN}$. For each trial the horizontal and vertical velocities are normalized by the magnitude to create normalized unit vectors in the direction of the velocity.

4.3.2 Model and Regression

The different movement parameters, (e.g. position) can be decoded in the simulated channels in which they were encoded. Cosine tuning has been done historically with both single units and LFPs (Georgopoulos, Kalaska et al. 1982; Heldman, Wang et al. 2006; Heldman 2007; Wang, Chan et al. 2007). In the simulated data discussed before and in the channels with the most significant tuning this can be seen just by categorizing the data by direction, position, or speed. In this case an individual channel and frequency bin (feature) is binned according to either position or direction to view the tuning of the raw data, Figure 4.3.2-3. To quantify the tuning of each feature, a regression to a model of the kinematics is

done for each movement parameter. These models are listed as equations 4.3.13-17 and are present for position, direction, speed, and velocity respectively.

$$\overline{P}=B_0+B_{p,x}\overline{x}+B_{p,y}\overline{y} \quad \textbf{(4.3.13)}$$

$$\overline{P} = B_0 + B_{d,x}\overline{\dot{x}}_d + B_{d,y}\overline{\dot{y}}_d \quad \textbf{(4.3.14)}$$

$$\overline{P}=B_0+B_s\overline{\dot{s}} \quad \textbf{(4.3.15)}$$

$$\overline{P}=B_0+B_{v,x}\overline{\dot{x}}+B_{v,y}\overline{\dot{y}} \quad \textbf{(4.3.16)}$$

For Equation 4.3.13-17 the variable $\overline{P}$ is the average spectral amplitude in a given frequency band and $\overline{x}$ and $\overline{y}$ are the mean cursor positions for that period. $\overline{P}$ is found by taking the percent deviation from baseline before it is entered in the equation. Similarly the movement kinematics are standardized as percentages of the maximum in order to normalize the data.

Equation 4.3.13 is a model for position and fits the signal to the mean position of the cursor for each sample. Similarly for Equation 4.3.14 the variable $\overline{P}$ is the same as in 4.3.13 but the $\overline{\dot{x}}_d$ and $\overline{\dot{y}}_d$ are the mean direction the cursor is moving. Equation 4.3.15 is setup for speed tuning and only has one component. By combining speed and direction Equation 4.3.16 models velocity, the two vectors $\overline{\dot{x}}$ and $\overline{\dot{y}}$ are the corresponding velocities of cursor movement.

The models use the average spectral amplitude as the dependent variables and the movement kinematics of position, direction, speed, and velocity as independent data, the weights or regression coefficients are represented by the *B* variables in the above equations. Each equation has a B_0 variable which corresponds to the cortical activity unrelated to movement kinematics. In addition there is a *B* value for each movement kinematic variable

fit to the equation. For example position has $B_{p:x}$ and $B_{p:y}$ in addition to the B_0 component, similarly direction has $B_{d:0,x,y,z}$, speed has $B_{s:0,s}$, and velocity has $B_{v:0,x,y,z}$. $B_{p:x}$ and $B_{p:y}$ together are the preferred gradient of a given feature. The magnitudes of the positional or directional B values are defined as the Depth of Modulation (DOM), shown in Equation 4.3.17. Features were statistically significant if their fit to the model had a corresponding p value of below 0.05 and a depth of modulation of greater then 0.05 (Heldman 2007).

$$DOM = \sqrt{B_{p,x}{}^2 + B_{p,y}{}^2} \quad \textbf{(4.3.17)}$$

4.3.3 Center Out

The Center Out task was broken down into three distinct periods which were analyzed separately; delay, movement, and holding. The kinematics and spectral data for these periods was averaged for each trial and then regressed to the models discussed in Equations 4.3.13-17. The mean amplitude of the period before target encoding (Baseline Period) of all trials was used to find the deviation from the mean for the other periods (Delay, Movement, and Holding). This was an ideal situation as there could be no task relevant tuning previous to the display of the target as the subject would have no knowledge of which target was going to be the goal target.

The movement and hold periods were analyzed separately, because the use of both periods separately allowed for some dissociation of kinematics. The Movement period was regressed to direction, speed, and velocity. The Hold period was regressed to position since it allowed for some dissociation of the position components from the direction and velocity components. Results on the simulated data are shown in Figure 4.3.3 where position and velocity data show the expected results and noise shows nothing significant.

The Delay period (post target introduction but prior to movement onset) was of particular interest as it had been designed to look at movement intention. This Delay period

was regressed to the direction, speed, velocity, or position of the following movement and also following hold period. This allowed for some measurement of intention and a quantification of which parameters were encoded in this time period and how they changed across time periods. It also allowed for a comparison across Delay and Movement periods in order to show which kinematic parameters remained constant from intention through movement.

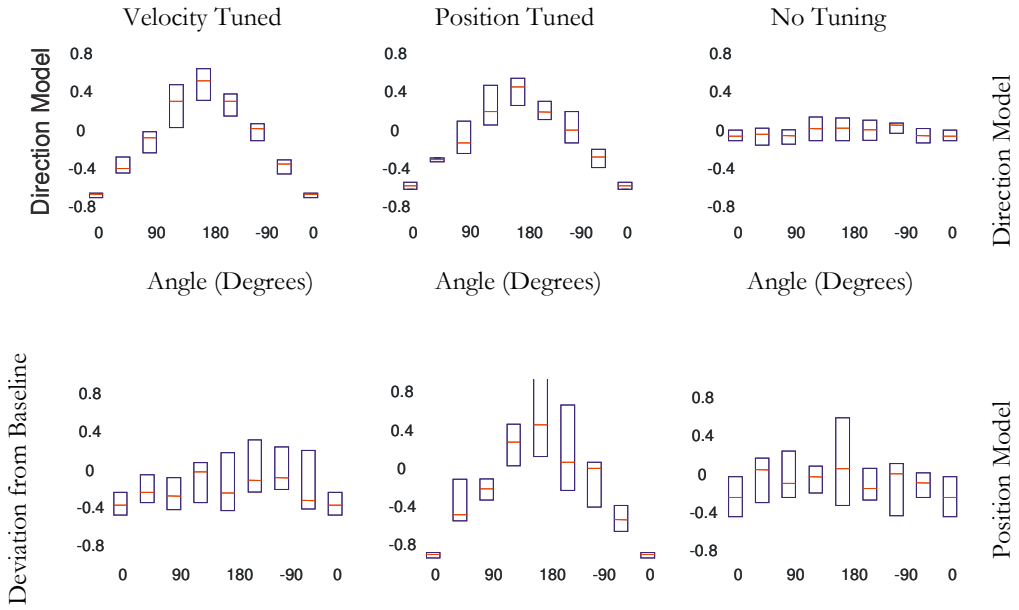

Figure 4.3.2: Center out results
Results for two models on three simulated channels. A frequency band of 75-105 Hz was used, the tuned band for the simulated data. The red line indicates the mean and blue boxes indicate 25th and 75th percentiles of data. It is important to note that the direction model shows positive results for velocity tuning and position tuning, but the position model only does for position encoding.

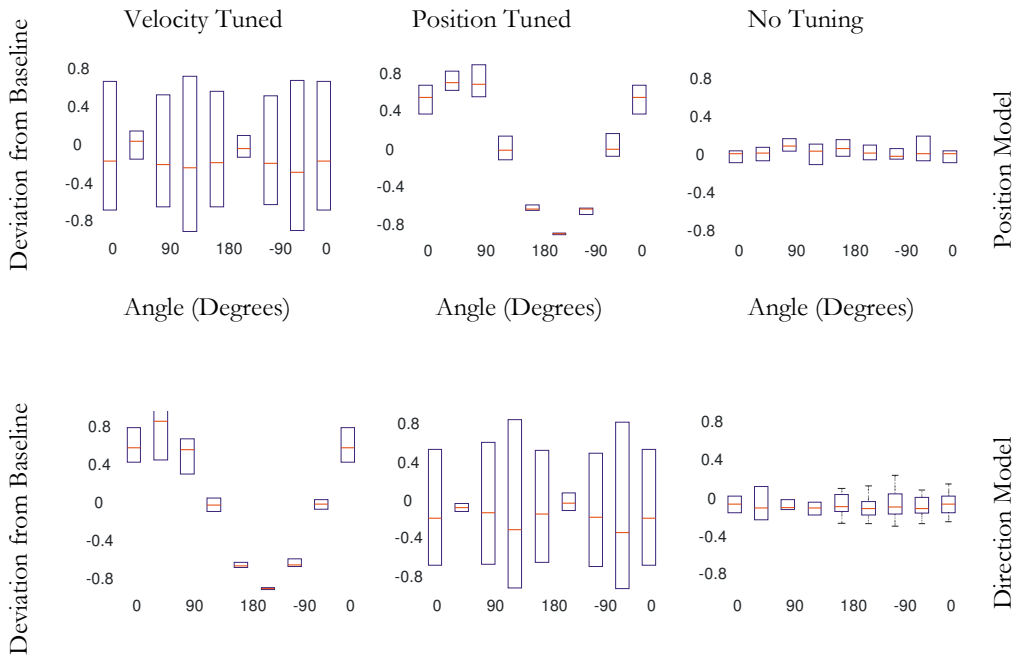

Figure 4.3.3: Tracing results for position and directional tuning.
In this case the orthogonality of the kinematics allows the dissociation of the two components. Due to this orthogonality the position model only shows position tuning and the direction model only shows direction tuning.

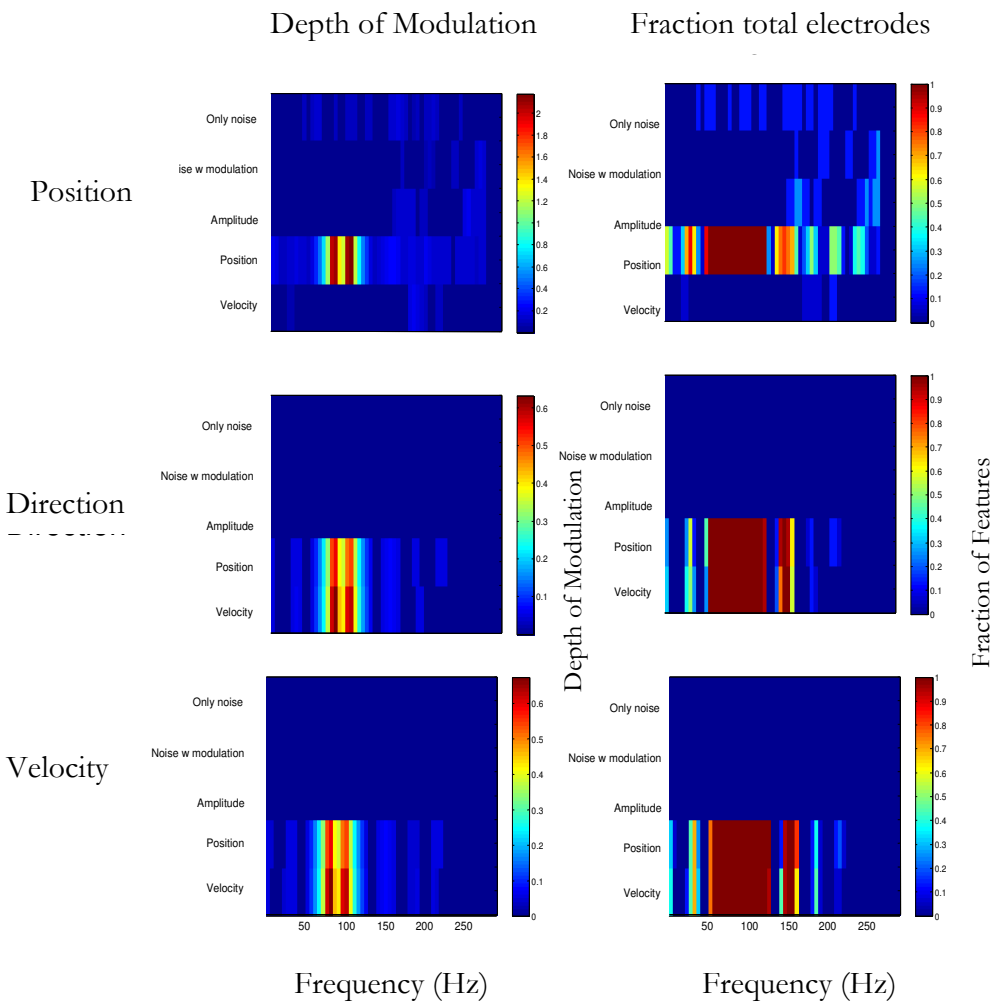

Figure 4.3.4: Analysis of simulated position, direction, and velocity
Encoding results in Center Out task. The position decoding only shows significant results for the position encoding on the left and it shows this in 100 percent of the electrodes, shown on the right. However, the Direction and velocity results yielded significant results for both position and direction tuning which can be seen in the left and right columns. These overall results were expected based on the tuning that was simulated and the analysis, in addition this correlates to the data shown in Figure 4.3.1of an individual channel.

4.3.4 Tracing

Tracing was first divided into 8 octants that mirrored the 8 targets shown in Center Out, shown in Figure 4.3.1. These octants were then analyzed as separate movements. This lent itself well to both creating a simple analysis that could take advantage of the experimental design containing multiple directions and radii, and comparing the tuning vectors across both tasks.

A baseline used to normalize the data similar to Center Out. However, no delay periods were present in this task so the baseline that was used for comparison was the mean of all trials (in all octants). This baseline was based on all of the data used for each feature and was not based on a trial by trial analysis.

Position, direction, and velocity were dissociated into separate components more easily in this task by virtue of the orthogonal nature of the task. Speed was easily dissociated as it is directionless and had little bearing on the position of the cursor (per Equation 4.3.9). Position tuning was found by a regression of the spectral features to the mean position of that octant for that trial. Similarly, velocity was regressed to the mean velocity of that octant for that trial. Direction was found by making all velocities unit vectors based on speed (Equations 4.3.11-12).

Using this method position, velocity, and direction could be correlated for an individual trial but they would not be correlated for all the combined trials, due to the reversal of directions. Data was simulated that performed the tracing perfectly (constant angular velocities and radius), and corresponding results of the analysis on simulated data can be seen in Figure 4.3.5. In this figure it can be seen that position has been successfully dissociated from velocity and direction in the simulated data and ensuing analysis.

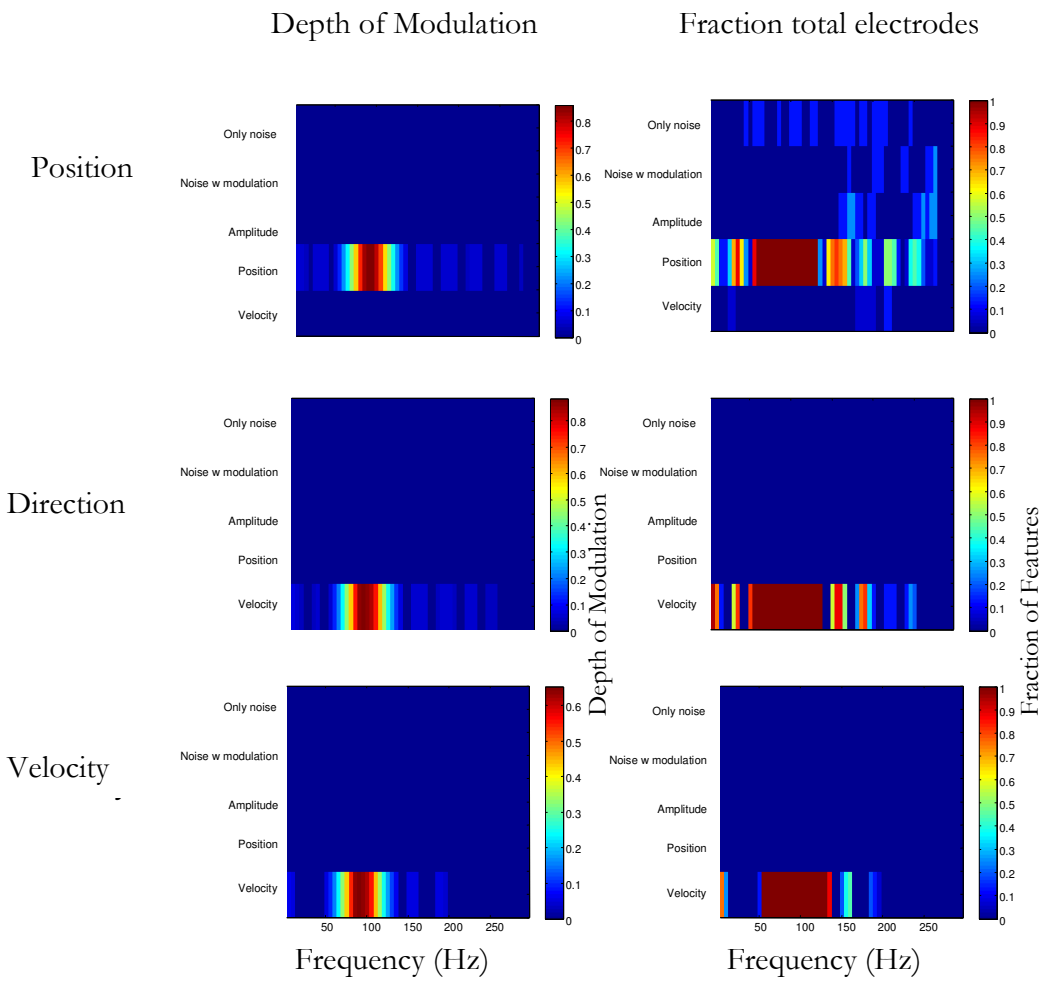

Figure 4.3.5: Tracing analysis of position and velocity.
Position and Direction/Velocity components have been successfully dissociated. Only the position encoded electrodes showed significant results for position model and similarly only velocity encoded electrodes showed significant results for direction/velocity model.

4.3.5 Comparison

The tuning vectors for features that were statistically significant by the given criteria across multiple different tasks Delay to Movement and Holding of Center Out, and also Movement and Holding of Center Out to Tracing were compared. These tuning vectors were compared by finding the angle between them, using Equation 4.3.18, the results from

the simulated data are shown in Figure 4.3.6. In Equation 4.3.18 variables *v1* and v*2* correspond to the vectors in two conditions, the equation finds *Theta* which is the angle between the two vectors. These angles were then histogrammed in octants in an effort to keep the level of discriminibility constant for comparison purposes. These binned results of tuned data can be compared to the same analysis done on random data to show that there is a consistency to the tuning, which was purposefully entered into the simulated data for testing purposes. If the angle between the two vectors was less than 45 degrees the two vectors were said to have similar tuning.

$$Theta = \arccos\left(\frac{v1 \circ v2}{|v1||v2|}\right) \quad \textbf{(4.3.18)}$$

Similarly these comparisons were made across different electrodes as a function of simulated distance. Distances were simulated for two and three dimensional coordinates. In terms of the simulated data only the surface coordinates were used as no third coordinate was entered, simulated (results shown in Figure 4.3.7). The angles between the vectors were found using Equation 4.3.18 and the mean was taken for each frequency and distance that had at least 5 comparisons in the actual data. This was done for comparisons between two statistically significant vectors and two non-statistically significant vectors.

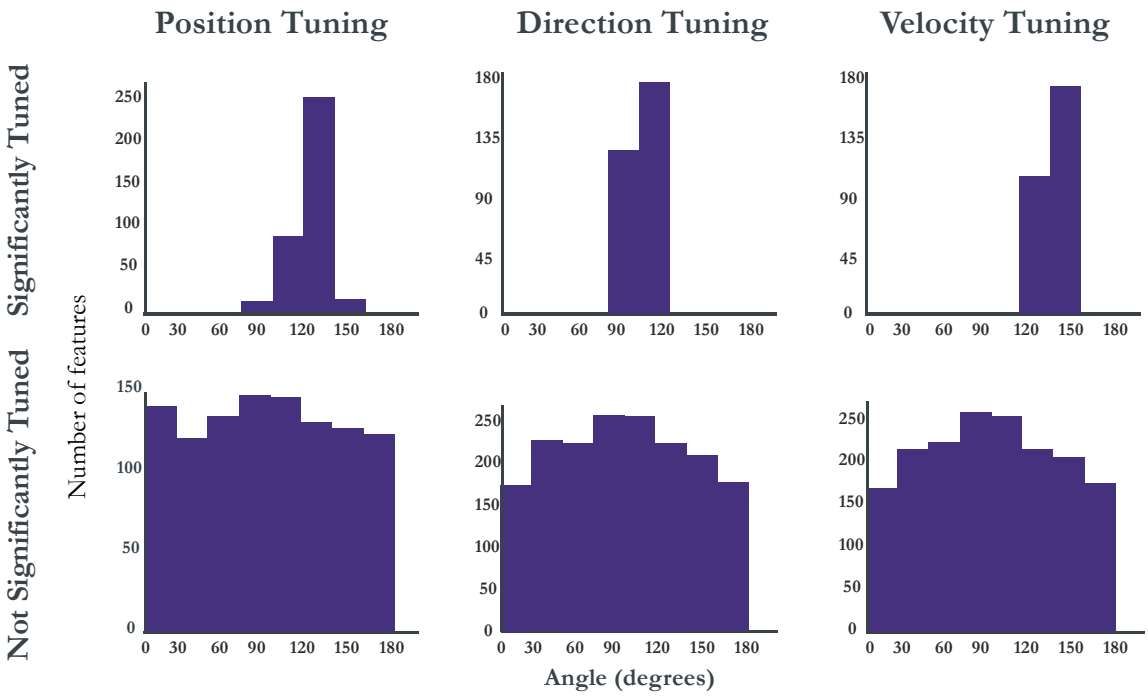

Figure 4.3.6: Position, Direction and Velocity simulated comparisons
Comparisons of tuning vectors across Center Out and Tracing tasks with the simulated data. The tuned data were simulated so that the vectors would be significantly tuned in the 90-150 Hz range. This clustering on the top row can be seen in comparison to the overall uniformity in the non tuned data on the bottom row. These results can be compared to figure 4.3.1-2 where the data for position and direction for Center Out are greatly out phase with that for Tracing.

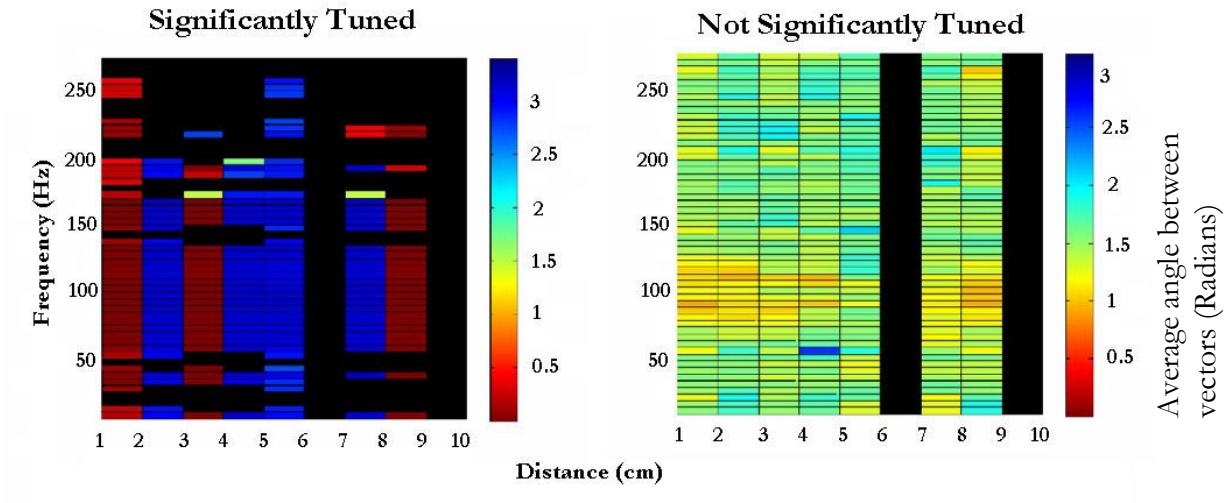

Figure 4.3.7: Distance tuning
Tuning of both Center Out and Tracing on simulated data. This is a measure of the difference between two vectors at some distance for position, velocity, or direction tuning. These vectors were setup on the tuned data to be in bands where they would either be at 0 degrees or 180 degrees. This is in respect to the un-tuned noise data on the right which shows all of its results to be averaging out to 90 degrees.

4.4 Analysis for Dorsolateral Prefrontal Cortex (DLPFC) encoding

The analysis for the target encoding in the DLPFC can be broken down into two categories, amplitude modulation and directional modulation. The amplitude modulation is a change in signal when the subject encodes any target. The directional modulation is expected to be a change in the signal that correlates to the position of the eventual target or direction the target is in from the current position. These are the two types of encoding that have been found in the DLPFC in previous studies using single units (Iba and Sawaguchi 2003; Funahashi, Takeda et al. 2004; Tsujimoto, Genovesio et al. 2008). It is unknown if these signals will be present in ECoG due to its difference from previous modalities.

4.4.1 Amplitude Encoding

Amplitude encoding determines whether there is a statistically significant change in magnitude over many trials on a given feature. This was determined by application of a standard *T*-test. To change this comparison to a trial-by-trial basis one condition was subtracted from another condition for each trial, to create a new Combined Distribution. This Combined Distribution was then subjected to a *lillie*-test to make sure that it was reasonably Gaussian (Conover 1980). After Gaussian distribution was assured, a *T*-test was performed on the Combined Distribution to test whether it was statistically different from zero ($p<0.05$).

Combined Distributions were found for each combination of conditions, Baseline, Delay, and Holding. If the *p* value for the *T*-test was less than 0.05, that feature was considered statistically significant; this is shown on the simulated data in Figure 4.4.1. In Figure 4.4.1 the simulated data shows tuning for amplitude encoding but no tuning for position or velocity encoding. The only portion that shows statistical significance is the amplitude encoded channel in the 30 Hz band centered around 90 Hz.

The absolute amplitude was also analyzed in order to qualitatively determine if there was a decrease or an increase in the amplitude across each period; this is shown for the simulated data in Figure 4.4.2. The percent deviation from the mean of all conditions is color scaled and shows the difference in the mean on a trial by trial basis. A mean of all conditions was used in this case since it can be used to see the change across all conditions including baseline and no increase in tuning is shown because of the relative change of baseline.

Temporal dynamics of the amplitude tuning were displayed for qualitative viewing; the simulated results for this are shown in Figure 4.4.2. A gradual increase across the

conditions can be seen in Figure 4.4.2 which is the same result that can be seen in Figure 4.1.3 when the amplitude encoding data was created. This correlation to the spectrogram is what should be seen given the analysis. It is worth noting that there is more smearing over frequency in 4.4.2 than 4.1.3. This is due to the spectral estimation that was used for 4.4.2 whereas 4.1.3 was a direct transformation (FFT).

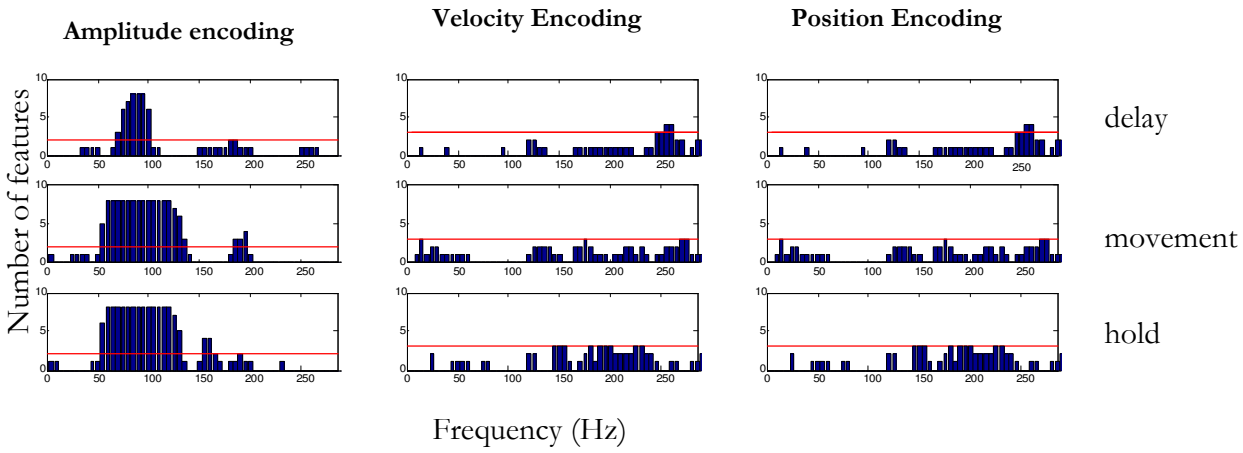

Figure 4.4.1: Amplitude decoding of simulated data.
Every channel within the encoded range showed up as being statistically significant. Velocity and position encoded channels showed no statistical significance when analyzed using an amplitude model.

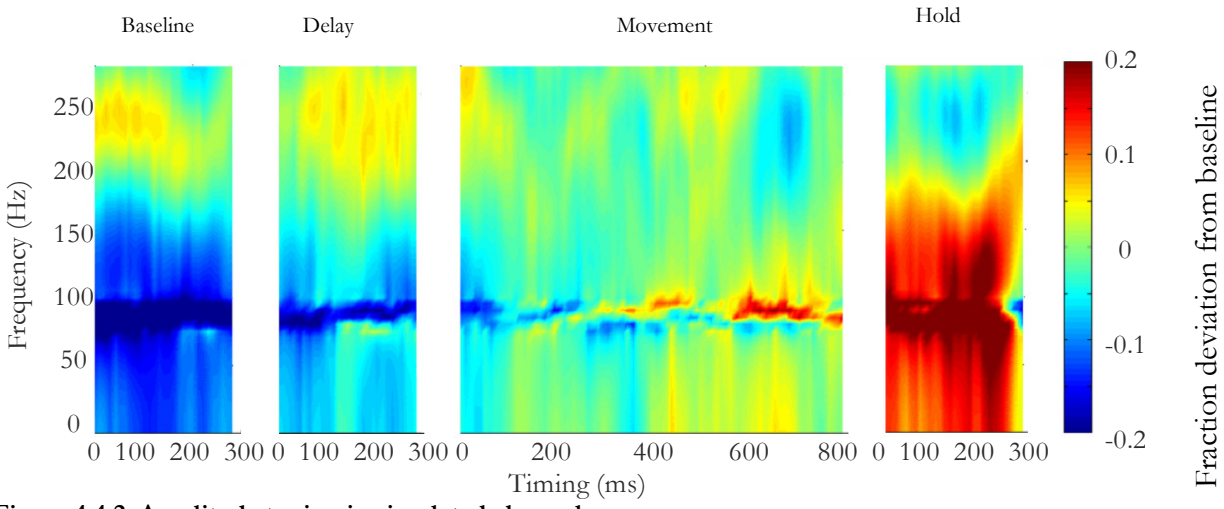

Figure 4.4.2: Amplitude tuning in simulated channels.
A gradual increase can be seen as the subject approaches any target. All targets were averaged for this figure.

4.4.2 Positional and Directional Encoding

Positional and Directional Encoding were not analyzed on a trial by trial basis, but rather used a baseline from the entire task period. The models that were used herein are Equations 4.3.1-2. For position, all three relevant time periods were compared to the eventual position of the goal target. For direction, the delay and movement period were compared to the direction the subject was moving in. In this case the criteria for being statistically significant were a p value less than 0.05 (no depth of modulation test was applied) and the position tuning is shown on the simulated data in Figure 4.4.3.

In this case the spectra from Delay, Movement, and Holding were normalized by the Baseline value for all trials. Baseline was used as normalization here as it did not contain any directional tuning so it would not insert any directional bias into the data. If a mean of all conditions was used as it was for amplitude tuning it could have inserted additional direction or positional information that was not in fact present.

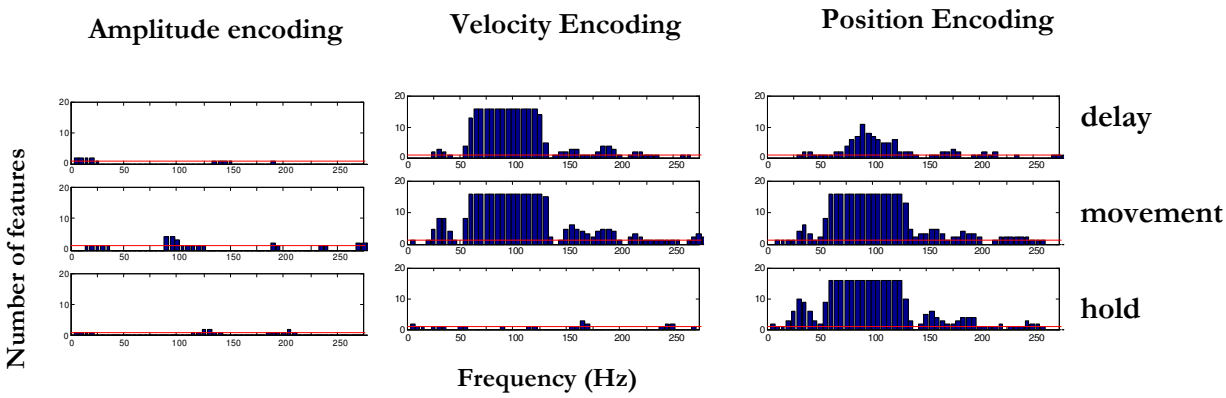

Figure 4.4.3: Decoding of simulated data.
Velocity and Position models show appropriate tuning. It is important to note that the hold period of velocity model encoding is flat because there is no movement. Amplitude encoding shows no position decoding that is statistically significant.

4.4.3 Decision Tree Analysis in the DLPFC

Decision trees are a data mining technique that uses a simple discriminibility test; an example decision tree is shown in Figure 4.4.4. A decision tree analysis takes a set of data and trains the tree. It does this by building a set of nodes by looking for features that best correspond to being on a target vs not being on a target. It creates the first node based on the feature which seemingly does the best job of separating being on a target vs not being on a target; separating the data into two groups. There continues to be some cases in each group; that is, on target and not on target are still mixed. This process is then continued through the lower nodes, dividing into smaller and smaller groups until all on target and not on target data is separate from each other.

When simulated data were tested the reasons for decision trees lack of discrimination became more obvious, results shown in Table 4.4.1. The first test on target tuned data showed good efficacy at 92% and the percentage on the test data was 100% correct so the tree is being formed correctly. The problem arises once position or velocity tuned data are

introduced. These data seem to create systematic noise as is evident by the decrease from row one to row two of Table 4.4.1.

When fitting the decision trees on all of the data it contained both data fitted for this test and confounding encoding. With the addition of the systematic position and velocity tuning the percent correct fell by 5%. In addition when the only the channels with systematic noise are used they actually drive the percent correct down to 20%, well below the 50% that could be acquired given chance probability. This problem was also apparent when the analysis was run on the actual data; the results of which can be seen in the Appendix. This issue of systematic position and velocity tuning seems to make it hard for machine learning to effectively cluster ECoG data, and will be a continued issue for those who try to do automated analysis.

Tuning	Percent correct	Percent correct on training set
Target Tuned	0.9351	1.0000
All Tuning	0.8881	1.0000
Position and Direction Tuning only	0.2062	1.0000

Table 4.4.1: Simulated Decision Tree Analysis
The target tuned data showed good efficacy for training the decision trees, however once other data was added the effectiveness of these trees fell drastically. The decision tree is being trained on systematic noise in this case and it can actually cause the tree to do far worse than chance probability seen in the last row.

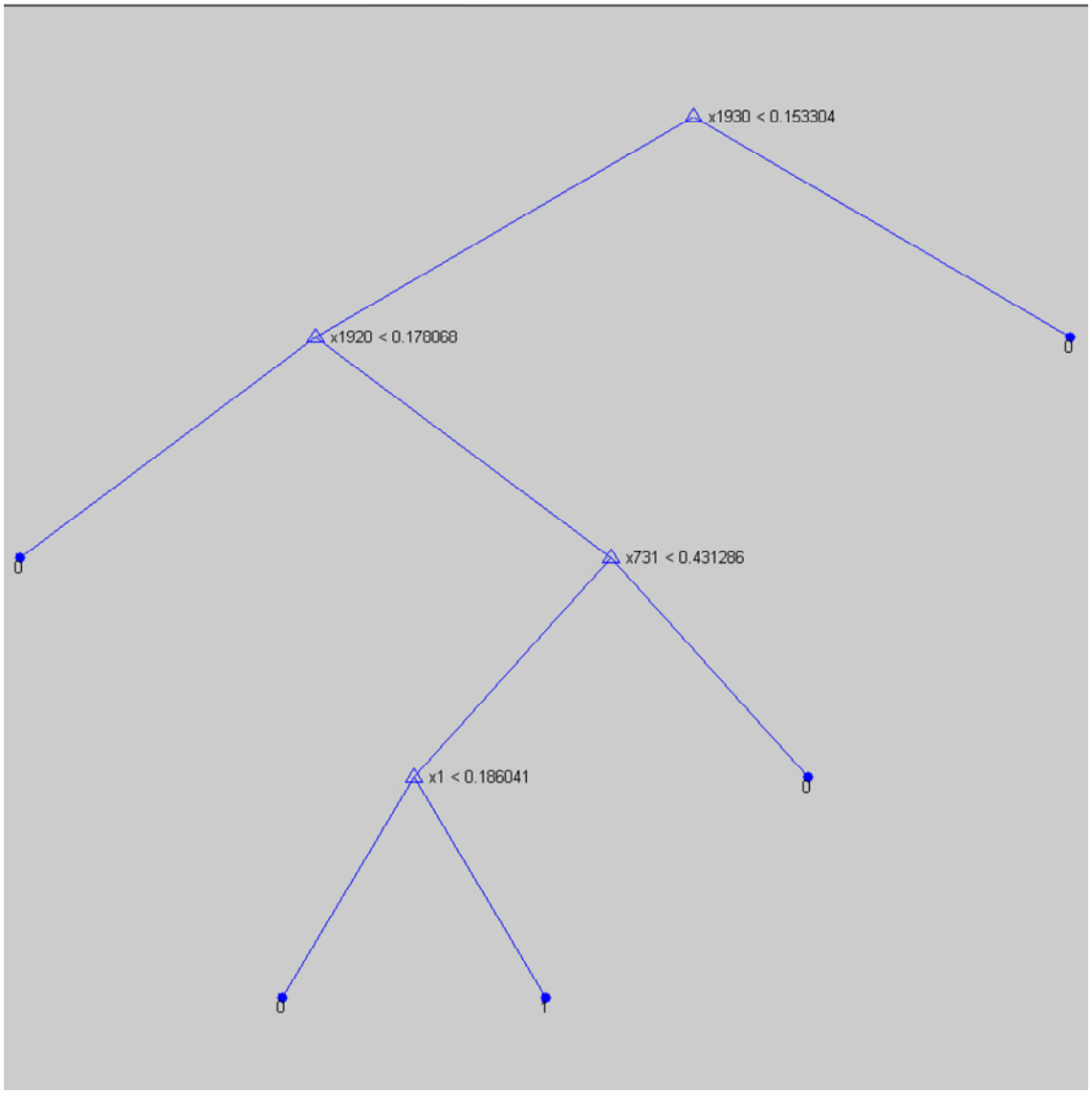

Figure 4.4.4: Example Decision Tree
An example decision tree corresponding to the Target Tuned data in row 2 of Table 4.4.1. The tree has clustered all of the data within only a few nodes and can discriminate on the test data at a rate of 100 percent.

5 Directional Encoding throughout the Brain

5.1 Introduction

Cortical activations were recorded using ECoG during arm movement tasks. The cortical activity was decoded using a cosine tuning model based on earlier studies. Historically these cosine tuned models have been applied in distinct regions using single units, (e.g. M1, premotor, DLPFC, MT, LIP); however, one of the advantages of ECoG is that many different functional areas can be recorded simultaneously and then compared (Georgopoulos, Kalaska et al. 1982; Moran and Schwartz 1999b; Leuthardt 2006). Cosine tuning has shown heavy correlations to the activity of single units during motor paradigms.

In these experiments two tasks will be performed to help elucidate the encoding of arm movements in ECoG gamma band activity. These two experiments were based on the classic Center Out task and Tracing task that were designed for use in non-human primates (Georgopoulos, Schwartz et al. 1986; Schwartz, Kettner et al. 1988). ECoG electrodes should offer a different view from the microscopic level of electrical activity that accompanies microelectrodes recording single cells or LFPs.

It is unknown whether positional or velocity information is encoded at the level of ECoG. It has been shown that directional tuning exists at the level of ECoG, however the design of the previous experiment did not dissociate kinematic parameters (Schalk, Kubanek et al. 2007). My hypothesis is that there is tuning of position, velocity, direction and speed. It is expected that speed will show the greatest modulation and most robust and widespread encoding (Heldman 2007). Finally, we hypothesize that this kinematic tuning, while widespread, will be more robust and have greater depth of modulation within the motor areas (Miller, Leuthardt et al. 2007).

5.2 Kinematics Encoding

The Center Out and Tracing tasks were performed and movement kinematics have been isolated from both tasks. The Center Out task allows both for separation of different movement periods and some disassociation of kinematics. It was redesigned specifically to isolate encoding during delay periods from movement responses so that planning encoding could be analyzed separately from the movement correlated signals. The Tracing task was redesigned to dissociate position kinematics from velocity kinematics in a 2 dimensional environment..

In center out and tracing if a subject moved in the wrong direction or began to move before the beginning of the trial it was eliminated. Less than 10% of the data were eliminated in this fashion. The bulk of the data was analyzed as approximately 70 trials for both tasks as the majority of the data conformed to these standards. All the trials longer than half a second and shorter than three seconds were accepted from the Center out task. In the tracing task the subject had to be moving the target for 300 ms for the trail to be accepted. Also, data with a radius greater than one, or less than 0.3 (0.3 is 30 % of the radius as it was standardized to a unit circle), was eliminated. Figures 5.2.1-2 shows the positions and velocities which were used to model the signal. It is with these limitations that the data in Figure 5.2.1-2 were selected and then used to create the models for Tracing.

The data in these tasks were normalized so that the regressions would be a percentage of the mean cortical activations, this was discussed in more detail in Chapter 4. Similarly, the respective ECoG data was normalized as a percent deviation from baseline. In this way the regressions weights that are formed using Equation 4.3.1-4 can be viewed as being related to the percent deviation from the mean based on the percentage of maximum extent for the related kinematic component.

Mean times were found for each location on all patients to account for any large variations in movement kinematics. The mean time to reach the target and the variance of the times taken to reach the target were analyzed for center out. For the Tracing task the mean time and the variance for the times in each octant were checked. Example results of timing are shown in Figure 5.2.3 and no patients showed significant variance across target or octants.

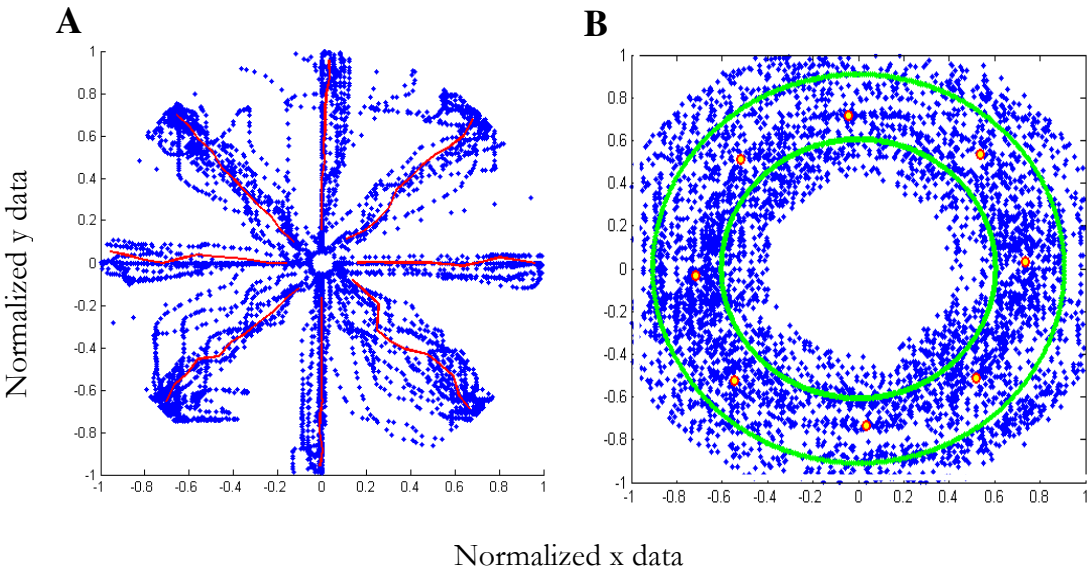

Figure 5.2.1: Positions and mean paths/positions.
These are the paths taken by one subject as they performed the Center Out and Arrow Tracing tasks. A) For Center Out the blue dots are the position held by the patient as he tried to capture the target. The red line in Center Out is the mean path the subject took. B) For Tracing the blue points are the positions held by the cursor as it traveled around the circle. The red points on the right are the mean position of the blue points in each octant. The green paths on the right are the path of the blue arrow (computer controlled) that is pushed around in a circle. Both the path of the small arrow and the large arrow can be seen as all this data was clustered together for analysis.

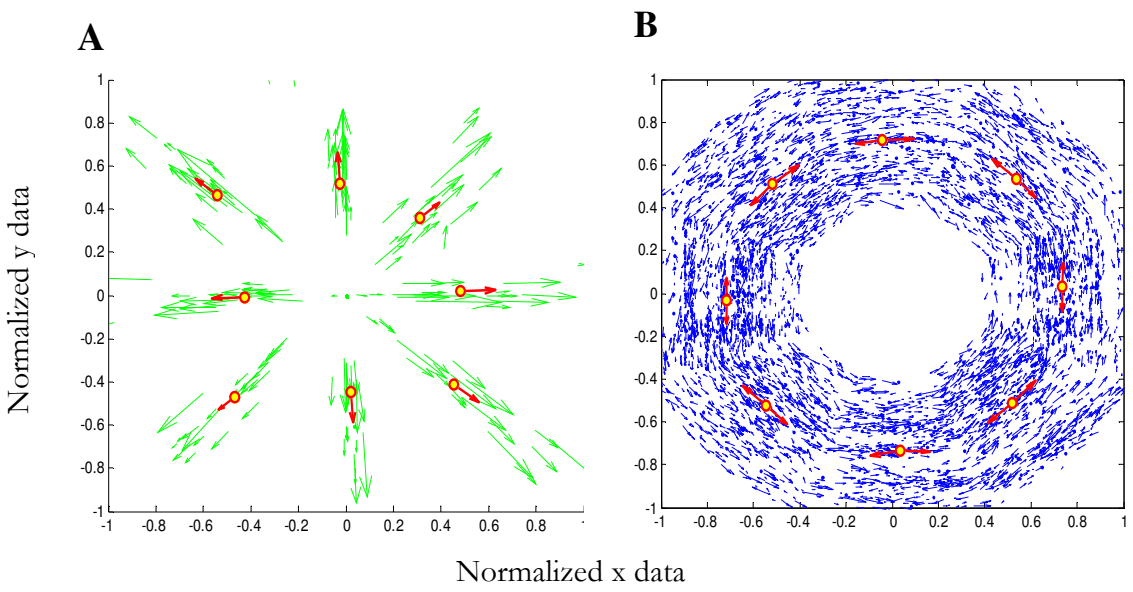

Figure 5.2.2: Velocity and mean velocity/mean position
These are the velocities produced in the paths taken by one subject as he moved to the targets in Center Out and pushed the arrow in Tracing. A) For Center Out the green arrows are all the velocities used in the center out analysis on this patient and they are located at their positions. The red arrows are the mean velocities for each target plotted at the mean position. B) For Tracing the blue arrows represent all the velocities used to create average values for the regression. The red arrows on the right are the mean velocity all originating from the mean position in that octant.

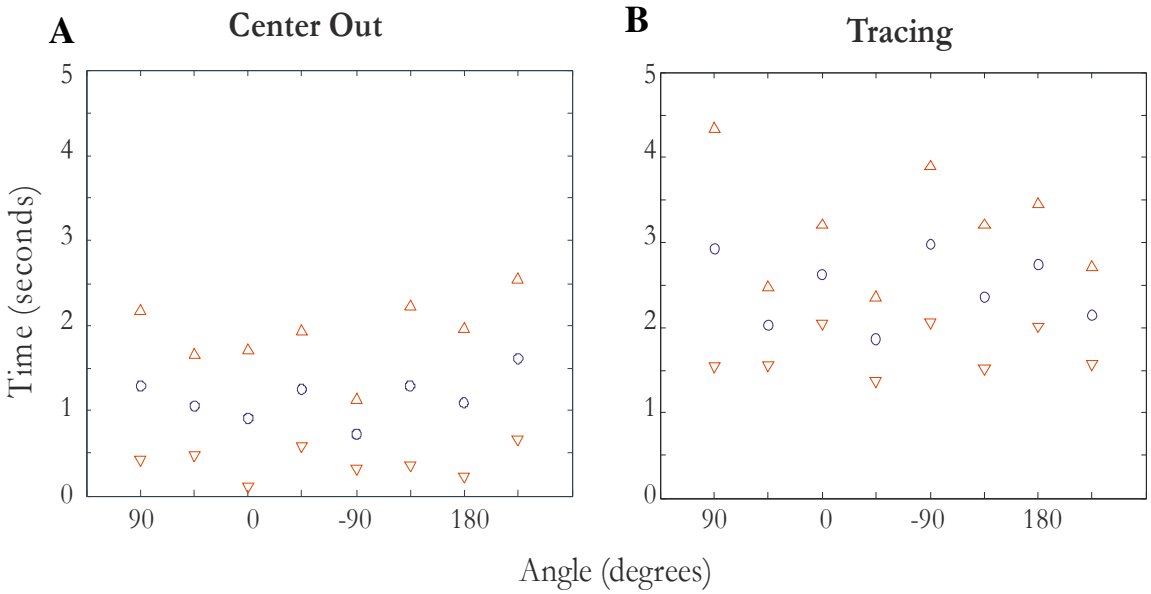

Figure 5.2.3: Mean movement times and variance
for trials in Center Out task or time spent in a particular octant for Tracing task. The blue circles represent the mean time spent in each of the conditions and the red triangles are one standard deviation above or below this mean. A) For Center Out the means were relatively consistent around 1.25 seconds and variances were relatively consistent across locations. B) For Tracing the means was relatively consistent around 2-3 seconds. The variances on this were more consistent except 90 degrees. Each trial started at 90 degrees causing the subject to have to restart there, increasing the variance in the eventual results.

5.3 Example Channel

In Chapter 4 one simulated channel's direction and position tuning were binned to both elucidate the cosine tuning as well as to show that the simulated data had the expected tuning. In this section one channel has been chosen that has particularly good tuning and exemplifies several patterns in the data that should be highlighted. For this channel one wide–band, high-frequency feature was taken and one wide–band, low-frequency feature. The raw data from these wide bands were grouped by their kinematic variables (i.e. direction, speed). By clustering these data the underlying tuning can be seen in this channel. In addition, the example channel was divided into 5 Hz bins (features). The 5 Hz features were arranged by frequency to demonstrate their tuning relationship to each other. Showing these 5 Hz bins with the wide band results help exemplify the population of features.

5.3.1 Direction, Velocity, Speed, and Position Tuning

Channel 31 in subject ZNZS is a good example of speed tuning as well as direction and velocity tuning. Two large bandwidths one low frequency, (8-32 Hz) and one high frequency (90-160) Hz were identified as being significantly tuned to the movement kinematics. While these bands were significantly tuned on this channel, the population as a whole had slightly wider bands (8-32, 70-160) that were significant as there is some variation from subject to subject. The bands that were significant for this channel were binned to show position, direction, and speed tuning.

An example of a non-tuned position encoding electrode is shown in Figure 5.3.1. It shows that there is, in fact, no significant position tuning ($p>.05$) for this example. In addition the right two plots in this figure show the tuning vectors by applying the position

model to this electrode in 5 Hz bins. Many of the channels do show good position tuning; however, this channel did not show significant position tuning but was chosen because it showed very good tuning for the other kinematics.

Direction binned spectra are shown in Figure 5.3.2. From Figure 5.3.2 it can be seen that the channel has particularly good direction tuning for high frequencies in Center Out. It is slightly hard to see, but the tuning for high frequency Tracing is also significant ($p<.05$ DOM > .05) and has almost the same preferred direction. The low frequencies of this direction tuning are out of phase with the high frequencies which is important to note because the high frequencies have been show to be opposite in amplitude from the low frequencies in other motor studies (Leuthardt, Schalk et al. 2004; Miller, Leuthardt et al. 2007). In addition, the right two plots in this figure show the tuning vectors by applying the direction model to this electrode in 5 Hz bins. This tuning shows good depth of modulation for direction and good wide band tuning that is significant. Lastly, it shows the phase reversal from low frequency to high frequency in more detail.

Speed tuning also shows an increase in slope of the higher frequency bin and a relative decrease in slope of the lower frequency bin. The plotted amplitude can be seen in Figure 5.3.3 and shows a relative increase as speed increases at higher frequencies in both Center Out and Tracing. In addition it shows a decrease in amplitude as speed increases in the lower frequency band of 8-32 Hz. The slope of this channel can be modeled as discussed in Chapter 4 and the associated vectors across the tasks can be compared. Speed slopes in 5 Hz bins appears on the right hand side of Figure 5.3.3 and shows the important phase reversal from low frequency to high frequency in its modulation. This speed slope is consistent between the Center Out and Tracing tasks.

Velocity cannot be binned like the other components because it is a mix of two components. In Figure 5.3.4 the tuning of large bandwidths can be seen for velocity and how they are very similar to direction. This similar tuning helps to exemplify the similarity between the two paradigms. This plot also helps to show that the preferred direction at a given frequency is generally very similar to the frequencies adjacent to it. There is a relatively constant change in preferred direction, so that across many frequencies there can be a large change in preferred direction. Though the velocity tuning cannot be binned like the other components the preferred direction can still be found for large bandwidths, and then compared.

5.3.2 Across task comparisons

Comparison of preferred direction for position, direction, velocity, and speed can be seen in Figure 5.3.5. These comparisons are of particular interest because of the differences this electrode shows between the statistically significant results and the tuning, which is not statistically significant. It is important to make comparisons across tasks because it gives an opportunity to look at how robust this tuning is across tasks; in addition comparison across tasks can lead to comparison across time.

In Figure 5.3.5 position tuning is the only example where in the high frequencies and low frequency preferred directions do not cluster. In all three other kinematics the difference between high and lower frequencies within a task is greater than the difference in the two high frequency preferred directions, or low frequency preferred directions, across tasks. This difference of position from the other examples helps to show that only the statistically significant vectors show tuning.

The directional high frequency tuning of Center Out matches up very well with the high frequency component of Tracing. By comparing Figure 5.3.5 to Figure 5.3.2 the matching of high frequency components in the raw data can also be compared to that of the tuning vector. Similarly the low frequency components can be compared across Figures 5.3.5 and 5.3.2 to see the similarity in tuning. Speed and Velocity tuning show similar results to direction tuning and have high frequency and low frequency match up. This comparison of tuning vectors is later calculated across all features for all subjects.

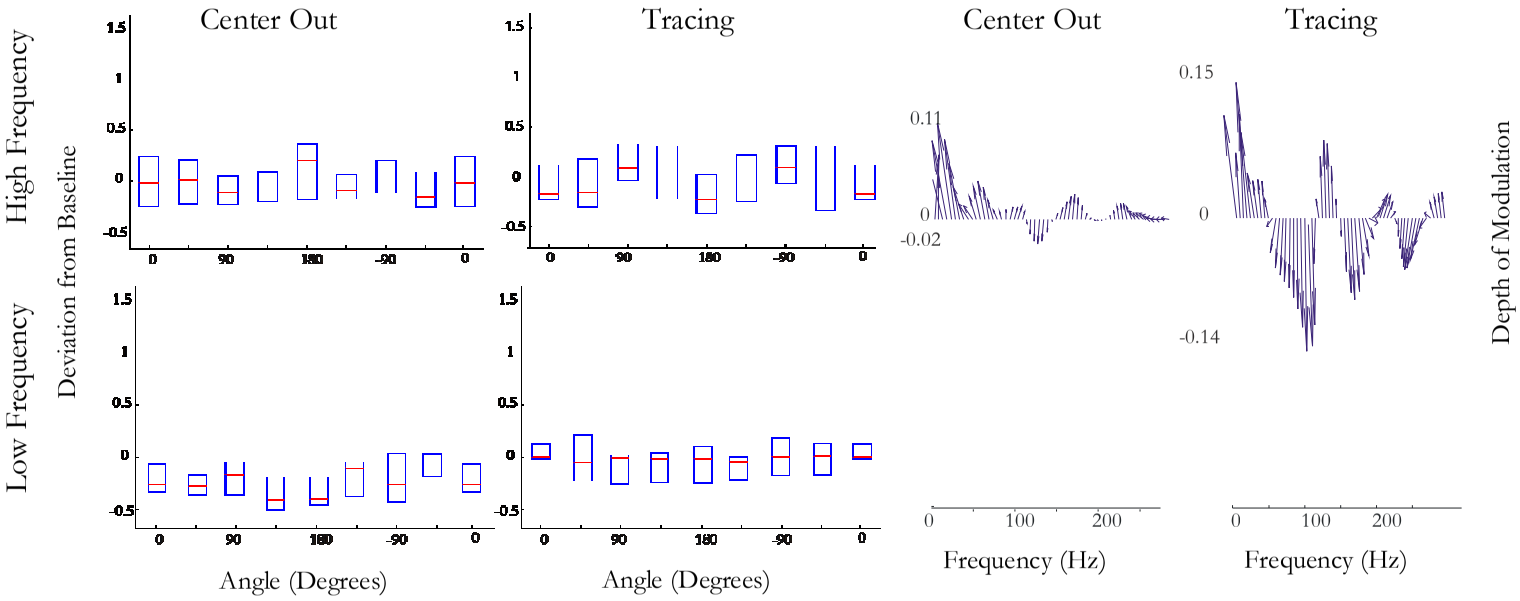

Figure 5.3.1: Position tuning on one channel.

This channel did not show particularly good position tuning but other channels did. On the left is a wide band taken from 110-160 Hz on this channel for high frequency and 8-32 Hz for low frequency. These two figures show non significant tuning for both the high frequency and low frequency bands.

The right two figures show the tuning vectors derived from applying the position model to this electrode in 5 Hz bins from .5-280.5 Hz. There are many more reversals from positive to negative tuning on this channel. This channel does not have statistically significant position tuning which may result in the higher number of phase reversals.

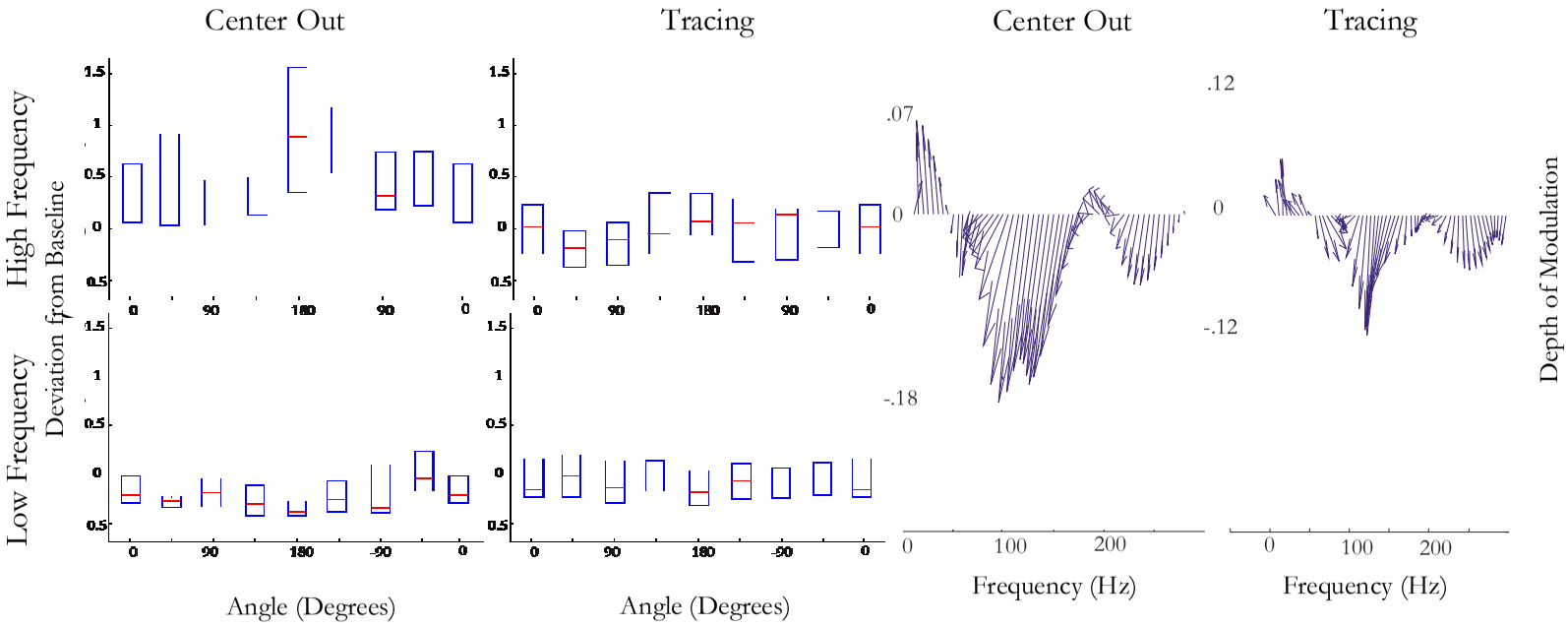

Figure 5.3.2: Direction tuning

This channel showed significant direction tuning for both Center Out and Tracing. On the left the high frequency band from 110 -160 Hz shows statistically significant direction tuning for both high frequency and low frequency Center Out. The direction tuning for both tasks in high frequency is 90 degrees out of phase with that of low frequency in Center Out.

The right two figures show the tuning vectors derived from applying the direction model to this electrode in 5 Hz bins from .5-280.5 Hz This channel shows good direction tuning and only one major phase reversal from positive to negative as it moves from the 8-32 Hz band to 70-160 Hz band that have both shown wide tuning.

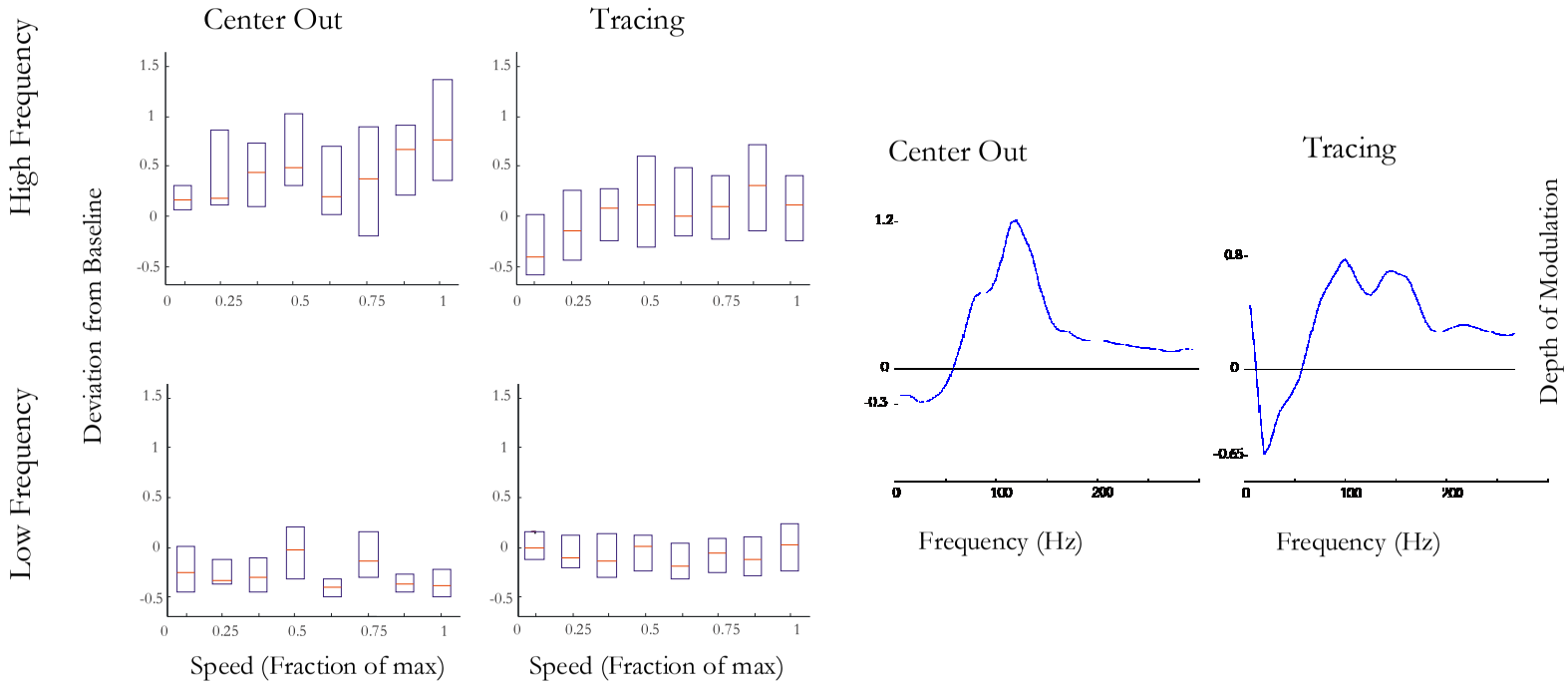

Figure 5.3.3: Speed tuning

This shows a relative increase in higher frequencies (110-160 Hz) as speed increases. Inversely the speed tuning at lower frequencies (8-32 Hz) negative and the amplitude decreases as speed increases.

The figures on the right showed the depth of modulation for speed tuning given 5 Hz bins from .5-280.5 Hz. These show a greater detail of the tuning on this channel and better show the phase reversal below 60 Hz.

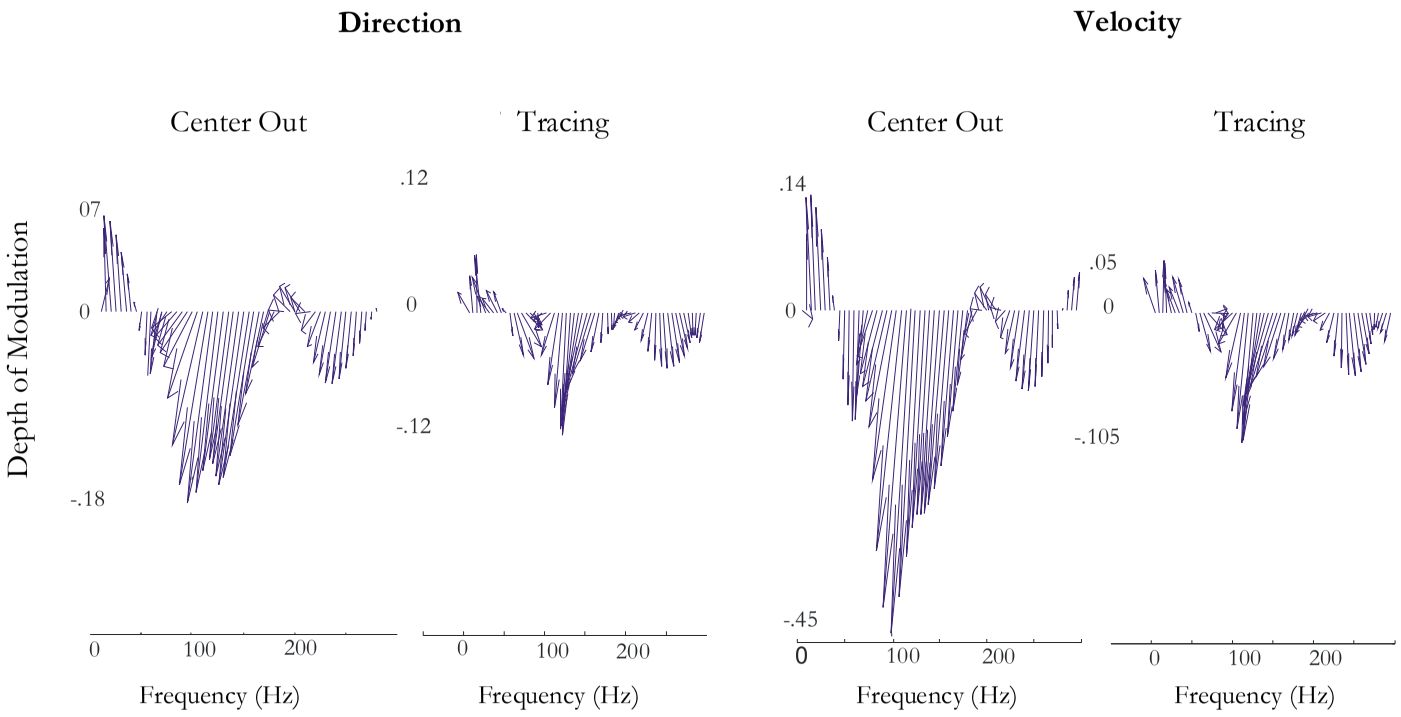

Figure 5.3.4: Comparison of direction and velocity tuning
This tuning of 5hz bins is very similar in this task only really showing a greater depth of modulation for velocity tuning. The comparison of these two plots underscores the similarity between direction and velocity tuning.

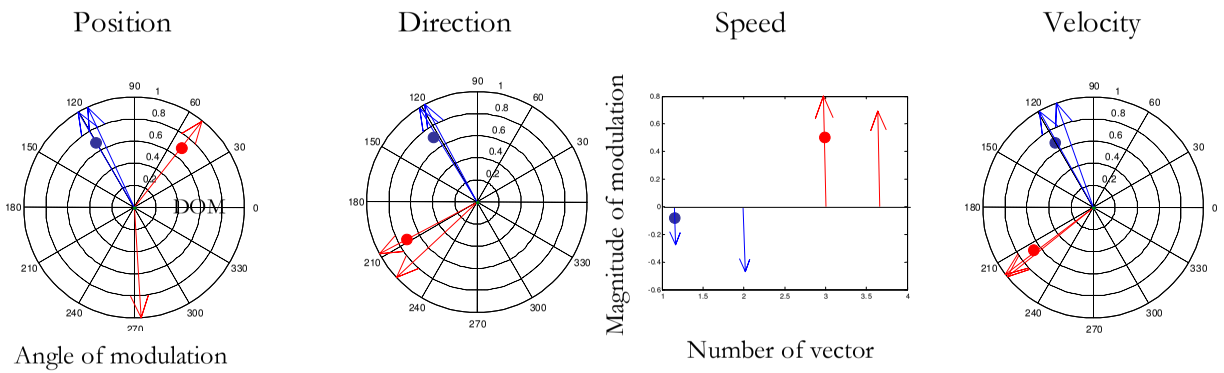

Figure 5.3.5: Comparison of angle between vectors for each movement component.

The arrows with the dots are for Center Out and the ones without are for Tracing. Blue Arrows represent low frequencies (8-32 Hz) and red arrows high frequencies (110-160 Hz). In direction, speed, and velocity there is significant correlation between the angles at higher and lower frequencies across tasks, but not between higher and lower frequencies on the same task. These are also the same vectors that showed statistically significant results in earlier analysis. This underscores the consistency of preferred direction in this recording modality as the measurements for these two tasks were actually taken on separate days.

The one exception is position. High frequency positions do not show good correlation across tasks however since the are not statistically significant it was expected. This underscores the correlation of the statistically significant vectors in these electrodes, while highlighting the non-statistically significant vectors lack of correlation across tasks.

5.4 Population Analyses

Now that it has been established that an individual electrode can show good kinematic tuning, tuning should be compared across the population. Within the population, any tuning was said to be statistically significant in a given channel if it had both $p<0.05$ for fit to the model and depth of modulation (DOM) > 0.05. This threshold for significance was applied to all four kinematics and allowed for distinguishing between results that were significant and could be applied to BCI and those that could not. It is of note that the depth of modulation portion of the test eliminated very few features so that of the p-value by itself may be a good indication of tuning.

There were three separate regressions, done on different periods; they are referred to as Center Out, Delay, and Tracing. Center Out was the movement period of the Center Out task for speed, velocity, and direction; Center Out was the hold period of the Center Out task for position tuning. Delay was the spectra from the Delay period of Center Out and the kinematics from the following movement period for direction, speed, and velocity; similarly it was the spectra from Delay and the kinematics from the hold period for position. Tracing was taken during the Tracing task once it was divided into octants.

5.4.1 Comparison Across all frequencies

The populations of all features show trends that are in line with previous studies that have shown motor cortical regions will have more consistent tuning than other areas. These trends are important because they allow us to see which Brodmann areas are encoding a reliable signal for each of these components. It is important to be able to pick out the most robust tuning in the cortex to create a reliable BCI using these components; if there are unreliable tuning, the features will not be controllable by a BCI user.

Tables were created by taking the criteria for significance and combining those features across Brodmann Area and kinematic component (Table 5.4.1-3). Each set of features was viewed for all frequencies and also across a region of interest in the high gamma band between 70-160 Hz. Each of the regressed periods showed differences but a few overall important trends are evident. These trends are dominant in the motor areas but show good tuning in other areas as well.

The Center Out task showed significance across a variety of different areas but only Brodmann Area 4 showed significance across virtually all the kinematics (Table 5.4.1). Brodmann Area 4 had statistical significance across all of the kinematic regressions except positions in all frequencies. This is consistent with earlier single unit studies which have shown that motor areas encode preferentially for velocity and direction rather than position.

The Center Out task also found clustering of statistical significance in the areas surrounding motor cortex. Brodmann Areas 8,6,1,2,3, and 43 all surround the motor area and all show statistical significance for velocity. In addition they all show statistical significance for one of the other components as well. Only the areas surrounding Brodmann Area 4 had statistical significance for more than one kinematic component in the region of interest.

Another trend seen in Table 5.4.1 is significant position tuning in Brodmann Areas 10 and 47. These two areas show position tuning in all frequencies and the region of interest. However, in the Center Out task the velocity and position kinematics are heavily correlated. Due to this correlation the ability to dissociate this position encoding from the velocity is reduced.

Interestingly, Delay Period shows statistical significance in a much broader array of areas than during movement (Table 5.4.2). During movement Brodmann Area 4 showed

statistical significance across most kinematics; however during the delay period, it is joined by Brodman Areas 6 9 10, and somatosensory (1,2,3). These broader activations across many features and areas in the region of interest during the delay period may be related to coordination of attention and movement.

The Delay Period shows an important trend in speed tuning; all areas except three are significant for speed tuning. This shows that there is some statistically significant component of speed that is being encoded in many locations of the cortex. The Delay Period also shows a cluster of statistical significance in position tuning in DLPFC and frontal areas. These areas are of particular interest because they have been implicated in planning motor action in other work. The Brodmann areas that show activation for this kinematic are areas 47, 46, and 9. This cluster is particularly highlighted because areas 8 and 10 do not show any position tuning and they surround the given areas. Area 10 and 9 both show significance for all of the other components which are likely particularly involved in motor planning

The Tracing task shows statistical significance in the most widespread area of the three regressed spectra periods. The wide regions of tuning likely are related to the nature of the task for two reasons. The first of which is that it requires continual control and significantly more attention than Center Out. The second is the correlated nature of some of the components in this task. While position and velocity have been designed to be orthogonal, there is significant correlation of the other components; also, there is continual updating of these components such that it is important for the cortex to encode for them continually.

The broad activation of cortex during the tracing task is of particular note in Brodmann areas 47, 46, 6, 4, 21, 22, and 38. Each of these areas showed tuning to most, if

not all, of the kinematic components in the region of interest. This region of interest is of particular importance because in this task the tuning is more widespread at frequencies outside of the region of interest than inside. This is likely based on previous research to be correlated to diffusion of lower frequency information. However, upon further review (Figures 5.4.1-4) the situation is much more complicated and frequencies above the region of interest are also playing a significant role.

5.4.2 Comparison across individual frequencies

The comparison across individual frequencies gives a better picture of the overall trends than the earlier tables. These trends are important to understand the underlying neural activity and also to show the Depth of Modulation and slopes. These depths of modulation are important because they are a measure of the signal to noise ratio of this encoding. A high signal to noise ratio is important to create a usable BCI in a noisy environments (i.e., a hospital room, or home). By taking the Depth of Modulation into account when considering kinematic encoding it takes this signal to noise ratio into account in addition to the statistical significance. The overall results were that there was broad activation of most of the components but there are a few trends that should be highlighted in the significant tuning.

Position tuning was found in all Brodmann areas and actually showed more significant results outside of motor areas than inside motor areas in some instances. The vast majority of position tuning occurs within the expected confines of 70-160 Hz as can be seen in Figure 5.4.1. However, there is significant position tuning at much higher frequencies and that is true in many brodmann areas. This was similar to what was shown in Table 5.4.1 where the number of features is widely spread both inside and outside of the normal high gamma band.

It was not surprising that position was found to be relatively ubiquitous. Position is found in attentional areas as well as eye movements (Curtis, Rao et al. 2004; Thompson, Biscoe et al. 2005). It is likely an earlier joystick based decoding study was using positional encoding to predict cursor movements (Schalk, Kubanek et al. 2007). We expected motor cortex to show preferential position tuning, which it did not; however motor cortex did show better tuning in other kinematic tuning.

Speed tuning was expected to be everywhere due to earlier results in LFPs (Heldman 2007). Speed tuning is seen in many locations (Figure 5.4.2), however, cortical activations are positively correlated to speed in primary motor (Brodmann area 4), and cortical activations are negatively correlated to speed elsewhere. While this was not expected it makes some sense because the rest of the cortical areas may be decreasing in amplitude as the subject pays more attention to the motor task. Putting more resources into the task would cause the area of interest, primary motor, to increase and other areas to decrease in tuning.

The Delay period shows strong positive depth of modulation across many areas. This is inverted from the speed tuning in the Movement period and the Tracing period, but can be explained as an attention effect. If the subject is paying more attention to a trial it is likely they will move more quickly in that trial. If they are paying more attention and are more engaged we would expect this high positive correlation to speed in many areas.

Direction tuning is found more predominantly in motor cortex than in other cortical areas (Figure 5.4.3). Primary motor cortex has been shown to encode direction preferentially in many different studies (Georgopoulos, Schwartz et al. 1986; Schwartz, Kettner et al. 1988; Turner, Owens et al. 1995). The relationship of direction to velocity also plays a significant

role in its dominant encoding in motor areas. Table 5.4.1-3 illustrates this as the motor areas and even premotor shows up statistically significant in almost every case.

Velocity tuning is the best kinematic tunings represented in motor areas, compared to other functional areas (Figure 5.4.4). Velocity is a combination of direction and speed which have both showed different motor results than the rest of the cortex. While experiments have shown show that direction, position and speed are all corollary to motor cortex responses. Velocity is encoded for more robustly, during movements than the other components.

When all four kinematics are considered, motor cortex shows the most stable depth of modulation and most reliable number of electrodes with activation across all four components. Many of the Brodmann areas show significant activation in one component or another; however Brodmann area 4 shows statistically significant activation across all of the components. In the 70-160 Hz band BA 4 is most likely to be tuned with 10-25 % of features having statistically significant activation.

While the motor area (Brodmann area 4) shows the best tuning and the most tuned features, many of the other areas show tuning as well. The hypothesis was that the motor area would show much better tuning than the other areas but many of the other areas also show good tuning. This large amount of encoding in other areas is not surprising given multiple other studies that have shown tuning in these other areas. These other areas may also prove useful for BCI given this tuning as these areas have shown the ability to be controlled for BCI by users.

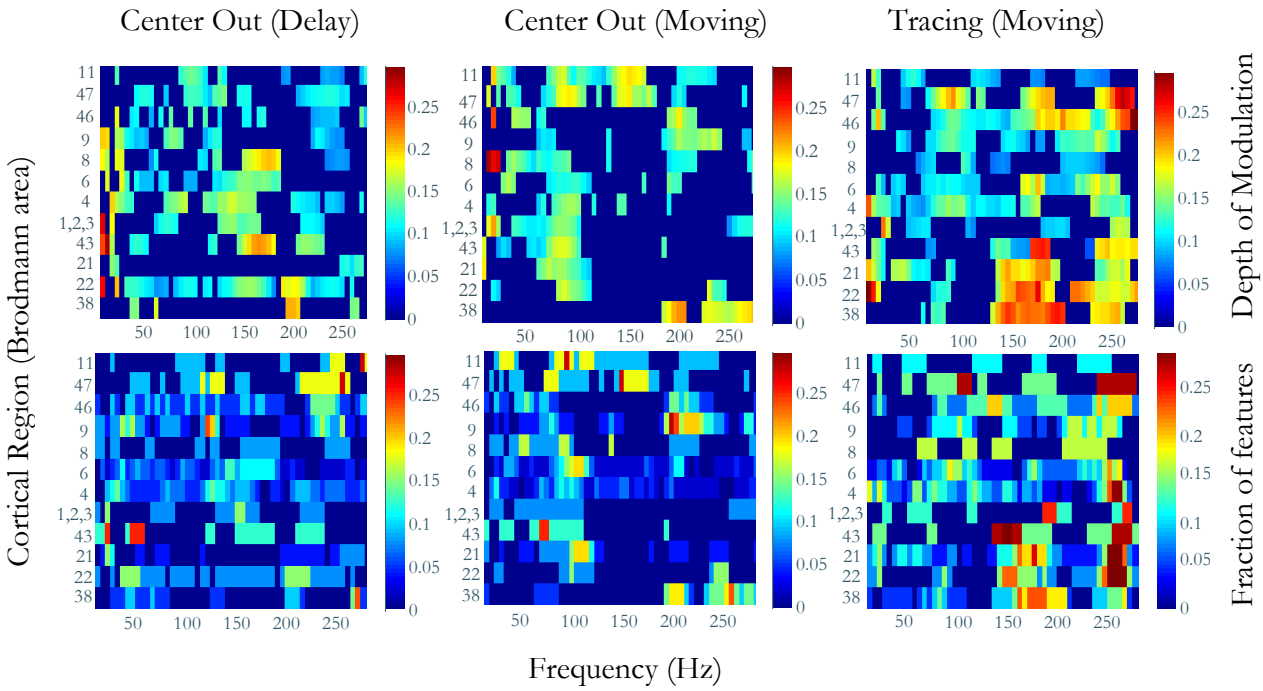

Figure 5.4.1: Population Position Tuning.
Position tuning was relatively ubiquitous.

During the Delay period the position tuning seems to cluster around the motor areas in the 150 Hz range. However, there is not the high level of clustering around primary motor that there is in other conditions. In addition it is important to point out the activity in the high frequency range (200-250 Hz) in the frontal areas during the delay period, correlates well with the percentage of features in that region and shows that there is significant activity being encoded there.

During the Center Out (Hold) period much of the activity moves to lower frequency ranges, except the frontal and dorsolateral prefrontal areas which show tuning from 110-250 Hz and 190-250 Hz respectively. It is interesting for the purposes of Aim 2 to point out the DLPFC high frequency tuning that shows up in the center out task during movement and delay. The Motor areas activation between 70-110 Hz is very similar to the activations that have been seen in other work (Leuthardt, Schalk et al. 2004; Miller, Leuthardt et al. 2007).

Tracing shows the most widespread activation of position, which is counter to its goal of dissociating position from other components. It is the only one of the three tasks that was tuned during actual movement and not a delay period. Tracing actually showed results in higher frequency ranges then some of the other tuning functions, particularly in areas 43,21,22, and 38 which are posterior parietal and temporal areas.

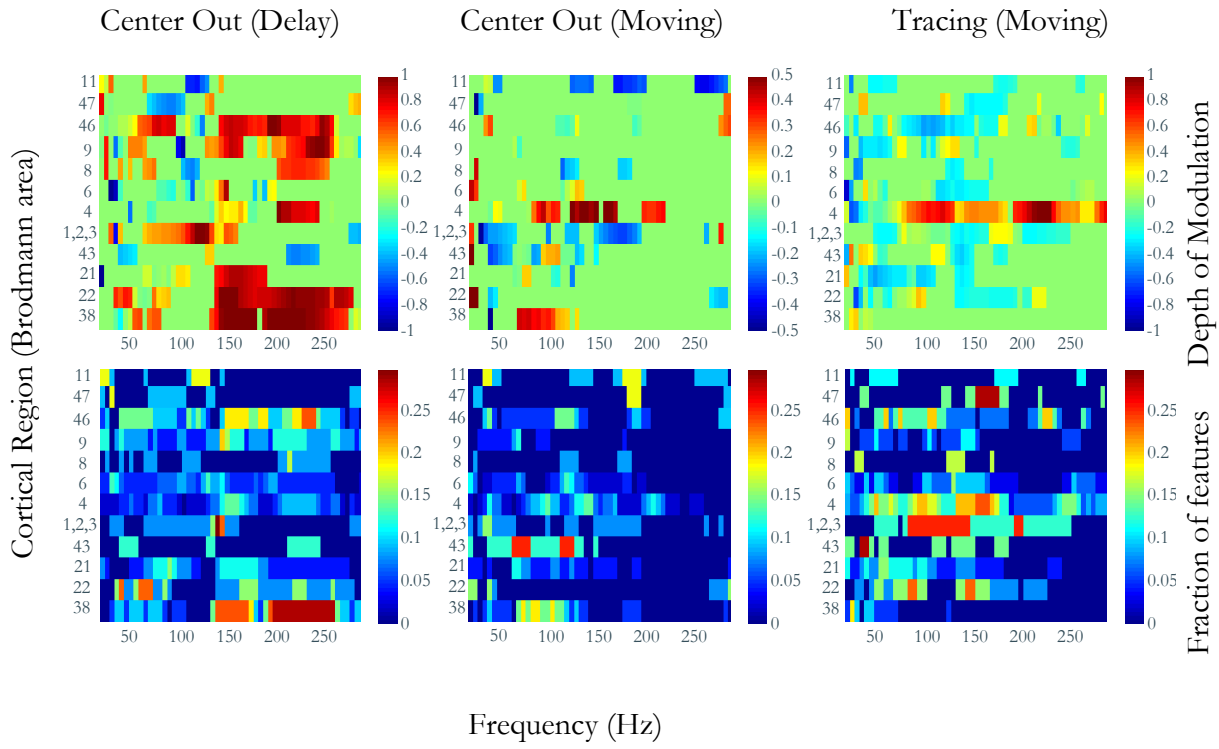

Figure 5.4.2: Population Speed tuning
Speed tuning is not nearly as widespread as expected. It was hypothesized to be the most widespread of the movement kinematics but it appear to be less widespread then position. It is best represented in Brodman area 4 (Primary motor) which correlates with previous results (Heldman 2007). In addition speed is the only

The speed tuning In Center Out (Movement) shows high positive correlation in Brodmann area 4 (Primary motor) and slight negative depth of modulation in other areas during actual movements. Its likely as the subject is devoting more resources to motor they are devoting less to other areas.

Tracing shows similar results to Center Out, in that there is an positive correlation to speed in area 4 but primarily negative outside of this area.

During delay there are high positive correlations in many cortical areas. This is likely an attention affect as the subject has to coordinate movements and if they are more engaged in a task during the delay there would be an expected increase in speed.

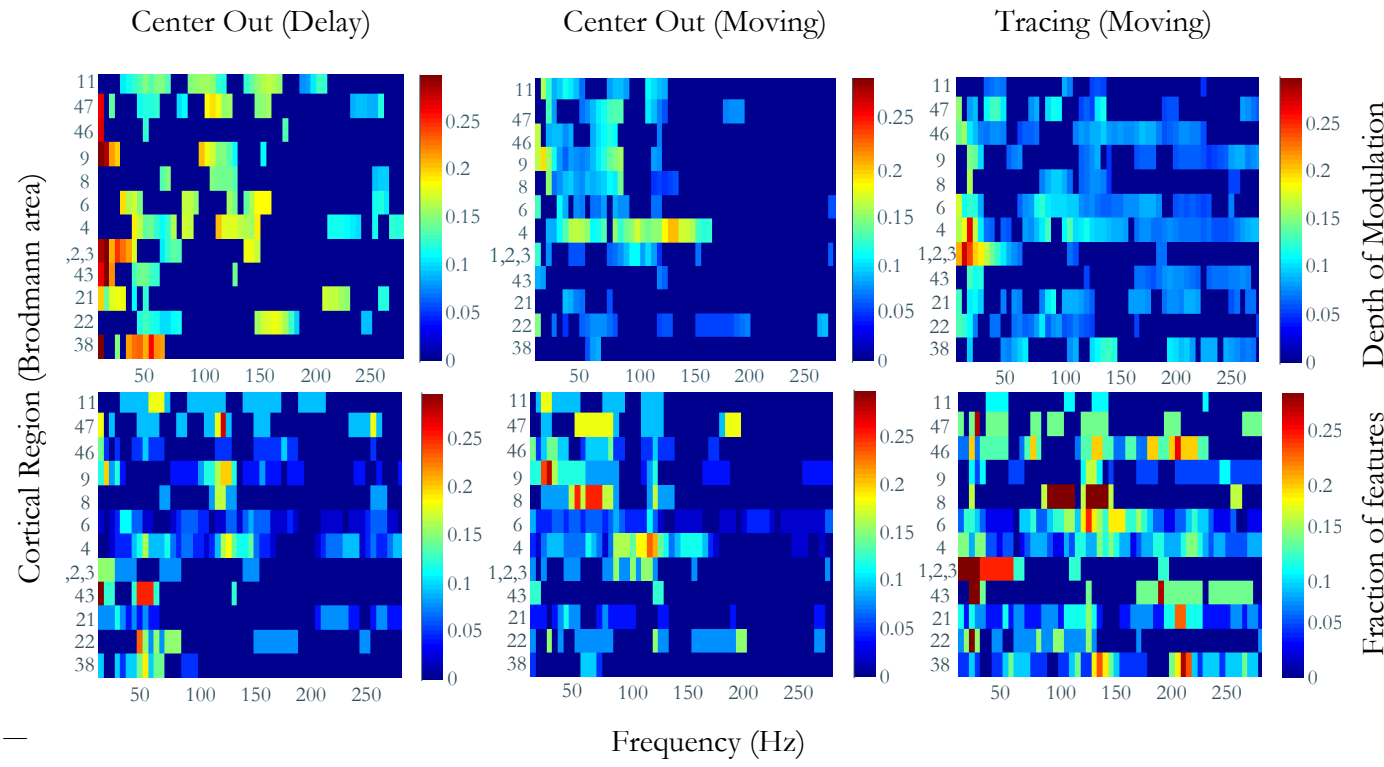

Figure 5.4.3: Population Direction Tuning
Direction tuningis encoded dominantly in primary motor, Brodmann area 4.

Direction tuning in center out (Movement) shows very focal results in the higher gamma band. This high frequency gamma activation is slightly reflected in Brodman areas 1,2 and 3 (Somatosensory). There is lower gamma frequency that is particularly interesting in the frontal areas as well. These frontal electrodes seem to be encoding for this at lower frequencies rather than the higher frequencies seen in Figure 5.4.1.

Tracing shows much more high frequency and relative broad activation compared to Center Out. It also shows interesting encoding at lower frequencies in somatosensory, and some breadth of tuning. These results suggest that motor dominantly represents direction over other cortical areas. Brodmann area 6 (Supplementary Motor and Pre Motor) show the most correlation to Brodmann area 4 (Primary motor) in this case.

Delay seems to show activation in the motor areas and frontal areas in higher gamma frequencies, it appears to show activation in the posterior parietal and temporal regions in lower frequencies.

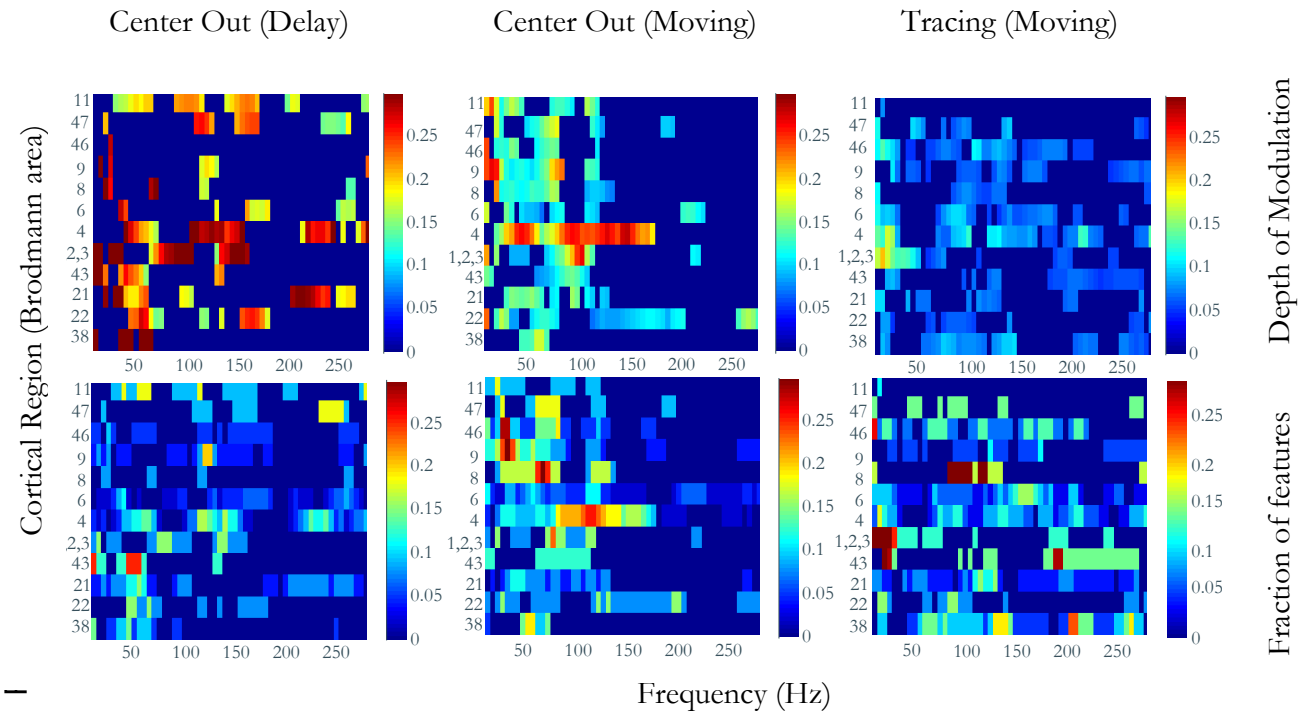

Figure 5.4.1: Population Velocity Tuning
Velocity was the most motor centered of all the kinematic tunings. Wide band activation at gamma frequencies occurs primarily in Brodmann area 4 or motor related areas in all three conditions. This makes sense given that we are tuning to velocity of arm movements and it uses the most kinematic data to tune. It is unlikely that attention or eye movement would be tuned for velocity; even as it is likely both would be tuned for position.

Center Out shows much stronger encoding in Brodmann area 4 (Primary motor) then in any other area. There is also some high frequency somatosensory as well as low frequency activation in most areas.

Tracing is broadly activated across many areas; however similar to direction (Figure 5.4.3) there is the heaviest activations in Brodmann area 4 and 6. The largest low frequency activation is in somatosensory (Brodmann areas 1,2,3, and 43).

Delay of velocity shows high frequency activation in Brodman area 4 (primary motor), Brodman areas 1,2 and 3 (somatosensory). There is additionally a high frequency activation in the frontal areas, Brodmann areas 11 and 47. The low frequency activation is primarily in temporal and posterial parietal cortex.

area	10	47	46	9	8	6	4	1,2,3	43	21	22	38	Totals	Motor Areas	Other Areas
electrodes	11	11	21	25	12	46	43	13	8	26	13	21	250	89	194
features	605	605	1155	1375	660	2530	2365	715	440	1430	715	1155	13750	4895	10670
features needed for significance	30.25	30.25	57.75	68.75	33	126.5	118.25	35.75	22	71.5	35.75	57.75	687.5	244.75	533.5
Position	44	38	41	84	30	120	101	23	18	52	17	57	625	221	501
direction	18	28	39	67	32	96	157	21	4	26	29	8	525	253	347
speed	29	10	46	16	8	68	124	27	29	37	13	54	461	192	310
velocity	17	21	53	76	39	115	226	26	13	44	41	19	690	341	438
70-160 hz features	198	198	378	450	216	828	774	234	144	468	234	378	4500	1602	3492
features needed for significance	9.9	9.9	18.9	22.5	10.8	41.4	38.7	11.7	7.2	23.4	11.7	18.9	225	80.1	174.6
position	27	23	2	14	9	64	51	7	7	32	8	2	246	115	188
direction	8	9	14	13	11	34	108	15	2	9	9	0	232	142	109
speed	7	0	21	3	5	35	72	10	15	20	0	31	219	107	137
velocity	8	7	17	14	14	43	157	15	8	20	15	0	318	200	146

Table 5.4.1: Center Out Movement and Hold Table.

This table shows the number of features that are statistically significant in different Brodmann areas and combinations of them. All frequencies were considered in the first four rows of position through velocity; correspondingly only a frequency range of interest 70-160 Hz is considered in the bottom four rows position through velocity. Green features show statistical significance for all frequencies. Red features show significance for the region of interest. Blue features show significance for all areas. Orange features show significance for motor areas. Purple features show significance for non-motor areas.

Brodmann area 4 (Motor) shows statistically significant results for almost every component. The only component it does not show a statistically significant number of features is position over the whole spectra.

Other areas do not show more than one or two regions of activation . Velocity seems to show some activation in the areas surround motor in the frequency range of interest; however none of the other components seem to show systematic activations when compared to motor.

Position activation was limited to the two frontal areas (10 and 47) showing significant activation, but no other kinematics. These two show results for both the frequency of interest and in all frequencies.

When Premotor and Motor are combined they show statistical significance for everything in the frequency of interest. However, when the other areas are combined they only show statistically significant activation for position, which yields itself to earlier results that showed position was widely tuned.

area	10	47	46	9	8	6	4	1,2,3	43	21	22	38	Totals	Motor Areas	Other Areas
electrodes	11	11	21	25	12	46	43	13	8	26	13	21	250	89	194
features	605	605	1155	1375	660	2530	2365	715	440	1430	715	1155	13750	4895	10670
features needed for significance	30.25	30.25	57.75	68.75	33	126.5	118.25	35.75	22	71.5	35.75	57.75	687.5	244.75	533.5
position	24	43	73	86	23	137	155	24	27	35	53	35	715	292	536
direction	31	27	25	59	12	89	152	17	14	40	25	27	518	241	349
speed	16	16	132	116	22	137	137	32	13	81	60	166	928	274	759
velocity	32	21	27	42	8	79	155	27	15	64	19	23	512	234	330
features 70-160 hz	198	198	378	450	216	828	774	234	144	468	234	378	4500	1602	3492
features needed for significance	9.9	9.9	18.9	22.5	10.8	41.4	38.7	11.7	7.2	23.4	11.7	18.9	225	80.1	174.6
position	8	17	25	31	7	63	68	13	6	3	16	5	262	131	181
direction	13	13	7	37	7	42	67	5	1	0	8	3	203	109	131
speed	10	7	44	38	4	61	54	22	2	41	14	46	343	115	267
velocity	13	8	9	26	2	27	59	19	2	7	7	2	181	86	103

Table 5.4.2: Center Out Delay Table

This table shows the number of features that are statistically significant in different Brodmann areas and combinations of them. All frequencies were considered in the first four rows of position through velocity; correspondingly only a frequency range of interest 70-160 Hz is considered in the bottom four rows position through velocity. Green features show statistical significance for all frequencies. Red features show significance for the region of interest. Blue features show significance for all areas. Orange features show significance for motor areas. Purple features show significance for non-motor areas.

The delay period shows activation across Brodmann area 4 (Primary motor) for every condition, it also shows activation for Brodmann area 6 (Premotor) for most of the kinmatics that were being recorded for in this case.

Somatosensory, Brodmann areas 1,2, and 3, shows significant activation for speed velocity and position when viewed in this format.

Frontal and Prefrontal areas, 10 and 9, both show significant activation in the frequency range of interest. This is particularly interesting because many of the areas between these areas and motor do not show significant activation.

Speed tuning is the most dominantly represented component with Position also being heavily represented. The broad activations of both of these components can be seen when scanning across their respective rows.

area	10	47	46	9	8	6	4	1,2,3	43	21	22	38	Totals	Motor Areas	Other Areas
electrodes	9	7	15	18	6	32	34	8	7	26	13	21	196	66	154
features	495	385	825	990	330	1760	1870	440	385	1430	715	1155	10780	3630	8470
features needed for significance	24.75	19.25	41.25	49.5	16.5	88	93.5	22	19.25	71.5	35.75	57.75	539	181.5	423.5
position	23	40	80	66	20	135	165	24	40	143	65	99	900	300	711
direction	10	25	77	41	24	158	163	31	30	106	32	94	791	321	597
speed	14	20	65	32	7	84	241	55	20	70	52	17	677	325	381
velocity	1	14	54	31	21	102	123	30	33	69	21	101	600	225	447
features in 70-160 hz	162	126	270	324	108	576	612	144	126	468	234	378	3528	1188	2772
features needed for significance	8.1	6.3	13.5	16.2	5.4	28.8	30.6	7.2	6.3	23.4	11.7	18.9	176.4	59.4	138.6
position	6	14	33	26	8	46	61	2	16	35	20	31	298	107	235
direction	5	10	26	11	21	87	57	2	1	33	16	33	302	144	243
speed	1	14	28	15	5	43	119	32	9	32	28	1	327	162	176
velocity	0	7	22	13	18	48	53	2	5	28	10	41	247	101	192

Table 5.4.3: Tracing Table.

Tracing shows the broadest activation of any of the tasks. When looking at the combined areas on the right only one component is not correlated to a statistically significantly level.

This table shows the number of features that are statistically significant in different Brodmann areas and combinations of them. All frequencies were considered in the first four rows of position through velocity; correspondingly only a frequency range of interest 70-160 Hz is considered in the bottom four rows position through velocity. Green features show statistical significance for all frequencies. Red features show significance for the region of interest. Blue features show significance for all areas. Orange features show significance for motor areas. Purple features show significance for non-motor areas.

Motor and Premotor, areas 6 and 4, show very significant activation in all kinematics in the frequency range of interest and virtually as significant activation in all frequencies.

Frontal areas and Posterior parietal areas seem to be more heavily recruited in this task then in previous tasks. Areas that demonstrate this frontal and posterior recruitment are 47 and 46 for frontal and 21 and 22 for posterior parietal.

Several areas show statistical significance in all frequencies but do not show this level of significance when only the frequency range of interest is viewed. Notable areas that exhibit this behavior include Somatosensory (1,2,3, and 43) and frontal eye fields (8).

Patient	Center Out Task		Tracing Task		Time Difference	
	Session	Date and Time	Session	Date and Time		
ZNZS	16	9/15/06 ~ 5:20 PM	7	9/10/06 ~ 4:52 PM	~ 5 days	
TOFS	3	2/16/07 ~ 11AM	1	2/15/07 ~ 1PM	~ 22 Hours	
TTES	7	3/31/07 ~ 11AM	7	3/31/07 11AM	Concurrent	
FOTE	1	4/28/07 ~ 10AM	1	4/28/07 ~ 10 AM	Concurrent	
ETOS	1	8/31/07 ~ 11 AM	2	8/31/07 ~ 3 PM	4 Hours	
FZFE	1	04/03/08 ~ 12:45 PM	1	04/03/08 ~ 1:15 PM	30 Minutes	

Table 5.4.4: Time difference
Time difference between recording of Center Out and Tracing. There is a large variance in the times between recording and helps to demonstrate the robustness of preferred direction at this level of recording.

5.5 Comparison of tuning vectors

5.5.1 Across Task Comparisons

Tuning vectors from the Delay period of Center Out to the Movement period are only separated by tens of milliseconds in time so we would expect a large amount of them to have similar tuning. Many of the features which are statistically significant, in both Delay and Movement, show similar tuning (Figure 5.5.1). The difference in angles between these periods is fairly small particularly in direction and position tuning where virtually all of the angles in the motor area between 70-160 Hz are near 0 degrees, Figure 5.5.2. Direction and position appear to be dominantly encoded between Delay and Movement; however this dominance becomes even more evident when looking at the region of interest.

The Comparison of Movement in Center Out to Tracing is in contrast to the earlier results because position actually shows the most significant results (Figure 5.5.3). To review the Delay compared to Movement of Center Out showed larger encoding in direction, Figure 5.5.4. This result makes sense based on the fact that direction only needs to remain constant for a few hundred milliseconds for Delay and Movement to correlate; position needs to remain constant for several seconds, because position is taken from the Hold period rather than the movement period.

Position is not dominant when Center Out movement is compared to Tracing and anatomy is limited to motor areas, Figure 5.5.4. The high gamma band of the motor area seems to show dominance of direction and velocity. However this does not tell the whole pictures, as one might expect that the position component has been removed by filtering out the results below 70 Hz and it was actually largely removed by filtering the results above 160

Hz. This is particularly interesting when combined with results from Chapter 6 which show activity in frontal regions for this band.

The robust nature of preferred direction across task is particularly good when the time between tasks is taken into account, (Table 5.5.4). This Table demonstrates that there is, in some cases, a long time between tasks and there is still a large correlation of preferred direction. This shows that the preferred direction of ECoG features is very stable, when compared to other recording modalities.

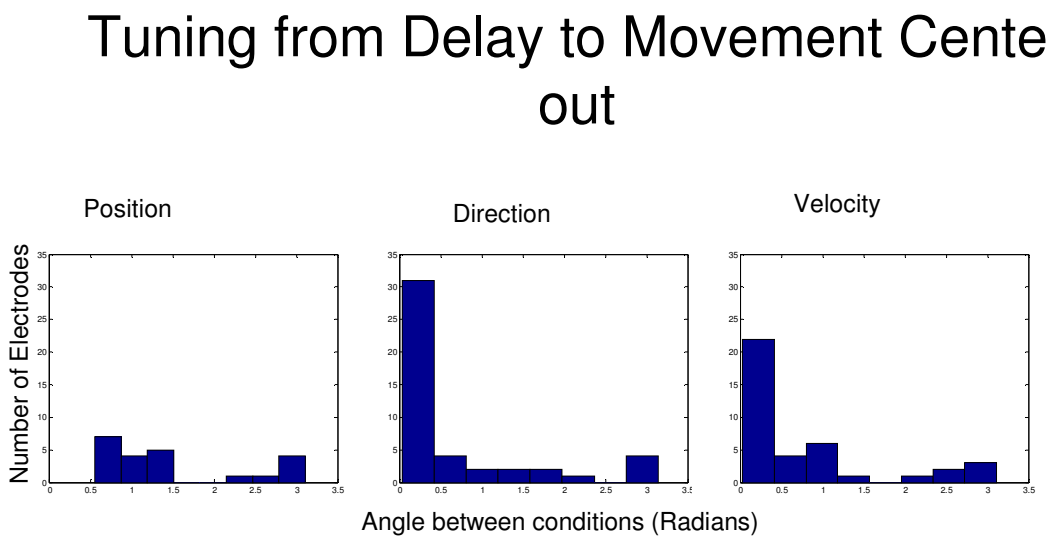

Figure 5.5.1: Comparison of Center Out Delay to Movement
Difference in Angles from Center Out Delay to Center Out Movement. Direction and Velocity appear to show significant encoding between the two periods in this task. Position tuning is not as nearly as stable between tasks.

Tuning from Delay to Movement Center out ROI

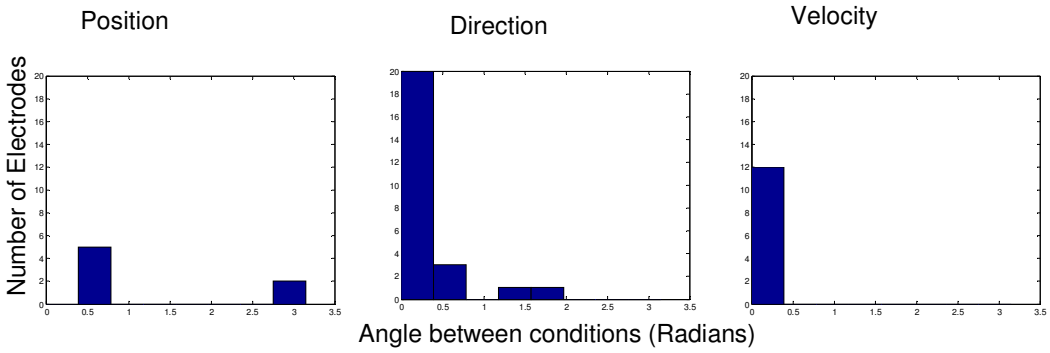

Figure 5.5.2: Angles in Region of interest (70 - 160 Hz) Comparison of Movement to Delay Comparison from Center Out Delay to Center Out Movement. This only further highlights the representation of direction and velocity during the delay period. This encoding remains constant across the movement period. However, position is not encoded for in the same way during Delay and Holding. This makes sense, as the position is different.

Tuning from Center out to Tracing

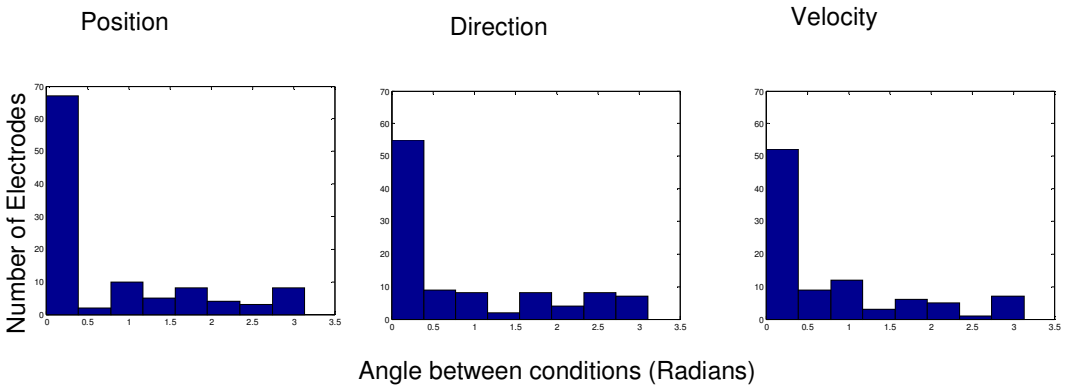

Figure 5.5.3: Comparison of Center Out and Tracing
Difference in tuning Angles from Center Out Movement to Tracing. All kinematic components that are statistically significant show primarily small difference between the two tasks. It is important to note that these tasks were often separated by days so this tuning is robust for long periods of time.

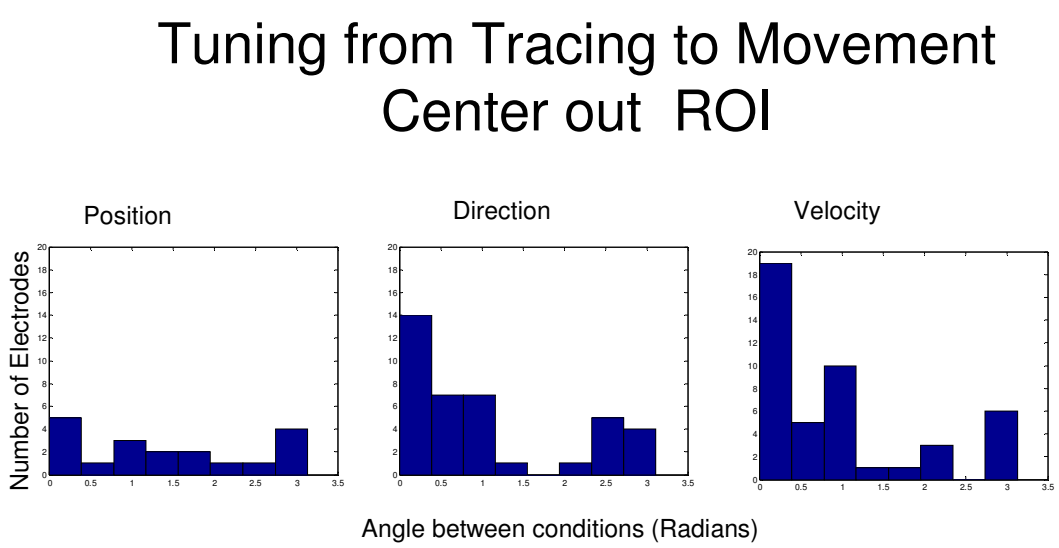

Figure 5.5.4: Angles in Region of interest (70 - 160 Hz) Center Out vs Tracing
Comparison of angles from Center Out Movement to Tracing. By looking at the frequency range of interest there appears to be robust velocity and direction encoding in the high gamma frequency range. Position is greatly reduced when this frequency range is looked at separately from low frequencies and frequencies greater than 160 Hz. In this case the frequency range greater than 160 Hz contains the bulk of the position vectors that were displayed in Figure 5.5.4.

5.5.2 Distance Comparisons

Distance comparisons showed very significant correlations across very large distances (8 cm on a standardized Talairach Brain) (Talairach and P. Tournoux PU - Thieme Medical Publishers 1988). These significant correlations across large distance could be mistaken for noise if it was not for the fact that the results which are not statistically significant and are actually noise show no correlation across distance, Figure 5.5.5. The significant correlations were surprising as it was expected correlation would fall off quickly with distance as had been seen with LFPs (Heldman 2007).

Heldman had used a different method for looking at correlation across distance. Here it is the angle between to vectors tuned to the same kinematic that is being compared. Heldman compared signal correlation in different frequency bands. These are fundamentally different metrics and while we see an increase in amplitude it is unknown whether the phases

are the same. If we return to the 5.4.1-4 figures and focus on the breadth of modulation on these figures it is even more unsurprising that we see this over these distances. The significant encoding of hand movements is present in many areas and over great distances in each of the analysis that are presented

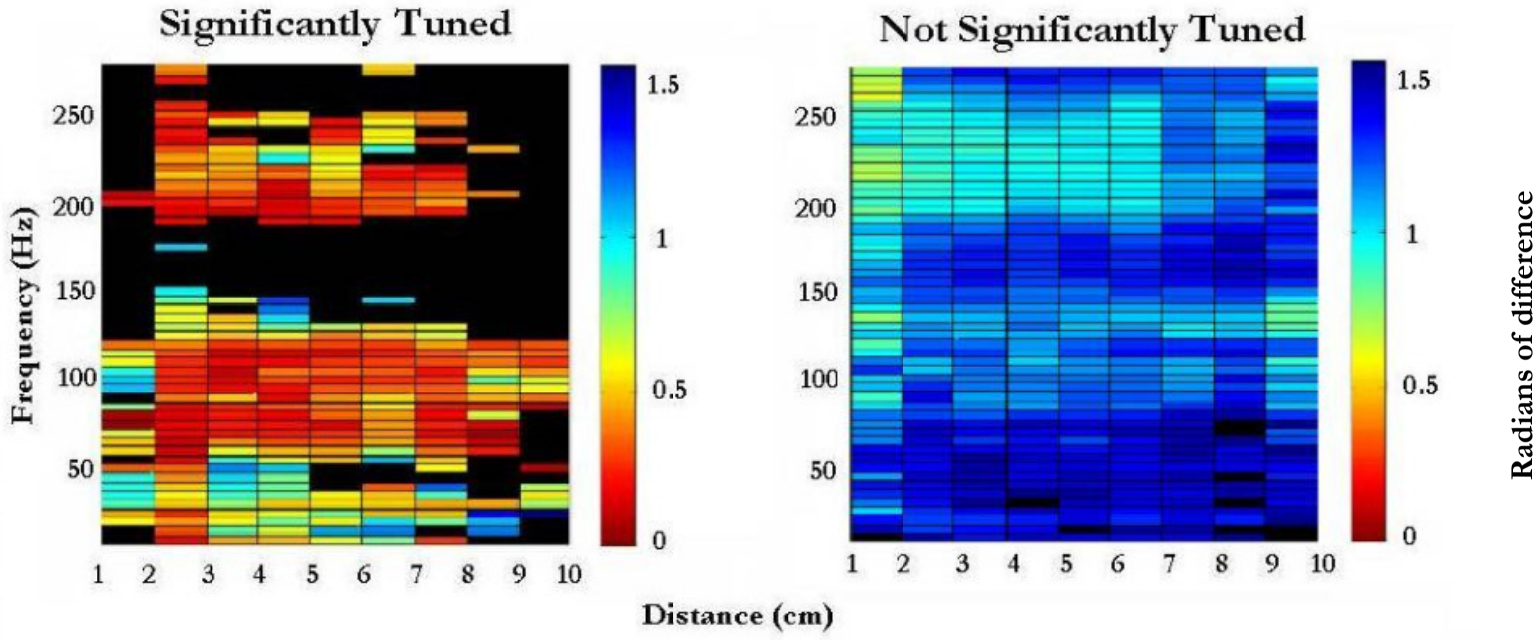

Figure 5.5.5: Comparisons of angles across distance.
The x-axis is distance as measured in centimeters and the y axis is frequency in 5 Hz bins. The figure on the left shows that there is a very small difference in statistically significant tuning even across larger distances. This was only true for the statistically significant features as the plot on the right shows the difference in angles between features that are not statistically significant; this difference is at noise level.

5.6 Discussion

ECoG recordings of spectra and tuning to the neural correlates showed widespread statistical significance throughout the brain. This widespread tuning showed a few interesting trends and areas that showed better tuning but many areas showed tuning that was robust enough to show significant involvement in the task. Many areas have shown this kind of tuning in previous studies using other recording modalities (Moran and Schwartz 1999a; Schwartz and Moran 1999c; Georgopoulos, Langheim et al. 2005; Wang, Chan et al. 2007). While there is tuning in all the functional areas, the high gamma band (70-160 Hz) seems to encode for these kinematics in the bulk of cases. The high gamma band is the frequency band where ECoG shows it's most promising results (Leuthardt, Schalk et al. 2004; G. Schalk 2007).

Signal to noise ratio is an important factor in controlling a useful BCI and the ECoG neural correlates of hand movements are encouraging in this respect. The purpose of quantifying depth of modulation was to help understand the signal to noise ratio that would be present in a BCI. In addition to showing statistical significance in a widespread number of Brodmann Areas there was also a relatively high depth of modulation in many of these areas. This means that these areas should be able to provide a robust signal when applied to a BCI.

The widespread tuning of ECoG throughout the cortex should allow for many independent control signals for BCI. Multiple different areas showed good tuning to the motor kinematics of hand movements and several of these areas have been previously tested in BCI (Andersen, Burdick et al. 2004; Ramsey, van de Heuvel et al. 2006). The use of these other cortical areas in BCI should be explored, using ECoG. It should not be necessary to

only use the motor cortex for BCI control as has been previously thought. This gives hope to those patients who have suffered cortical injuries of the motor cortex (i.e., stroke). In these cases other cortical areas may be able to operate BCI to help compensate for some of these motor deficits.

Tuning across different tasks is robust and should create a more stable BCI than single units. Single Unit BCIs are not only plagued by encapsulation, but they require complicated models that must be continually updated due to plasticity of individual neurons (Schwartz 2004). The preferred direction of individual neurons change within a matter of hours (Velliste, Ferel et al. 2008). Herein we have shown that the preferred direction in features of ECoG can be similar for days (Table 5.5.4). The stability of these features will be useful for home use of ECoG BCI as they will not need to be updated or maintained as much as other BCI modalities.

The widespread correlation of tuning vectors could prevent the creation of multi-dimensionality BCI using ECoG. However, previous results have shown that even closely related electrodes can be operated independently with training (Heldman 2007). ECoG has also shown a good amount of plasticity when training to use a BCI (Leuthardt, Schalk et al. 2004; Leuthardt 2006; Schalk, Miller et al. 2008). The important factor is to find tuned features with good signal to noise ratios that are controllable by the user, so that online learning can start. We have shown that tuned features with a good signal to noise ratio can be found throughout the cortex.

6 Dorsolateral Prefrontal Cortex (DLPFC) Encoding

Previously, the DLPFC has demonstrated encoding of target information in both humans and non human primates (Niki and Watanabe 1976; D'Esposito, Ballard et al. 2000). Consistently the DLPFC shows a physiological change correlated to task related targets, both across humans and primates, as well as across experimental modalities. (Curtis, Rao et al. 2004). We have recorded ECoG data which shows physiological responses of the DLPFC during a target based task.

We tested for both directional and non directional signals in order to better elucidate encoding of information at the level of ECoG. Our purpose in identifying DLPFC target selection signals is to create a binary selection signal, which could be used for a mouse click in a BCI. While much of the research on this area has focused on the directionality of these signals it has also been shown to encode non directional signals, which are potentially useful for this type of selection (Tsujimoto, Genovesio et al. 2008). In addition it was expected that directional tuning would be found based on previous studies in local field potentials (LFPs) and ECoG, which have demonstrated robust directional tuning (Heldman 2007; Schalk, Kubanek et al. 2007).

We have found both non-directional and directional encoding in DLPFC ECoG. The encoding shows unique results above 150 Hz, a result of note given previous studies have shown encoding between 70-150 Hz(Miller, Leuthardt et al. 2007). It is also indicated from the results that the tuning of signals at the level of ECoG tend to move to higher frequencies as they move forward. These signals were isolated with the hopes of using them in BCI, however, the efficacy of this signal as a mouse click is still in question as it has not been shown to be effective for determining whether a subject is on their goal.

6.1 *DLPFC electrodes*

Electrodes contra-lateral to hand movement were chosen from seven patients that had coverage on either the right (17 electrodes) or on the left (24 electrodes) hemisphere. Consistent with previous fMRI reports, electrodes which covered Brodmann areas (BA) 46 and 9 were chosen. (D'Esposito, Ballard et al. 2000). In previous reports DLPFC is located near the intersections of BA 9 and 46, so electrodes outside of a approximately 1 cm radius were eliminated. These electrodes are shown in Figure 6.1.1 and are clustered around the important location in DLPFC.

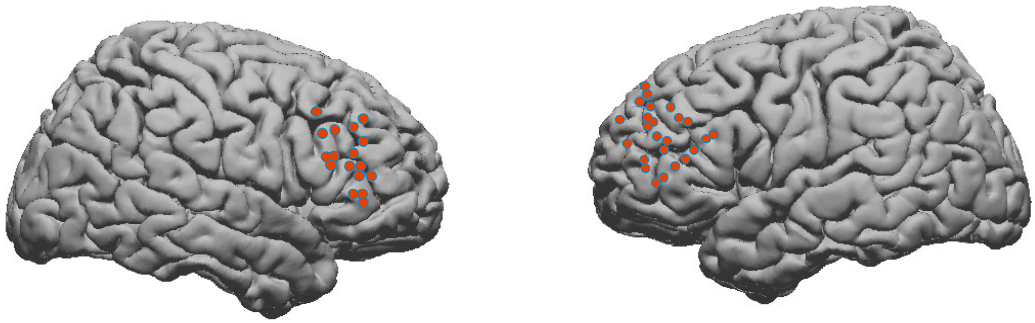

Figure 6.1.1: Dorsolateral Prefrontal Cortex Electrodes
Electrodes that were chosen were in the DLPFC, more specifically, they were in Brodmann areas 9 and 46. The wider distribution on the left cortex is due to subject electrode location rather than selection.

6.2 *Unique frequency response of DLPFC*

Electrodes in motor areas have historically shown a frequency response from approximately 70 Hz to 150 Hz (Miller, Leuthardt et al. 2007). Response from DLPFC electrodes, however, have a separable bandwidth ranging approximately from 160 Hz to 250 Hz. These differences are shown in the example in Figure 6.2.1. The response in DLPFC for goal tuning, and position tuning, was in the 160-250 Hz band. Goal tuning was shown as a simple comparison of mean cortical activation across two time periods. Position tuning can not be shown by a simple amplitude change between time periods (Figure 6.2.2). In

order to view the position tuning at these levels the bandwidth from 160 – 250 Hz needs to be combined and viewed based on target location.

Position tuning shows no absolute difference across different periods but does across different targets. Goal tuning shows no difference across targets but shows a difference across periods. Goal tuning of a wide high frequency band for two electrodes is shown in Figure 6.2.3; electrode 1 shows no goal tuning and electrode 2 shows a large change once the subject is on any target. The features displayed in Figure 6.2.3 and Figure 6.2.4 were created using a bandwidth between 160 Hz – 250 Hz as it showed typical tuning seen in electrodes in the DLPFC. Figure 6.2.4 has position tuning for electrode 1 but only during the Hold period, electrode 2 shows no position tuning. This shows that we should expect some position tuning throughout the population and some goal tuning; and each of these tunings may be represented in separate electrodes.

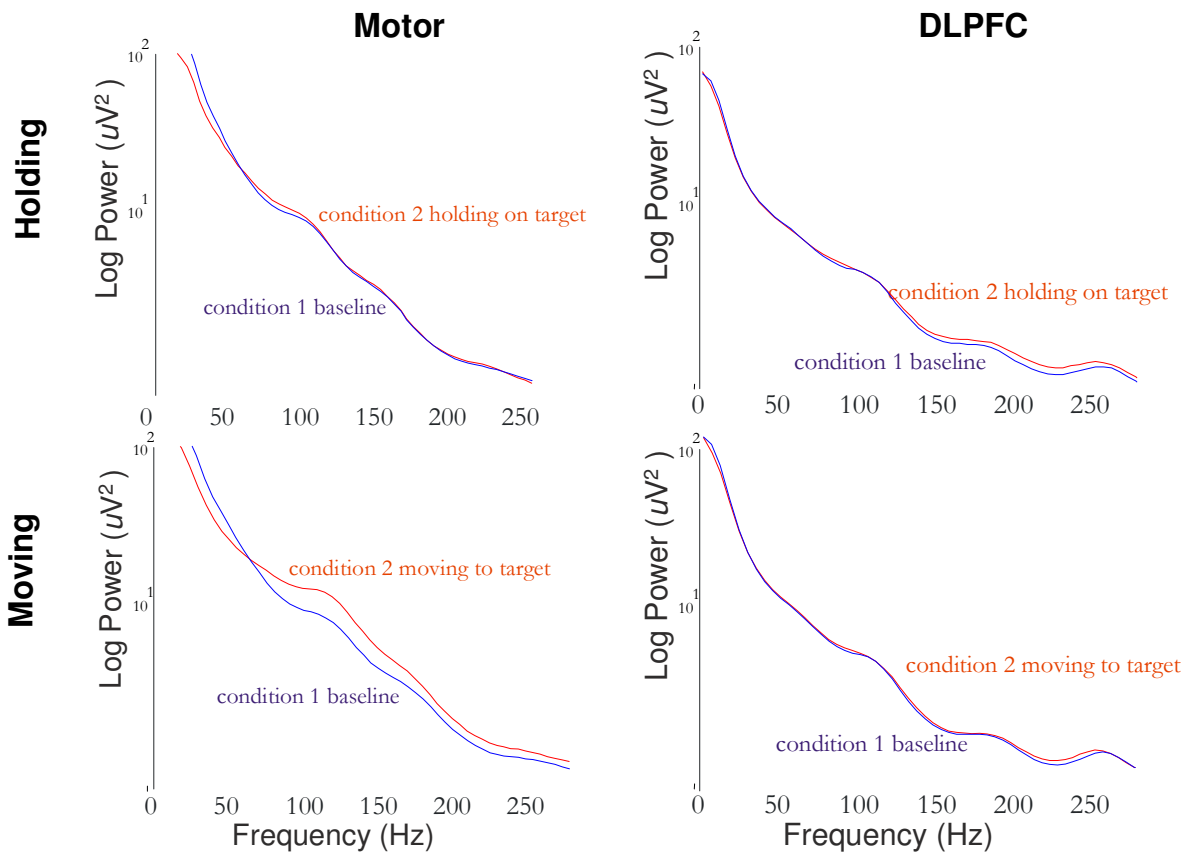

Figure 6.2.1: Example of DLPFC encoding from two channels.
Difference in amplitude of ECoG power from a motor electrode during a holding vs rest and a DLPFC electrode for holding vs rest. The difference in magnitude can be seen at different frequencies, particularly the magnitude below 120 Hz for the motor electrode and above 160 Hz for the DLPFC electrode. During the movement the motor electrode shows much broader tuning including in the high frequency band. The greatest difference in activations is in the 100 Hz region for the motor electrode during movement. There is no large difference in activation between baseline and movement for the DLPFC electrode.

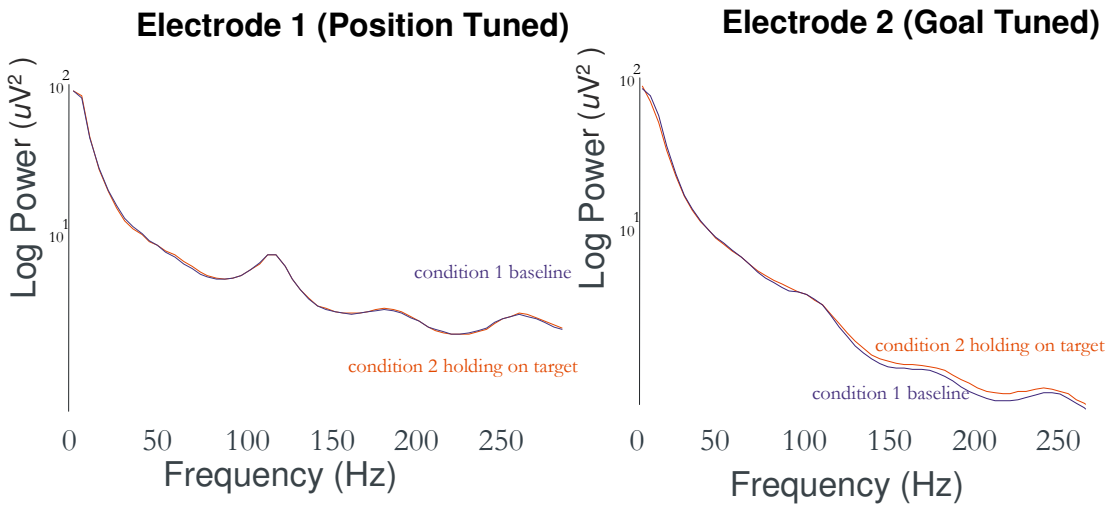

Figure 6.2.2: Comparison of two DLPFC electrodes
One electrode with directional tuning for position(left) vs goal tuning (right). The x-axis shows the frequency (Hz) and the y-axis shows Log Power of both conditions. There is no obvious difference in amplitude for the position tuned electrode. The goal tuned electrode shows a large change in amplitude in the higher frequency band.

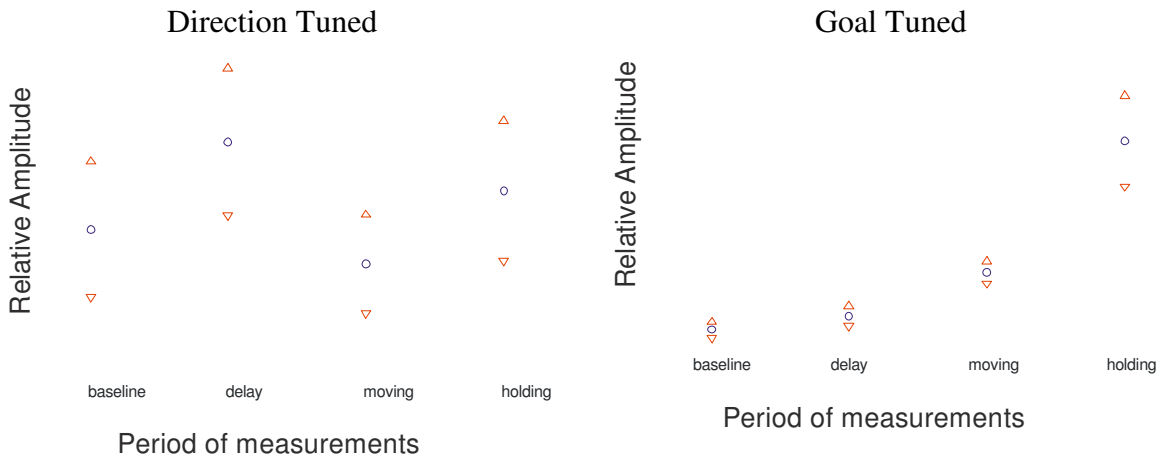

Figure 6.2.3: Comparison of two electrodes with different tuning in DLPFC
The figure displays a wide band high frequency (160-250 Hz) across different periods of Center Out. Relative amplitude is percent deviation from the mean of all periods. The blue circles represent the mean and the red triangles represent the mean plus or minus the standard deviation. By comparing these different periods, the goal tuned electrode can be seen to change in amplitude by a significant amount over these periods (thus the name goal tuning). The directional tuned electrode shows no systematic change over these periods.

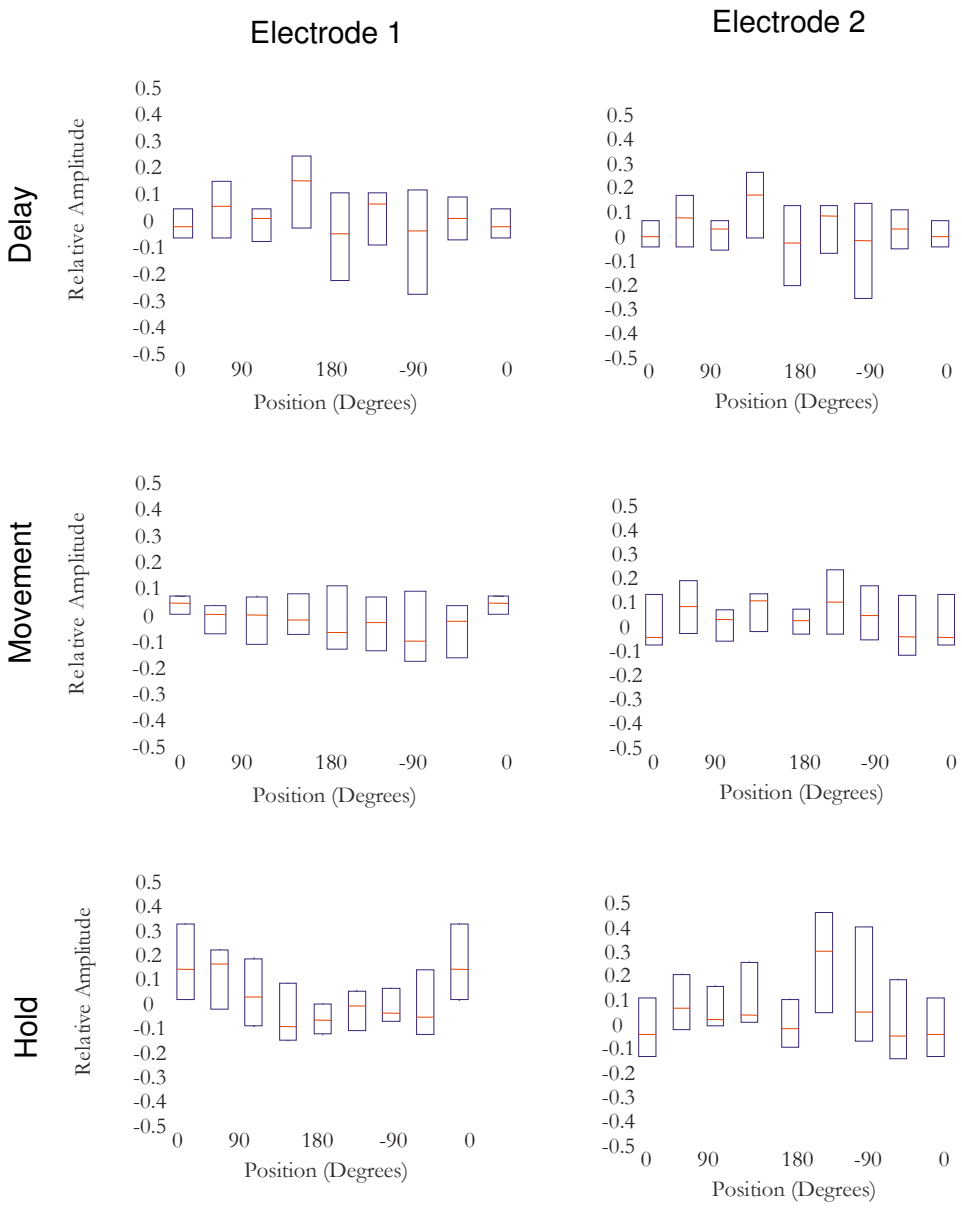

Figure 6.2.4: Comparison of wide band frequency across angle for two electrodes.
The red lines are the median of the data in that group, the lower bound on the box is the lower quarter and the upper bound is the upper quartile. The relative amplitude is percent deviation from baseline. The only state that shows statistically significant position tuning is the Hold period on Electrode 1. Features were said to be statistically significant if they had a $p < 0.05$ for their fit to the model. The rest of the periods show no statistically significant or obvious position tuning.

6.3 *Result from all features*

6.3.1 Comparison of Center Out periods

The goal tuning of one electrode which exemplified the response that was seen across the DLPFC, was discussed earlier. To quantify the response across the population of electrodes a T-test was used on each feature and then binned by frequency as discussed in Chapter 4. Results from the binned T-test can be seen in Figure 6.3.1. Statistical significance was determined by whether the number of electrodes exceeded what would be expected based on a binomial distribution at $p < .05$.

The goal tuning for comparison of Baseline to Delay, in the population, showed statistically significant results in the expected gamma range. However, when Baseline and Delay was compared to the Hold period the frequencies demonstrating significant alteration moved to a higher range. This is also demonstrated in Figure 6.2.1 for individual electrodes, these spectral changes are in a higher frequency range than has been traditionally demonstrated for motor associated ECoG activations.

Because of the more established experience and prior documented cortical physiology associated with movements, these three delay periods were also compared to the movement period. When all three periods were compared to the movement period, there was a broader tuning which was consistent with previous reported spectral changes (Miller, Leuthardt et al. 2007) . The results in Figure 6.3.2 show broad tuning for comparisons from movement to baseline and holding. Consistent with the proposed notion that DLPFC is more involved with motor planning than motor execution, the delay period versus the movement period showed little difference. (Tanji and Hoshi 2001; Astafiev, Shulman et al. 2003).

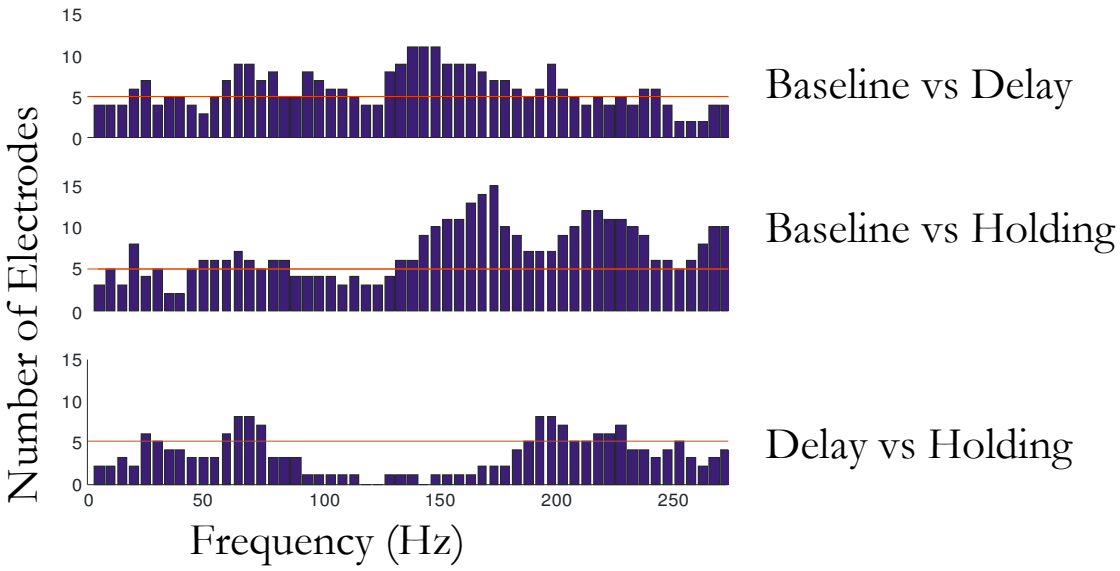

Figure 6.3.1: Comparison of delay periods for goal tuning.
Any number of electrodes greater than the red lin is statistically significant. Each of these comparisons shows statistical significance in different bands, and these results can be compared to Figure 6.3.3. Baseline vs Delay shows encoding of a target as the subject acquires their goal This is broadly tuned primarily around the spectra range related to motor activation. There is, however, some activation in the higher frequency range associated with the DLPFC. Baseline vs Holding shows primarily high frequency activation associated with the DLPFC. Delay vs Holding show a couple of bands that reached statistical significance but is a less striking activation than the comparison of Holding to Baseline.

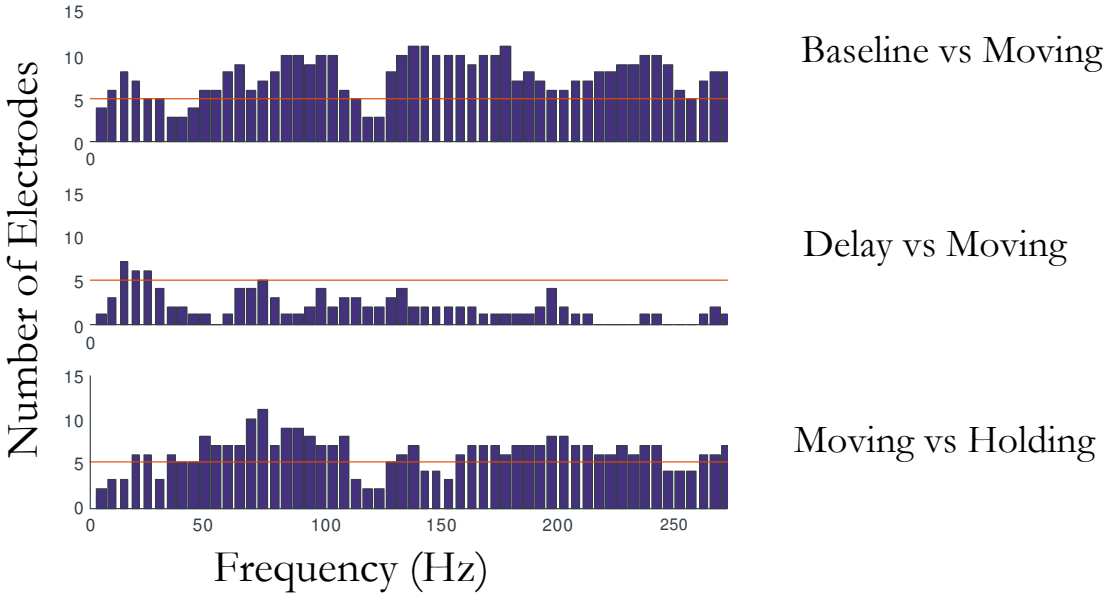

Figure 6.3.2: Movement period compared to other periods for goal tuning.
Any number of electrodes greater than the red line is statistically significant. Movement should show a broad difference when compared to most periods. This is the case for the comparison of Baseline to Holding, but the Delay period shows very little that is significant. The lack of statistically significant results in Delay vs Moving is interesting.

The DLPFC sites demonstrate a consistent change in spectral power to create the statistically significant results seen in Figure 6.3.1. This change was also evaluated over time by analyzing the amplitude deviation for each of the examined periods (baseline, delay, movement, and holding). This is shown in Figure 6.3.3. Percent deviation from the mean showed a decrease at all the higher frequencies during baseline. Respectively an increase in amplitude at the higher gamma frequencies (160 Hz and above) during delay was seen when the spectra of the entire population was evaluated. During the movement period, however, there was a broader band of increased spectral power encompassing which was different from that seen during the delay period. Most strikingly there was a large increase of amplitude at frequencies over 160 Hz during holding period. This is the largest percent deviation from the mean seen throughout these results. This percent deviation from the

mean was a measure of the goal encoding and does not change for position or direction tuning.

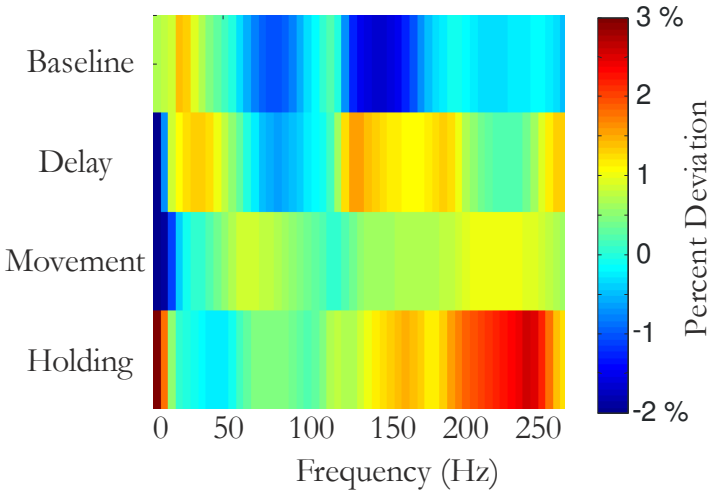

Figure 6.3.3: All electrode percent deviation from the mean for each period.
The color scale goes from -2-3% deviation from the mean. Each of the periods has a unique spectral deviation from the mean. Baseline and Movement are responses we have seen before; Baseline shows an increase at lower frequencies and a decrease at higher frequencies and Movement shows the opposite. The Delay period and Hold period show more interesting responses when compared to the others. Both Delay and Hold periods show an increase beginning in much higher frequencies than the movement period, and multiple unique bands that are not seen in Movement periods.

6.3.2 Position and Direction Tuning in the DLPFC

Position and direction fitting to the cosine tuned model were calculated as described in Chapter 4,. The analyses was different from Chapter 5 in that $p<0.05$ was used but no magnitude of tuning was placed as a threshold for significance. Positions were tuned to the target location and direction is tuned to the direction of the trial.

Position tuning showed statistically significant results in the higher frequency band particularly during the hold period. There are statistically significant results for both position and direction tuning, shown in Figure 6.3.4. The direction components were largely significant at lower frequencies in bands that had been previously implicated in other ECoG experiments (Miller, Leuthardt et al. 2007). The hold period shows the best position tuning (Figure 6.3.4) of any time period and this was primarily seen in frequencies above 160 hz. The delay period also shows its most significant results in the higher frequency band 150-250 Hz. The movement period tuning to position is best represented at lower frequencies, which is similar to the movement period of tuning of direction.

Directional tuning was seen in both periods (movement and delay) and was represented primarily in lower frequencies. Position appears to be preferentially encoded at higher frequencies, whereas direction appears to be preferentially encoded at lower frequencies. This low frequency vs high frequency dichotomy is interesting when comparing different kinematic variables as it helps elucidate the different neuronal populations involved in the activities.

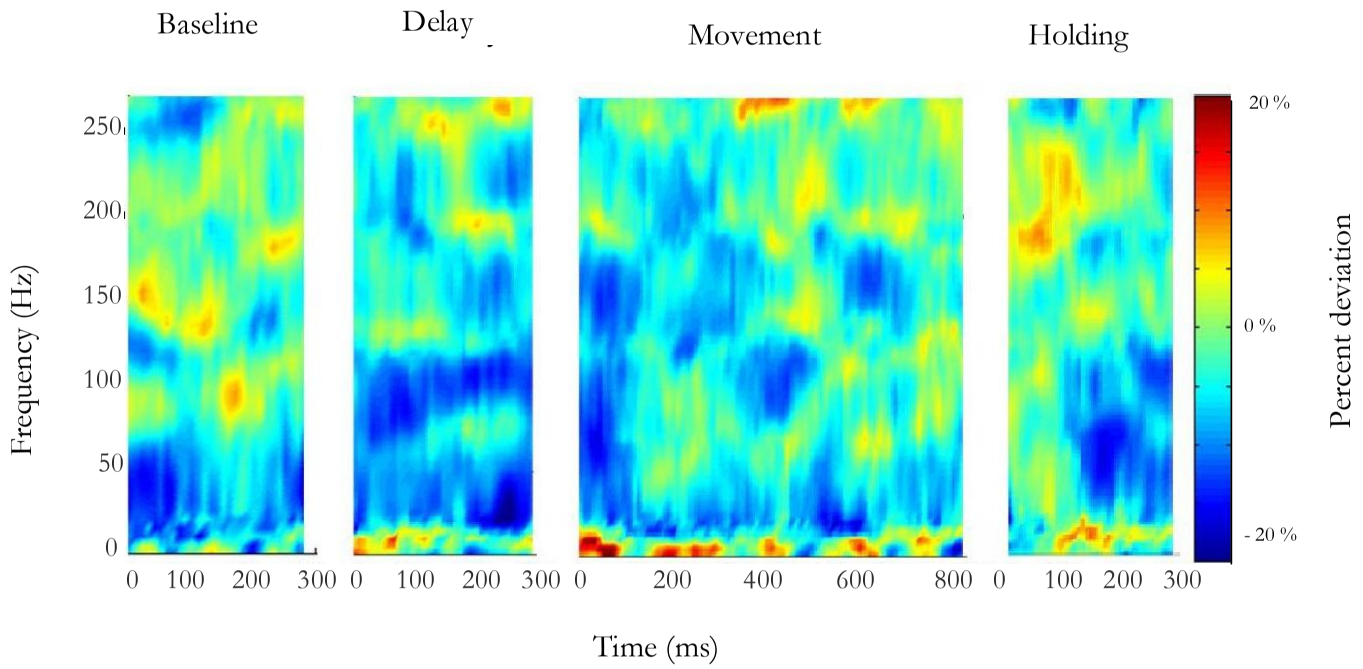

Figure 6.3.4: Temporal periods for encoding of a target goal.
This plot is the temporal information for one electrode over time. The activity is the percent deviation from the mean of all periods. This percent change is represented in the color from -20 to 20%. This figure can be compared to Figure 6.3.3. which shows the average over all electrodes used in this study for each period. The activations across time are similar for both this one electrode throughout time and the population as a whole.

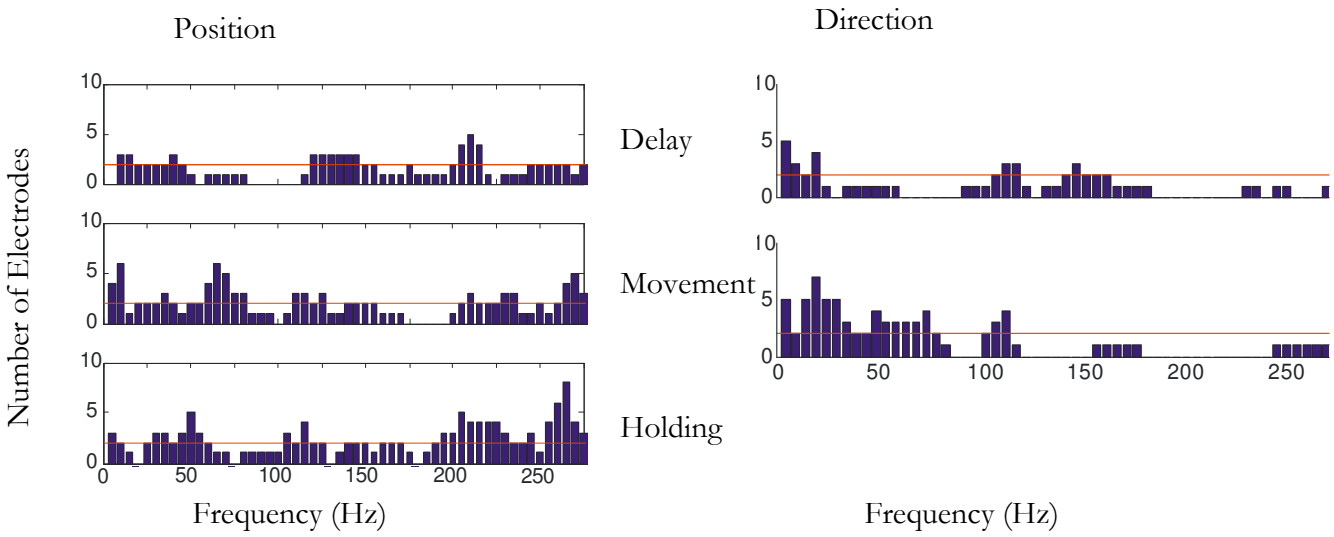

Figure 6.3.5: Tuning of position and direction in the DLPFC.
Any number of electrodes greater than the red lin is statistically significant. Position encoding is shown for all three periods. Direction is shown for the two it could be represented in, namely, delay and movement. Position seems to be encoded at higher frequencies similar to the results in the goal tuning. The results are most significant during the Hold period but also show some significance during the Delay period. Direction seems to be encoded at lower frequencies and is primarily encoded during the actual movement.

6.3.3 Comparison to other functional areas

Two electrodes were show in Figure 6.1.1 to demonstrate the difference in spectra of an electrode in a motor area from that in the DLPFC. The motor and DLPFC populations show similar results to Figure 6.1.1. There is broad tuning across the gamma range in the motor area and high frequency band (160-250 Hz) tuning above those typically expected in the DLPFC, shown in Figure 6.3.6. This shift to higher frequencies appears to continue as detection moves farther anterior. The highest percentages of electrodes that show differences are in the frontal areas (Brodmann areas 47 and 11). In addition the frontal areas show nothing statistically significant in bands below this high frequency range.

This trend is of importance as it appears that cortical areas can encode information at higher frequencies than has been seen previously in ECoG. It has been shown in other studies that higher frequency Local Field Potentials (LFPs) are encoding information in cortices of animals (Jones and Barth 1999; Jones, MacDonald et al. 2000; Staba, Ard et al. 2005). However, in humans this is largely unexplored territory and warrants further investigation. Unfortunately 280 Hz and higher is near the limit of what the amplifiers could handle in terms of magnitude so higher frequency information could not be obtained.

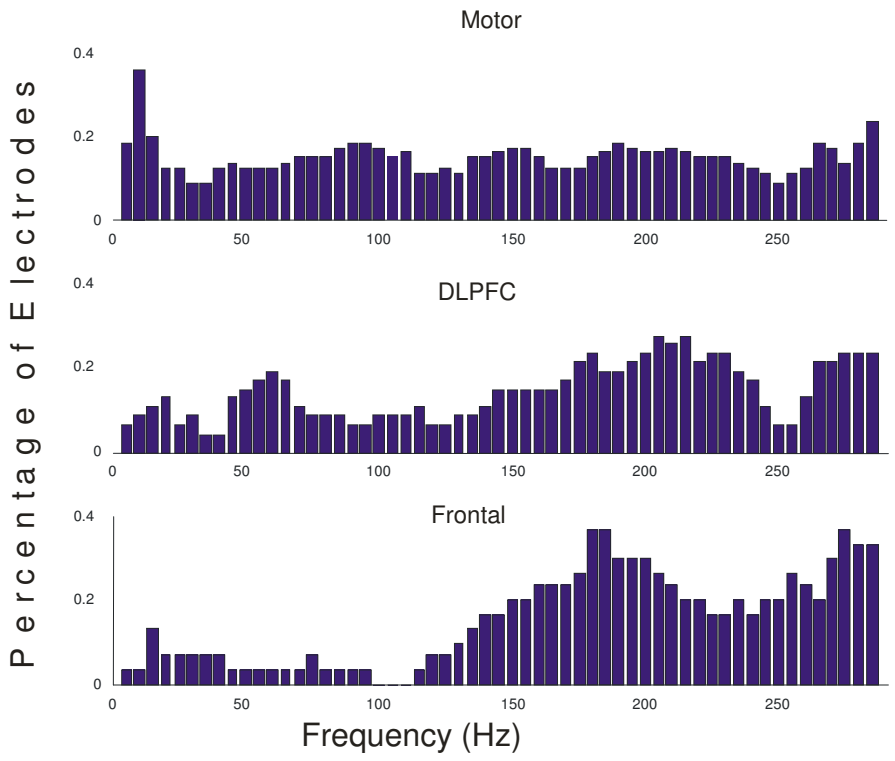

Figure 6.3.6: Cortical Progession
Demonstrates the goal (non directional) analysis of Baseline vs Holding comparison for each of the different functional areas has a different frequency response. The motor areas show a broad tuning across many frequencies for this comparison. The DLPFC shows a greater response in the higher frequency range 150-250 Hz than in the lower frequency range. Finally the Frontal areas show a much greater response in high frequency components than in low frequency components.

6.4 Discussion

A non-directional goal signal has been found and tested for efficacy as a mouse click which was the original goal of Specific Aim 2. This goal signal while identified has not been proven effective in a closed loop BCI. It is unclear as to whether a subject will be able to control this signal but it is likely given other work done in ECoG for BCI (Ramsey, van de

Heuvel et al. 2006; Felton, Wilson et al. 2007). With training a subject should be able to control this signal given some level of efficacy.

It is encouraging that direction encoding is found and this may prove effective for BCI in the future as well given that other BCI studies have shown effectiveness in this area (Ramsey, van de Heuvel et al. 2006). Position tuning is not as well represented in this area as in motor areas. We hypothesize that this could be because of overlapping receptive fields. This was an issue for Heldman et al in previous local field potential work with receptive fields in motor areas (Heldman 2007).

Despite decreased representation of both non-directional goal signals and directional signals over single units, the DLPFC ECoG activity could be useful in BCI. This area has proven to be controllable by other studies and it encodes for both signals that were examined. Further examination of this area would likely be able to identify more signals of use and find more support for use of this area in BCI. It is a particularly good candidate for BCI if more traditional available areas have been damaged (i.e. stroke).

7 Conclusions

There were two aims proposed in Chapter 1 of this thesis and each had results that have implications that will affect the understanding of what is encoded in ECoG as well as the type of BCI it can be used for. In Specific Aim 1 we looked at the tuning of arm movement kinematics in different cortical regions. The results showed that there was encoding of kinematics in many areas of the cortex that could be useful for BCI. In Specific Aim 2 the experiments were designed to find a goal encoding signal in the Dorsolateral Prefrontal Cortex (DLPFC), which could be used as a binary selection control (i.e., Mouse Click). These experiments found a signal encoding for goal targets, and also explored how the DLPFC encodes direction and position information.

7.1 Specific Aim 1: Tuning of Cortical Potential to Arm movements

In Aim 1 it was proposed to determine the tuning of arm movement kinematics in neural signals collected using ECoG features. Experiments were designed to dissociate the movement kinematics of velocity and position. Velocity would further be decomposed into direction and speed. These four variables were then correlated to features of the ECoG signals collected. Specific results were expected based on previous work which had shown tuning of these kinematic variables in different portions of the brain (DeAngelis, Cumming et al. 1998; Moran and Schwartz 1999b; Pochon, Levy et al. 2001; Schalk, Kubanek et al. 2007).

In this study the motor areas did show higher correlation to two of the kinematics related to movement, direction and velocity. These two components have shown strong

encoding in motor cortex in previous single unit studies (Moran and Schwartz 1999b; Schwartz and Moran 1999c). In addition these components were represented in the 70-150 Hz band, which was expected, as recent studies had shown activation for motor tasks (Miller, Leuthardt et al. 2007). These two components fit neatly into the existing understanding of how motor actions are controlled by and correlated to neural activity recorded by ECoG. The remaining two kinematic components (position and speed) display much broader tuning in neuro-anatomy and frequency.

Speed was expected to have widespread representation based on previous work by Heldman et al (Heldman 2007). Expectedly the motor areas showed a positive correlation to speed; however, all other areas showed a negative correlation to speed during actual movements. This could be explained as an attention effect. As a subject concentrates more on their movements they focus more resources on the motor areas, increasing motor activation and decreasing other areas at the same time they are moving faster. During the Delay period of the Center Out task, more areas showed a positive correlation to the following speed. This can be described as an attention effect as well; more attention during preparation would correlate to higher activations and thus a positive correlation to the speed during the following movement (Cisek 2006).

Position was encoded in most of the locations that were examined (i.e., frontal, motor, posterior parietal, and temporal) and at higher frequencies than have been seen previously in motor based tasks. The positions in the task were correlated across many different aspects of the task (i.e., attention, and movement) in these experiments; thus, it is not surprising that many of the areas are correlated.

The higher frequency encoding of position is possibly related to smaller cortical units being recruited than the motor areas that drive direction and velocity. Larger groups of

neurons seem to manifest themselves at lower frequencies and thus if position is being represented by smaller cortical units we may likely see position represented at higher frequencies (Nunez and Srinivasan 2006). There is some evidence even within primary motor cortex, fewer neurons represent position than other kinematics (Georgopoulos, Kalaska et al. 1982; Wang, Chan et al. 2007). In addition position is not unique to motor cortex as it is represented for eye movements and attention areas as well, this helps support that position is represented at higher frequencies in motor cortical ECoG data.

Comparison of preferred directions across tasks yielded very robust and encouraging results. The angles between preferred directions of the same component (e.g., position) were hypothesized to show very little difference across the two separate tasks (Tracing and Center Out) based on previous studies (Moran and Schwartz 1999b). Delay and Movement of Center Out seemed to be most similar for direction and velocity. The actual position of the cursor is very different during Hold than Delay, this seems to indicate that in most cases cortex is encoding for the cursor position and not the target position. All three components (velocity, position, and direction) were the same across the Movement period of Center Out and Tracing. This stability across different movements helps support its relationship to hand position and the robust nature of this encoding. In addition, the stability of these comparisons is particularly impressive as they are performed hours apart.

Stability in preferred direction is supported by our understanding of the receptive fields. Single cells may change their encoding due to plasticity, and micro LFPs have issues with overlapping receptive fields; ECoG records from many cortical columns and it is likely the encoding of a movement remains relatively stable at this macroscopic level. From a BCI standpoint this stability in preferred directions is ideal for an ECoG BCI paradigm.

Finally, it was hypothesized that the distant electrodes particularly at higher frequencies would show dissimilar preferred directions. The results show a high level of correlation in preferred directions, even at 8cm distance on the surface of the cortex. These results led to the further test of features showing non-statistically significant tuning over the surface of the cortex, these un-tuned features showed no correlation based on distance. The data seems to indicate that the cortex is keeping a relatively constant representation of this task. However, many of the factors in this experiment are correlated, so this may be particular to this experiment.

7.2 Specific Aim 2: DLPFC encoding

It was hypothesized that the DLPFC would show goal and/or position encoding in the Center Out task and both types of encoding were found. Goal encoding was found to be heavily represented in this area of cortex, and at higher frequencies than anticipated. ECoG direction encoding was also represented at higher frequencies, but not as well as single units in the same area (Iba and Sawaguchi 2003; Funahashi, Takeda et al. 2004; Tsujimoto, Genovesio et al. 2008).

The gradual increase to higher frequency representations in the cortex as one move from motor to frontal areas raises interesting questions about what signals we are recording using ECoG. As discussed earlier, smaller groups of neurons seem to manifest at higher frequencies than larger groups. This manifestation is likely correlated to the amount of cortical area involved in the processing, indicating there are many smaller cortical areas manifesting higher frequency signals. Future research should explore the actual sizes of these areas as well as the smallest area that ECoG can reliably detect.

These higher frequency bands in DLPFC were statistically significant primarily during planning stages rather than movement periods. This held true for both the non directional signals and the directional signals found through fitting to the cosine tuning model. This result helps us to again conclude that the DLPFC is involved in planning of motor responses rather than executing these movements.

When the spectral amplitude of all electrodes in the DLPFC are compared across periods the higher frequency encoding of attention components remains dominant. While there is broad activation in the movement period, which is possibly a bleed over from motor areas, the high frequency component is dominant for the baseline, delay, and hold periods when compared to the average of all periods. This higher frequency dominance of attention period becomes more apparent as the electrodes move further anterior. This is likely because fewer of the neurons are involved in movement as the electrodes are further anterior then if they are adjacent to motor areas or smaller cortical groups are involved in processing in these anterior areas.

Overall changes in activation (power) of DLPFC were much smaller than motor areas, which was why a trial by trial analysis had to be used. This more sensitive analysis seems to show that ECoG is maturing as a recording paradigm and will need more complicated and robust analysis and decoding algorithms in the future. Increased sensitivity of analysis and recordings will demand careful experimental design in the future.

7.3 Application to BCI and implications for neuroscience

Generalized ECoG feature tuning found in non-motor cortical regions is quite useful to BCI. It has yet to be seen whether these non-motor regions can be controlled by a user, however it is likely given the history of BCI and ability of users to learn to control them

(Wolpaw, McFarland et al. 2003; Leuthardt, Schalk et al. 2004; Kubler, Nijboer et al. 2005). Identification of tuning vectors for use in a multiple degree of freedom BCI, could help create a BCI using only a few electrodes in different cortical areas. Encouragingly these preferred directions in ECoG recordings seem to be more stable than single units, making it easier to create a more robust BCI.

The robust tuning across time and tasks is encouraging but the common tuning across different anatomical locations may require additional training. The high degree of correlation across features on different electrodes in the same time period of each task needs to be addressed. The features need to be independently controllable by the user in order to obtain multidimensional control. This high degree of correlation raises concerns about the possible independence of these features.

The DLPFC does show promise as an area that could be used for BCI since it has both goal encoding and direction tuning. This attention area can be controlled by users, so it should prove useful for BCI. In addition, motor areas tend to degrade after neural injury so this frontal attention area may be a more stable location to allow a user to control a BCI (Andersen, Burdick et al. 2004).

Use of the DLPFC for a mouse click will likely require some training by the user. As we showed in Chapters 4, the directional signals interfere with the goal encoding signals for some types of decoding. It is likely that a novel decoding algorithms combined with user training will be required. With this type of set up it should have some efficacy as a mouse click signal.

7.4 Future Work

Applying results of Aim1 and 2 to a closed-loop BCI application is the next logical step in development. We have shown detection of the desired control signals but not

whether a subject can actively control the available signals. Both aims show promise but there are issues with regarding to whether these are in fact controllable effects. However, we cannot be certain whether the identified signals are controllable until closed loop experiments have been conducted.

In attempting or achieving closed loop control these signals will change. As discussed in Chapter 2, when closed loop control is achieved on signals they change in different ways. The signals identified in this thesis will undoubtedly change when they are put into a closed loop system. Based on previous experience, it is likely the signals will be able to achieve better control than what initial results have indicated (Heldman 2007).

Correlation of features across different electrodes is the next stage of analysis. While this thesis viewed each electrode as an independent source, more neuroscience and BCI work can be done by quantifying the interactions of these features. An analysis that quantifies electrode locations should be able to greatly increase our understanding of the interaction of cortical areas. ECoG creates an opportunity to look at these interactions on time and spatial scales that other modalities cannot.

Correlation of information across electrodes could also greatly increase the efficacy and accuracy of a BCI. Activity across different electrodes provides additional dimensions to the data (in this case an increase by 2^{64}). Use of this additional dimension of data could provide more degrees of freedom then current BCI systems. It also provides the opportunity to create a system that can be used by patients to lead more normal lives (i.e., multidimensionality, asynchronous control). If these opportunities of ECoG are taken advantage of, it could provide real improvement over existing BCI technology and more importantly to patient's lives.

References

A.H.A. (2007). Heart Disease and Stroke Statistics.

Andersen, R. A., J. W. Burdick, et al. (2004). "Cognitive neural prosthetics." Trends Cogn Sci **8**(11): 486-93.

Andersen, R. A., J. W. Burdick, et al. (2004). "Recording advances for neural prosthetics." Conf Proc IEEE Eng Med Biol Soc **7**: 5352-5.

Andersen, R. A., S. Musallam, et al. (2004). "Selecting the signals for a brain-machine interface." Curr Opin Neurobiol **14**(6): 720-6.

Anderson, C. W., E. A. Stolz, et al. (1998). "Multivariate Autoregressive Models for Classification of Spontaneous Electroencephalographuc Signals During Mental Tasks." IEEE Trans Biomed Eng **45**: 277-286.

Anderson, N. R., K. Wisneski, et al. (2009). "An Offline Evaluation of the Autoregressive Spectrum for Electrocorticography." IEEE Trans Biomed Eng.

Barkley, G. L. (2004). "Controversies in neurophysiology. MEG is superior to EEG in localization of interictal epileptiform activity: Pro." Clin Neurophysiol **115**(5): 1001-9.

Berger, H. (1929). "Ueber das Electroenkephalogramm des Menschen." Arch Psychiat Nervenkr **87**: 527-570.

Bertrand, O. "EEG/MEG oscillatory synchronization in sensory and cognitive functions."

Birbaumer, N. (2006). "Brain-computer-interface research: coming of age." Clin Neurophysiol **117**(3): 479-83.

Birbaumer, N., A. Kubler, et al. (2000). "The thought translation device (TTD) for completely paralyzed patients." IEEE Rehabilitation **8**(2): 190-193.

Bremer, F. (1958). "Cerebral and cerebellar potentials." Physiol Rev **38**(3): 357-88.

Brodmann, K. (1905). "Beiträge zur histologischen Lokalisation der Grosshirnrinde: dritte Mitteilung: Die Rindenfelder der niederen Affen." Journal für Psychologie und Neurologie.

Carmena, J. M., M. A. Lebedev, et al. (2005). "Stable ensemble performance with single-neuron variability during reaching movements in primates." J Neurosci **25**(46): 10712-6.

Castillo, E. M., P. G. Simos, et al. (2004). "Integrating sensory and motor mapping in a comprehensive MEG protocol: clinical validity and replicability." Neuroimage **21**(3): 973-83.

Cisek, P. (2006). "Preparing for speed. Focus on "Preparatory activity in premotor and motor cortex reflects the speed of the upcoming reach"." J Neurophysiol **96**(6): 2842-3.

Cohen, D. (1968). "Magnetoencephalography: evidence of magnetic fields produced by alpha rhythm currents." Science **161**: 784-6.

Cohen, M. S. and S. Y. Bookheimer (1994). "Localization of brain function using magnetic resonance imaging." Trends Neurosci **17**(7): 268-77.

Conover, W. J. (1980). Practical Nonparametric Statistics.

Corbetta, M. and G. L. Shulman (2002). "Control of goal-directed and stimulus-driven attention in the brain." Nat Rev Neurosci **3**(3): 201-15.

Crone, N. E., L. Hao, et al. (2001). "Electrocorticographic gamma activity during word production in spoken and sign language." Neurology **57**(11): 2045-53.

Curtis, C. E., V. Y. Rao, et al. (2004). "Maintenance of Spatial and Motor Codes during Oculomotor Delayed Response Tasks." J. Neurosci. **24**(16): 3944-3952.

D'Esposito, M., D. Ballard, et al. (2000). "The role of prefrontal cortex in sensory memory and motor preparation: an event-related fMRI study." Neuroimage **11**(5 Pt 1): 400-8.

Daemon, T. "Talairach Daemon." from (http://ric.uthscsa.edu/projects/talairachdaemon.html).

Dalton, A. J. (1969). "Discriminative conditioning of hippocampal electrical activity in curarized dogs." Comm. Behav. Biol **3**: 283-287.

Dean J. Krusienski, D. J. M., Jonathan R. Wolpaw (2006). "An Evaluation of Autoregressive Spectral Estimation Model Order for Brain-Computer Interface Applications." IEEE 28the EMBSE International Conference.

DeAngelis, G. C., B. G. Cumming, et al. (1998). "Cortical area MT and the perception of stereoscopic depth." Nature **394**(6694): 677-80.

di Pellegrino, G. and S. P. Wise (1993). "Visuospatial versus visuomotor activity in the premotor and prefrontal cortex of a primate." J. Neurosci. **13**(3): 1227-1243.

Donoghue, J. P. (2002). "Connecting cortex to machines: recent advances in brain interfaces." Nat Neurosci **5 Suppl**: 1085-8.

Donoghue, J. P., J. N. Sanes, et al. (1998). "Neural discharge and local field potential oscillations in primate motor cortex during voluntary movements." J Neurophysiol **79**(1): 159-73.

Evarts, E. V., C. Fromm, et al. (1983). "Motor Cortex control of finely graded forces." J Neurophysiol **49**(5): 1199-1215.

Evarts, E. V. and J. Tanji (1976). "Reflex and intended responses in motor cortex pyramidal tract neurons of monkey." J Neurophysiol **39**(5): 1069-80.

Fetz, E. E. (1999). "Real-time control of a robotic arm by neuronal ensembles." Nat Neurosci **2**(7): 583-4.

Fetz, E. E. and D. V. Finocchio (1971). "Operant conditioning of specific patterns of neural and muscular activity." Science **174**(7): 431-5.

Fetz, E. E. and D. V. Finocchio (1975). "Correlations Between Activity of Motor Cortex Cells and Arm Muscles During Operantly Conditioned Response Patterns." Exp Brain Res **23**: 217-240.

Fetz, E. E., D. V. Finoccio, et al. (1971). "Sensory and motor responses of precentral cortex cells during compatible passive and active joint movements." j-np **43**: 1070-1089.

Foxe, J. J. and G. V. Simpson (2002). "Flow of activation from V1 to frontal cortex in humans. A framework for defining "early" visual processing." Exp Brain Res **142**(1): 139-50.

Fu, Q. G., J. I. Suarez, et al. (1993). "Neuronal specification of direction and distance during reaching movements in the superior precentral premotor area and primary motor cortex of monkeys." J Neurophysiol **70**(5): 2097-116.

Funahashi, S., C. J. Bruce, et al. (1989). "Mnemonic coding of visual space in the monkey's dorsolateral prefrontal cortex." J Neurophysiol **61**(2): 331-349.

Funahashi, S., C. J. Bruce, et al. (1990). "Visuospatial coding in primate prefrontal neurons revealed by oculomotor paradigms." J Neurophysiol **63**(4): 814-831.

Funahashi, S., C. J. Bruce, et al. (1993). "Dorsolateral prefrontal lesions and oculomotor delayed-response performance: evidence for mnemonic "scotomas"." J. Neurosci. **13**(4): 1479-1497.

Funahashi, S., K. Takeda, et al. (2004). "Neural mechanisms of spatial working memory: contributions of the dorsolateral prefrontal cortex and the thalamic mediodorsal nucleus." Cogn Affect Behav Neurosci **4**(4): 409-20.

Fuster, J. M. and G. E. Alexander (1971). "Neuron Activity Related to Short-Term Memory." Science **173**(3997): 652-654.

G Schalk, J. K., K J Miller, N R Anderson, E C Leuthardt, J G Ojemann, D Limbrick, D Moran, L A Gerhardt, J R Wolpaw (2007). "Decoding two-dimensional movement trajectories using electrocorticographic signals in humans." Journal of Neural Engineering.

G. Schalk, J. K., K.J. Miller, N. Anderson, E.C. Leuthardt, J.G. Ojemann, D.Limbrick, D. Moran, L.A. Gerhardt, J.R. Wolpaw (2007). "Decoding Two-Dimensional

Movement Trajectories Using Electrocorticographic Signals in Humans." Neural Engineering.

Gassert, R., L. Dovat, et al. (2005). "Multi-joint arm movements to investigate motor control with FMRI." Conf Proc IEEE Eng Med Biol Soc **5**: 4488-91.

Georgopoulos, A. P. (1995). "Current issues in directional motor control." Trends Neurosci **18**(11): 506-10.

Georgopoulos, A. P., J. F. Kalaska, et al. (1982). "On the relations between the direction of two-dimensional arm movements and cell discharge in primate motor cortex." J Neurosci **2**(11): 1527-37.

Georgopoulos, A. P., R. E. Kettner, et al. (1988). "Primate motor cortex and free arm movements to visual targets in three-dimensional space. II. Coding of the direction of movement by a neuronal population." J Neurosci **8**(8): 2928-37.

Georgopoulos, A. P., F. J. Langheim, et al. (2005). "Magnetoencephalographic signals predict movement trajectory in space." Exp Brain Res **167**(1): 132-135.

Georgopoulos, A. P., A. B. Schwartz, et al. (1986). "Neuronal population coding of movement direction." Science **233**(4771): 1416-9.

Guger, C., G. Edlinger, et al. (2003). "How many people are able to operate an EEG-based brain-computer interface (BCI)?" IEEE Trans Neural Syst Rehabil Eng **11**(2): 145-7.

Heldman, D. (2007). Epidural Electrocorticography and Intra-Cortical Local Field Potentials in Motor Cortex During Volitional Arm Movements and Their Applications to Neural Prosthetic Control. Biomedical Engineering.

Heldman, D. A., W. Wang, et al. (2004). "Local field potential spectral tuning in primary motor cortex." Soc. Neurosci. Abstr. **421.22**.

Heldman, D. A., W. Wang, et al. (2006). "Local field potential spectral tuning in motor cortex during reaching." IEEE Trans Neural Syst Rehabil Eng **14**(2): 180-3.

Hochberg, L. R., M. D. Serruya, et al. (2006). "Neuronal ensemble control of prosthetic devices by a human with tetraplegia." Nature **442**(7099): 164-71.

Huk, W. J. and J. Vieth (1993). "[Functional imaging of the brain. Magnetoencephalography (MEG)]." Radiologe **33**(11): 633-8.

Iba, M. and T. Sawaguchi (2003). "Involvement of the dorsolateral prefrontal cortex of monkeys in visuospatial target selection." J Neurophysiol **89**(1): 587-99.

Jahanshahi, M., G. Dirnberger, et al. (2001). "Does the pre-frontal cortex contribute to movement-related potentials? Recordings from subdural electrodes." Neurocase **7**(6): 495-501.

Jarvelainen, J. and M. Schurmann (2002). "The motor cortex approximately 20 Hz rhythm reacts differently to thumb and middle finger stimulation: an MEG study." Neuroreport **13**(10): 1243-6.

Jerbi, K., J. P. Lachaux, et al. (2007). "Coherent neural representation of hand speed in humans revealed by MEG imaging." Proc Natl Acad Sci U S A **104**(18): 7676-81.

Jones, M. S. and D. S. Barth (1999). "Spatiotemporal organization of fast (>200 Hz) electrical oscillations in rat Vibrissa/Barrel cortex." J Neurophysiol **82**(3): 1599-609.

Jones, M. S., K. D. MacDonald, et al. (2000). "Intracellular correlates of fast (>200 Hz) electrical oscillations in rat somatosensory cortex." J Neurophysiol **84**(3): 1505-18.

Jueptner, M. and C. Weiller (1995). "Review: does measurement of regional cerebral blood flow reflect synaptic activity? Implications for PET and fMRI." Neuroimage **2**(2): 148-56.

Kai J. Miller, E. C. L., Gerwin Schalk, Rajesh P. N. Rao, Nicholas R. Anderson, Daniel W. Moran John W. Miller, and Jeffrey G. Ojemann (2007). "Spectral Changes in Cortical Surface Potentials during Motor Movement." The Journal of Neuroscience.

Kawaguchi, S., S. Ukai, et al. (2005). "Information processing flow and neural activations in the dorsolateral prefrontal cortex in the Stroop task in schizophrenic patients. A spatially filtered MEG analysis with high temporal and spatial resolution." Neuropsychobiology **51**(4): 191-203.

Kipke, D. R., R. J. Vetter, et al. (2003). "Silicon-substrate intracortical microelectrode arrays for long-term recording of neuronal spike activity in cerebral cortex." IEEE Trans Neural Syst Rehabil Eng **11**(2): 151-5.

Kostov, A. and M. Polak (2000). "Parallel man-machine training in development of EEG-based cursor control." IEEE Trans Rehabil Eng **8**(2): 203-5.

Krusienski, D. J. (2008). Personal Communication Concerning the MEM Filter.

Krusienski, D. J., G. Schalk, et al. (2006). "A mu Rhythm Matched Filter for Continuous Control of a Brain-Computer Interface." IEEE Biomed: submitted.

Kubler, A., F. Nijboer, et al. (2005). "Patients with ALS can use sensorimotor rhythms to operate a brain-computer interface." Neurology **64**(10): 1775-7.

Kubota, K. and S. Funahashi (1982). "Direction-specific activities of dorsolateral prefrontal and motor cortex pyramidal tract neurons during visual tracking." J Neurophysiol **47**(3): 362-376.

Kubota, K. and H. Niki (1971). "Prefrontal cortical unit activity and delayed alternation performance in monkeys." J Neurophysiol **34**(3): 337-347.

Lancaster, J. F., Peter. "Talairach Daemon." from (http://ric.uthscsa.edu/projects/talairachdaemon.html).

Leuthardt, E. C. (2006). "What's holding us back? Understanding barriers to innovation in academic neurosurgery." Surg Neurol **66**(4): 347-9; discussion 349.

Leuthardt, E. C., Miller, K.J., Schalk, G, Rao, R.N., and Ojemann, J.G. (2006). "Electrocorticography-Based Brain Computer Interface - The Seattle Experience." IEEE - Neural Systems and Rehabilitation Engineering.

Leuthardt, E. C., G. Schalk, et al. (2006). "The emerging world of motor neuroprosthetics: a neurosurgical perspective." Neurosurgery **59**(1): 1-14; discussion 1-14.

Leuthardt, E. C., G. Schalk, et al. (2004). "A brain-computer interface using electrocorticographic signals in humans." J Neural Eng **1**(2): 63-71.

Leuthardt, E. C., Schalk, G., Moran, D., and Ojemann, J.G. (2006). "The Emerging World of Motor Neuroprosthetics, A Neurosurgical Perspective." Neurosurgery **59**(1): 1-14.

Levy, C. E., D. S. Nichols, et al. (2001). "Functional MRI evidence of cortical reorganization in upper-limb stroke hemiplegia treated with constraint-induced movement therapy." Am J Phys Med Rehabil **80**(1): 4-12.

Licklider, J. C. R. (1960). "Man-Computer Symbiosis." IRE Transactions on Human Factors in Electronics **1**: 4-11.

Lotze, M., M. Erb, et al. (2000). "fMRI evaluation of somatotopic representation in human primary motor cortex." Neuroimage **11**(5 Pt 1): 473-81.

Marple, S. L. (1987). Digital spectral analysis with applications. Englewood Cliffs, N.J., Prentice-Hall.

Martin, T., J. M. Houck, et al. (2006). "MEG reveals different contributions of somatomotor cortex and cerebellum to simple reaction time after temporally structured cues." Hum Brain Mapp **27**(7): 552-61.

Matelli, M., G. Rizzolatti, et al. (1993). "Activation of precentral and mesial motor areas during the execution of elementary proximal and distal arm movements: a PET study." Neuroreport **4**(12): 1295-8.

McCarthy, G., A. Puce, et al. (1996). "Activation of Human Prefrontal Cortex during Spatial and Nonspatial Working Memory Tasks Measured by Functional MRI." Cereb. Cortex **6**(4): 600-611.

McFarland, D. J., A. T. Lefkowicz, et al. (1997). "Design and operation of an EEG-based brain–computer interface with digital signal processing technology." Behavior Research Methods, Instruments, & Computers **29**(3): 337-345.

McFarland, D. J., T. Lefkowicz, et al. (1997). "Design and operation of an EEG-based brain-computer interface (BCI) with digital signal processing technology." BEHRESMETH **29**: 337-345.

McFarland, D. J., W. A. Sarnacki, et al. (2005). EEG-based two-dimensional movement and target selection by a non-invasive brain-computer interface in humans: emulating full mouse control. Society for Neuroscience, Washington D.C.

Mellinger, J., G. Schalk, et al. (2005). A brain-computer interface (BCI) based on magneto-encephalography (MEG).

Mellinger, J., G. Schalk, et al. (2007). "An MEG-based brain-computer interface (BCI)." Neuroimage **36**(3): 581-93.

Menon, V., G. H. Glover, et al. (1998). "Differential activation of dorsal basal ganglia during externally and self paced sequences of arm movements." Neuroreport **9**(7): 1567-73.

Merlet, I. (2001). "Dipole modeling of interictal and ictal EEG and MEG paroxysms." Epileptic Disord **Special Issue**: 11-36.

Miller, K. J., E. C. Leuthardt, et al. (2007). "Spectral changes in cortical surface potentials during motor movement." J Neurosci **27**(9): 2424-32.

Miller, K. J. M., S.
Hebb, A., R. Rao, et al. (2007). "Cortical electrode localization from X-rays and simple mapping for electrocorticographic research: The 'Location on Cortex' (LOC) package for MATLAB." Journal of Neuroscience Methods **162**(1-2).

Moran, D. W. and A. B. Schwartz (1999a). "Motor cortical representation of speed and direction during reaching." J Neurophysiol **82**(5): 2676-92.

Moran, D. W. and A. B. Schwartz (1999b). "Motor cortical activity during drawing movements: population representation during spiral tracing." J Neurophysiol **82**(5): 2693-704.

Moran, D. W. and A. B. Schwartz (2000). "One motor cortex, two different views." Nat Neurosci **3**(10): 963; author reply 963-5.

Moseley, M. E., A. deCrespigny, et al. (1996). "Magnetic resonance imaging of human brain function." Surg Neurol **45**(4): 385-91.

Nakamura, A., T. Yamada, et al. (1998). "Somatosensory homunculus as drawn by MEG." Neuroimage **7**(4 Pt 1): 377-86.

Nakata, H., K. Inui, et al. (2005). "Somato-motor inhibitory processing in humans: a study with MEG and ERP." Eur J Neurosci **22**(7): 1784-92.

Nicolelis, M. A., D. Dimitrov, et al. (2003). "Chronic, multisite, multielectrode recordings in macaque monkeys." Proc Natl Acad Sci U S A **100**(19): 11041-6.

Niki, H. (1974). "Prefrontal unit activity during delayed alternation in the monkey. I. Relation to direction of response." Brain Res **68**(2): 185-96.

Niki, H. and M. Watanabe (1976). "Prefrontal unit activity and delayed response: Relation to cue location versus direction of response." Brain Research **105**(1): 79-88.

Nirkko, A. C., C. Ozdoba, et al. (2001). "Different ipsilateral representations for distal and proximal movements in the sensorimotor cortex: activation and deactivation patterns." Neuroimage **13**(5): 825-35.

Norton, E. D. A. P.-. (1928). The Basis of Sensation.

NSCIA, N. S. C. I. A. (2007). "http://www.spinalcord.org/html/injury.php."

Nunez, P. L. and R. Srinivasan (2006). Electric Fields of the Brain: The Neurophysics of EEG, Oxford University Press.

Penfield, W. and E. Boldrey (1937). "Somatic Motor and Sensory Representation in the Cerebral Cortex of Man Studied by Electrical Stimulation." **60**: 389-443.

Pesaran, B., J. S. Pezaris, et al. (2002). "Temporal structure in neuronal activity during working memory in macaque parietal cortex." Nat Neurosci **5**(8): 805-11.

Pfurtscheller, G. and A. Aranibar (1977). "Event-related cortical desynchronization detected by power measurements of scalp EEG." Electroencephalogr Clin Neurophysiol **42**(6): 817-26.

Pfurtscheller, G. and R. Cooper (1975). "Frequency dependence of the transmission of the EEG from cortex to scalp." Electroencephalogr Clin Neurophysiol **38**(1): 93-6.

Pfurtscheller, G., C. Neuper, et al. (1997). "EEG-based discrimination between imagination of right and left hand movement." Electroencephalogr Clin Neurophysiol **103**(6): 642-51.

Pochon, J. B., R. Levy, et al. (2001). "The role of dorsolateral prefrontal cortex in the preparation of forthcoming actions: an fMRI study." Cereb Cortex **11**(3): 260-6.

Polit, A. and E. Bizzi (1979). "Characteristics of motor programs underlying arm movements in monkeys." J Neurophysiol **42**(1 Pt 1): 183-94.

Press, W. H., S. A. Teukolsky, et al. (1992). Numerical Recipes in C.

Ramsey, N. F., M. P. van de Heuvel, et al. (2006). "Towards human BCI applications based on cognitive brain systems: an investigation of neural signals recorded from the dorsolateral prefrontal cortex." IEEE Trans Neural Syst Rehabil Eng **14**(2): 214-7.

Rao, S. M., J. R. Binder, et al. (1993). "Functional magnetic resonance imaging of complex human movements." Neurology **43**(11): 2311-8.

Rektor, I., D. Sochurkova, et al. (2006). "Intracerebral ERD/ERS in voluntary movement and in cognitive visuomotor task." Prog Brain Res **159**: 311-30.

Roland, P. E., E. Skinhoj, et al. (1980). "Different cortical areas in man in organization of voluntary movements in extrapersonal space." J Neurophysiol **43**(1): 137-50.

Sanes, J. N. and J. P. Donoghue (1993). "Oscillations in local field potentials of the primate motor cortex during voluntary movement." Proc Natl Acad Sci U S A **90**(10): 4470-4.

Sasaki, K., A. Nambu, et al. (1996). "Studies on integrative functions of the human frontal association cortex with MEG." Brain Res Cogn Brain Res **5**(1-2): 165-74.

Sawaguchi, T. and I. Yamane (1999). "Properties of Delay-Period Neuronal Activity in the Monkey Dorsolateral Prefrontal Cortex During a Spatial Delayed Matching-to-Sample Task." J Neurophysiol **82**(5): 2070-2080.

Schalk, G. (2005). Personal Communication.

Schalk, G., J. Kubanek, et al. (2007). "Decoding two-dimensional movement trajectories using electrocorticographic signals in humans." J Neural Eng **4**(3): 264-75.

Schalk, G., D. J. McFarland, et al. (2004). "BCI2000: a general-purpose brain-computer interface (BCI) system." IEEE Trans Biomed Eng **51**(6): 1034-43.

Schalk, G., K. J. Miller, et al. (2008). "Two-dimensional movement control using electrocorticographic signals in humans." J Neural Eng **5**(1): 75-84.

Scherberger, H., M. R. Jarvis, et al. (2005). "Cortical local field potential encodes movement intentions in the posterior parietal cortex." Neuron **46**(2): 347-54.

Schmidt, E. M. (1980). "Single Neuron Recording From Motor Cortex As a Possible Source of Signals for Control of External Devices." Ann Biomed Eng **8**: 339-349.

Schwartz, A. B. (1993). "Motor cortical activity during drawing movement: population representation during sinusoid tracing." j-np **70**: 28-36.

Schwartz, A. B. (1994). "Direct cortical representation of drawing." Science **265**(5171): 540-2.

Schwartz, A. B. (2004). "Cortical neural prosthetics." Annu Rev Neurosci **27**: 487-507.

Schwartz, A. B., X. T. Cui, et al. (2006). "Brain-controlled interfaces: movement restoration with neural prosthetics." Neuron **52**(1): 205-20.

Schwartz, A. B., R. E. Kettner, et al. (1988). "Primate motor cortex and free arm movements to visual targets in three-dimensional space. I. Relations between single cell discharge and direction of movement." J Neurosci **8**(8): 2913-27.

Schwartz, A. B. and D. W. Moran (1999c). "Motor cortical activity during drawing movements: population representation during lemniscate tracing." J Neurophysiol **82**(5): 2705-18.

Schwartz, A. B., D. W. Moran, et al. (2004). "Differential representation of perception and action in the frontal cortex." Science **303**(5656): 380-3.

Schwartz, A. B., D. M. Taylor, et al. (2001). "Extraction algorithms for cortical control of arm prosthetics." Curr Opin Neurobiol **11**(6): 701-7.

Staba, R. J., T. D. Ard, et al. (2005). "Intracortical pathways mediate nonlinear fast oscillation (>200 Hz) interactions within rat barrel cortex." J Neurophysiol **93**(5): 2934-9.

Stam, C. J. (2005). "Nonlinear dynamical analysis of EEG and MEG: review of an emerging field." Clin Neurophysiol **116**(10): 2266-301.

Stippich, C., P. Freitag, et al. (1998). "Motor, somatosensory and auditory cortex localization by fMRI and MEG." Neuroreport **9**(9): 1953-7.

Takeda, K. and S. Funahashi (2002). "Prefrontal task-related activity representing visual cue location or saccade direction in spatial working memory tasks." J Neurophysiol **87**(1): 567-88.

Takeda, K. and S. Funahashi (2002). "Prefrontal Task-Related Activity Representing Visual Cue Location or Saccade Direction in Spatial Working Memory Tasks." J Neurophysiol **87**(1): 567-588.

Talairach, J. and I. P. Tournoux PU - Thieme Medical Publishers (1988). Co-Planar Sterotaxic Atlas of the Human Brain.

Tanji, J. and E. Hoshi (2001). "Behavioral planning in the prefrontal cortex." Curr Opin Neurobiol **11**(2): 164-70.

Taylor, D. M., S. I. Tillery, et al. (2002). "Direct cortical control of 3D neuroprosthetic devices." Science **296**(5574): 1829-32.

Thompson, K. G., K. L. Biscoe, et al. (2005). "Neuronal basis of covert spatial attention in the frontal eye field." J Neurosci **25**(41): 9479-87.

Toro, C., C. Cox, et al. (1994). "8-12 Hz rhythmic oscillations in human motor cortex during two-dimensional arm movements: evidence for representation of kinematic parameters." Electroencephalogr Clin Neurophysiol **93**(5): 390-403.

Toro, C., G. Deuschl, et al. (1994). "Event-related desynchronization and movement-related cortical potentials on the ECoG and EEG." Electroencephalogr Clin Neurophysiol **93**(5): 380-9.

Touge, T., K. J. Werhahn, et al. (1995). "Movement-related cortical potentials preceding repetitive and random-choice hand movements in Parkinson's disease." Ann Neurol **37**(6): 791-9.

Tsujimoto, S., A. Genovesio, et al. (2008). "Transient Neuronal Correlations Underlying Goal Selection and Maintenance in Prefrontal Cortex." Cereb Cortex.

Turner, R., A. Howseman, et al. (1998). "Functional magnetic resonance imaging of the human brain: data acquisition and analysis." Exp Brain Res **123**(1-2): 5-12.

Turner, R., J. J. Owens, et al. (1995). "Directional variation of spatial and temporal characteristics of limb movements made by monkeys in a two-dimensional work space." J Neurophysiol **74**(2): 684-697.

Vaadia, E., D. A. Benson, et al. (1986). "Unit study of monkey frontal cortex: active localization of auditory and of visual stimuli." J Neurophysiol **56**(4): 934-952.

Velliste, M., S. Ferel, et al. (2008). "Cortical control of a prosthetic arm for self-feeding." Nature.

Vetter, R. J., J. C. Williams, et al. (2004). "Chronic neural recording using silicon-substrate microelectrode arrays implanted in cerebral cortex." IEEE Trans Biomed Eng **51**(6): 896-904.

Vidal, J. J. (1973). "Toward direct brain-computer communication." Annu Rev Biophys Bioeng **2**: 157-80.

Vidal, J. J. (1977). Real-time detection of brain events in EEG.

Vidal, J. J. (1977). "Real-time detection of brain events in EEG." IEEE Procedings. Special Issue on Biological Signal Processing and Analysis. **65**: 633-664.

Wang, W., S. S. Chan, et al. (2007). "Motor cortical representation of position and velocity during reaching." J Neurophysiol **97**(6): 4258-70.

Weiskopf, N., K. Mathiak, et al. (2004). "Principles of a brain-computer interface (BCI) based on real-time functional magnetic resonance imaging (fMRI)." IEEE Trans Biomed Eng **51**(6): 966-970.

Weiskopf, N., R. Veit, et al. (2003). "Physiological self-regulation of regional brain activity using real-time functional magnetic resonance imaging (fMRI): methodology and exemplary data." Neuroimage **19**(3): 577-586.

Wilson, J. A., E. A. Felton, et al. (2006). "ECoG factors underlying multimodal control of a brain-computer interface." IEEE Trans Neural Syst Rehabil Eng **14**(2): 246-50.

Wisneski, K. J., N. Anderson, et al. (2008). "Unique Cortical Physiology Associated With Ipsilateral Hand Movements and Neuroprosthetic Implications." Stroke **39**(12): 3351-3359.

Wolpaw, J. R. (2004). "Brain-computer interfaces (BCIs) for communication and control: a mini-review." Suppl Clin Neurophysiol **57**: 607-13.

Wolpaw, J. R. and N. Birbaumer (2005). Brain-computer interfaces for communicaton and control. Cambridge, Cambridge University Press.

Wolpaw, J. R., N. Birbaumer, et al. (2002). "Brain-computer interfaces for communication and control." Clin Neurophysiol **113**(6): 767-91.

Wolpaw, J. R. and D. J. McFarland (1994). "Multichannel EEG-based brain-computer communication." Clin Neurophys **90**(6): 444-449.

Wolpaw, J. R. and D. J. McFarland (2004). "Control of a two-dimensional movement signal by a non-invasive brain-computer interface in humans." Society for Neuroscience Abstracts. In press.

Wolpaw, J. R., D. J. McFarland, et al. (1991). "An EEG-based brain-computer interface for cursor control." Clin Neurophys **78**(3): 252-259.

Wolpaw, J. R., D. J. McFarland, et al. (2003). "The Wadsworth Center brain-computer interface (BCI) research and development program." IEEE Trans Neural Syst Rehabil Eng **11**(2): 204-7.

Zetterberg., L. (1969). "Estimation of parameters for a linear difference equation with application to EEG analysis." Math. Biosci.: 227-275.

Zimmerman, J. E., Theine, P., and Harding, J.T. (1970). "Design and operation of stable rf-biased superconducting point-contact quantum devices, etc." Journal of Applied Physics **41**: 1572-1580.